Marco Antonino Tribulato, BSc

Investigation of immobilization and performance of Z_{basic2}-tagged *Lm*SPase and *Tv*DAAO in a glass microreactor

MASTER'S THESIS

to achieve the university degree of

Diplom-Ingenieur

Master's degree programme: Biotechnology

submitted to

Graz University of Technology

Supervisor

Univ.-Prof. Dipl.-Ing. Dr.techn. Bernd Nidetzky

Institute of Biotechnology and Biochemical Engineering

Graz, July 2015

AFFIDAVIT

I declare that I have authored this thesis independently, that I have not used other than the declared sources/resources, and that I have explicitly indicated all material which has been quoted either literally or by content from the sources used.
The text document uploaded to TUGRAZonline is identical to the present master's thesis.

Date		Signature

Acknowledgements

Abstract

The performance of enzymatic reactions in microstructured flow reactors for biocatalysis is becoming increasingly interesting. Here, a non-covalent strategy for immobilization of enzymes in a glass microreactor is investigated. The polycationic linker peptide Z_{basic2} was employed as a silica-binding module (SBM), allowing fully reversible attachment of a fusion protein to the microchannel walls featuring an either unmodified or functionalized surface exhibiting sulfonate groups.

Two industrially relevant enzymes were chosen as the fusion partners, the monomeric sucrose phosphorylase from *Leuconostoc mesenteroides* (*Lm*SPase), and the dimeric D-amino acid oxidase from *Trigonopsis variabilis* (*Tv*DAAO). Ideal loadings were estimated to be 106 mU (Z_{basic2}_*Lm*SPase) and 58.4 mU (Z_{basic2}_*Tv*DAAO), based on comparison of the geometrical dimensions of microchannel and enzyme. Regarding the Z_{basic2}_*Lm*SPase, initial bound activities showed low reproducibility. However, the best experiments yielded values of 50-60 mU. Found stability was low, but could partially be improved by stepwise modification of the reaction medium. Values for the catalytic effectiveness (bound activity/eluted activity) of ~30% suggest that the enzyme exhibits a lower activity when being immobilized.

A three step immobilization was employed to achieve a sufficiently high and reproducible loading of Z_{basic2}_*Tv*DAAO, which catalyzes an oxygen-dependent reaction. Apparent initial activities were around 35.5 and 33.7 mU in the unmodified and functionalized microchannel, respectively. CLSM images created by exploiting the autofluorescence of the cofactor $FAD_{oxidized}$ reveal a homogeneous covering of the microchannel surface. Long term performance of Z_{basic2}_*Tv*DAAO was evaluated using two experimental setups. In the first configuration, substrate mix continuously passed the microreactor. Half-life time was found to be ~40 h on both surfaces. The apparent activity showed a dependency on the residence time. The second configuration was a recycling setup with intermediary reuptake of oxygen. After a recycling time of ~60 h keto acid concentrations of ~15 and ~12 mM were obtained in working volumes of 3.75 and 5 mL, respectively. A considerable contribution of surface functionalization to enhanced enzymatic stability could not be observed. Real-time optical sensing was employed for monitoring of oxygen consumption and provided valuable information.

Zusammenfassung

Die Durchführung enzymkatalysierter Reaktionen in kontinuierlichen mikrofluidischen Reaktoren für die Biokatalyse gewinnt zusehends an Interesse. Im Rahmen dieser Arbeit wird eine nicht-kovalente Strategie für die Immobilisierung von Enzymen in Glas-Mikroreaktoren untersucht. Das positiv geladene Peptid Z_{basic2} wurde als *silica-binding module* (SBM) eingesetzt und ermöglichte die reversible Adsorption eines Fusionsproteins an die Oberfläche eines nicht-modifizierten bzw. eines mit Sulfonatgruppen funktionalisierten Mikrokanals.

Zwei industriell relevante Enzyme wurden als Fusionspartner ausgewählt, die monomere Saccharose-Phosphorylase aus *Leuconostoc mesenteroides* (*Lm*SPase) sowie die dimere D-Aminosäureoxidase aus *Trigonopsis variabilis* (*Tv*DAAO). Die idealen Beladungen wurden unter Einbeziehung der geometrischen Gegebenheiten des Mikrokanals und der Enzyme auf 106 mU (Z_{basic2}_*Lm*SPase) und 58.4 mU (Z_{basic2}_*Tv*DAAO) geschätzt. Bezüglich der Z_{basic2}_*Lm*SPase zeigten die anfänglichen Werte der immobilisierten Aktivitäten eine geringe Reproduzierbarkeit, wobei in den erfolgreichsten Versuchen jedoch Werte im Bereich 50-60 mU erzielt wurden. Die beobachtete Stabilität war ebenfalls gering, konnte allerdings durch schrittweise Anpassung des Reaktionsmediums verbessert werden. Die Werte für die katalytische Effizienz (gebundene Aktivität/eluierte Aktivität) von ~30% weisen darauf hin, dass das Enzym im immobilisierten Zustand eine geringere Aktivität zeigt.

Um eine ausreichend hohe und reproduzierbare Beladung mit Z_{basic2}_*Tv*DAAO zu gewährleisten, wurde die Immobilisierung in drei Stufen durchgeführt. Die scheinbaren anfänglichen Aktivitäten im funktionalisierten und nicht-funktionalisierten Mikrokanal waren 33.7 bzw. 35.5 mU. Die – anhand der Autofluoreszenz des Kofaktors FAD ermöglichten – CLSM-Bilder offenbaren eine homogene Verteilung auf der Oberfläche des Mikrokanals. Zur Beurteilung der Langzeitstabilität wurden zwei verschiedene Versuchsanordnungen eingesetzt. In ersterer passierte der Substratmix kontinuierlich den Mikroreaktor, die dabei gefundene Halbwertszeit der Aktivität lag bei ~40 h. Die scheinbare Aktivität zeigte dabei eine klare Abhängigkeit von der Verweildauer im Mikroreaktor. In der zweiten Anordnung wurde der Substratmix mit dazwischengeschalteter Sauerstoffzufuhr rezykliert. Nach einer Rezyklierungszeit von 60 h wurden in den Arbeitsvolumen von 3.75 und 5 mL Ketosäurekonzentrationen von ~15 bzw. ~12 mM erreicht. Ein nennenswerter Beitrag der Oberflächenfunktionalisierung zur Stabilisierung konnte nicht beobachtet werden. Die zusätzliche, optische Erfassung des Sauerstoffverbrauchs in Echtzeit lieferte weitere wertvolle Informationen.

Contents

1   Introduction

Throughout the recent years, the use of microstructured flow reactors – henceforth referred to as microreactors – in biocatalysis has been extensively studied and acknowledged for several benefits. The first and most obvious of these advantages, arising from their small reaction volume, is the reduced demand of reagents, solvents and (bio)catalysts which offers the possibility to enhance safety and benignity for health and environment. During process development, the favorable controllability enables rapid screening of enzymes out of a number of potential candidates, as well as the selection of substrates (1–4). Hazardous reagents or (by)products are deployed or generated, respectively, in a limited amount and even reactions exhibiting a considerable explosive potential may be performed at negligible risk. In further consequence a small-sized and mobile microreactor setup might allow for operation directly at the point of use, therefore aiding to retain risky conversions at remote sites or to minimize transportation effort of the respective reagent or product (1, 5, 6). Using only small amounts of starting material, process conditions can be screened and evaluated in a fast manner. These conditions may even include novel process windows involving high pressure, temperature and concentrations which might not be accessible in a feasible way when using traditional large scale reactors (1).

The rigorous decrease of the reactor dimensions in microscale technology features a dramatic increase of the surface to volume ratio with typical values in the range of 10.000 to 50.000 m²/m³, which in combination with channel dimensions well below 1 mm to provide short diffusion paths, results in efficient heat and mass transfer. The thereby achieved higher reaction efficiency is the most appropriate contribution to process intensification (1), a term relating to the strong reduction of reactor dimensions while adhering to given production goals or improving key process parameters like product yield or selectivity (4). The transfer of several reactions traditionally performed in batch mode to continuous flow chemistry has been reviewed and shown to be often accompanied with better performance (1, 2, 5–7). Performing reactions in continuous systems at steady state allows for better control and hence reproducibility (2). The usually high space time yield and selectivity observed in microfluidic systems also contribute to regarding them as a promising example of "green" technology (1, 2, 5). Spatial and temporal control of reaction can be established by modification of the flow and/or length of the microreactor channel. Controlling the residence time of a reactive species may be crucial due to constraints emerging from comparison of reaction and mixing time in

view of very fast reactions, as well as from thermodynamic limitations (1). With their generally reduced input of mechanical energy to achieve fast mixing, microreactors also show higher energy efficiency in contrast to traditional reactors of larger scale. Effective mixing is of particular significance when regarding mass transport in multiphase reactions (e.g. immiscible liquids), where establishment of a high interfacial area e.g. promotes the contact between a reagent in the first and another reagent – or the (bio)catalyst – in the second phase. High surface to volume ratio can also assist in the *in situ* separation of product, aiming at increasing product purity, overcoming thermodynamic constraints and prevention of catalyst inactivation (1).

Troublesome scale-up, which is encountered frequently in conventional reactor technology, can be avoided as the transfer to production scale can be achieved by parallelization of a number of microreactors (numbering-up) (1, 4, 5). However, in reality the additional equipment required for operation and monitoring of several microreactors (pumps, sensors, etc.) in parallel might significantly increase the associated costs. Distribution of a stable and uniform flow over a high quantity of microreactor channels might be crucial especially when maintaining flow conditions during multiphase reactions (6, 8).

In view of the continuous processing, the performance of enzymatic conversions using microreactors is highly favored by immobilization of the desired enzyme in the reaction volume. A particularly interesting opportunity is the realization of cascade reactions involving several immobilized enzymes, made possible when considering their respective reaction rates, as well as pH and temperature optima. Popular model enzymes for investigating the efficiency of immobilization include glucose oxidase, horseradish peroxidase and alkaline phosphatase, because they are inexpensive, easily available and provide well-established analytical assays for characterization (9). Although a vast number of immobilization protocols have been developed for beads and microchannels, the immobilization process during the preparation of an enzymatic microreactor is still facing challenges. Implementation of immobilized enzymes into the microchannel can be accomplished in several ways. Immobilization on beads used for generation of a packed bed is a useful method for achieving a high volumetric activity, but may create a considerably high pressure drop (4, 10, 11). This can be avoided by immobilizing on the channel walls, but usually at the expense of a lower potential activity. To increase enzyme loading, the available surface can be extended by etching or coating of the microchannel or by introduction of nanosprings and other nanostructures on the surface (1, 9, 11).

Besides extending enzymatic stability and ensuring high loading, the ideal immobilization strategy has to fulfill several further requirements, such as applicability to a number of different enzymes. No chemical modification of the surface should be necessary. The enzyme should be immobilized in an oriented manner which means that the immobilization does not affect catalytic characteristics like activity and substrate affinity. Additionally, it should be selective for the desired enzyme to enable immobilization from a crude mixture without the need of preceding purification causing expenses regarding labor, time and money. The employed method has to maintain a stable retention of the enzyme under operational conditions, but also allow for an efficient removal. If enzymatic activity becomes insufficient, e.g. by exceeding the total turnover number, this reversibility of attachment provides the opportunity to reuse the solid support for a renewed loading with fresh enzyme (3, 4, 12, 13).

A promising strategy considered to meet the above stated requirements well is non-covalent adsorption between the surface and a domain which was genetically fused to the enzyme of interest (4). The deployment of a polyhistidine domain (His tag) for attachment to a surface featuring immobilized divalent metal ions (Co^{2+}, Cu^{2+}, Ni^{2+}, Zn^{2+}) is a successful and widespread strategy, but usually implies modification of the carrier (4, 14, 15). Furthermore, using this label in metal affinity chromatography for protein purification has revealed drawbacks like co-purification of histidine-rich host enzymes (16). A polyarginine domain comprising nine arginine residues has been utilized as a tag to allow for direct immobilization of proteins onto unmodified silica resin (17). In an early study, a polyarginine tag was fused to the C-terminal end of human urogastone. Only a minimal influence on the tertiary structure of urogatone was assumed, but in contrast it was supposed that the tag might alter the tertiary structures of proteins with a hydrophobic C-terminal (18). Silica-based materials like glass are attractive supports for biotechnological applications and show favorable optical characteristics enabling direct visualization of the reaction (9, 13). Although the various silica materials differ in their exact composition, they share the feature that the surface provides slightly acidic silanol groups ($pK_a \approx 6\text{-}7$). Deprotonation in aqueous environment at neutral pH results in a negative charge displayed on the surface. Besides, the siloxanes included in the structure also add hydrophobic properties. As a consequence, the immobilization of a protein on an unmodified silica surface might include ionic, hydrophobic and van der Waals interactions as well as hydrogen bondings (13). The generation of a protein chimera comprising the protein of interest and a silica-binding module (SBM) was proposed. The SBM is a small protein named Z_{basic2}, a variant of the Z domain derived from the B domain of staphylococcal protein A, genetically engineered to increase the number of arginine residues. It is a bundle of three

helices with a length of 58 amino acids and a size of 7 kDa. The addition of positive charge by the Z_{basic2} linker peptide is promoting the strength of interaction between the fusion protein and the anionic support (12, 13). Using a chimera, whereas one part is just responsible for attachment to the surface, greatly reduces the risk of a negative influence on the desired biocatalytic activity and is regarded an advantage over polyarginine tags. The Z_{basic2} linker peptide also functions as an independent folding unit, a feature which is missing in small peptide tags like the His-tag and supporting the employment of the SBM (19). The usefulness of Z_{basic2} was found to be independent of whether it was fused to the N- or C-terminus. Furthermore, no indication was detected that Z_{basic2} affects the expression of recombinant protein in *E. coli* (13). Z_{basic2} was already successfully employed for immobilization of enzymes on controlled pore glass, both unmodified or functionalized with amino and sulfonate groups, as well as on other commercial anionic supports (12, 13, 19). It has to be noted that the author did not find any published reports investigating immobilization of Z_{basic2} fusion proteins on the inner surface of a microreactor, as also remarked in a recent review (1).

For this thesis, two industrially applied enzymes – sucrose phosphorylase from *Leuconostoc mesenteroides* (*Lm*SPase) and D-amino acid oxidase from *Trigonopsis variabilis* (*Tv*DAAO) – were selected as the fusion partners for the Z_{basic2} linker peptide. *Lm*SPase is a monomeric enzyme which catalyzes the conversion of sucrose and phosphate to α-D-glucose-1-phosphate and D-fructose. Apart from this hydrolytic reaction, the enzyme also performs transglycosylation reactions where new α-D-glycosides are formed (20). *Tv*DAAO is a homodimer catalyzing the oxidative deamination of D-amino acids to their corresponding α-keto acids, besides producing ammonia and hydrogen peroxide (21). Carrier bound preparations of the enzyme play an important role in the transformation of Cephalosporin C during the production of various cephem antibiotics (22). The Z_{basic2} peptide was genetically fused to the N-termini of the enzymes, *Lm*SPase and *Tv*DAAO therefore featuring one and two tags, respectively. Moreover, the Z_{basic2} SBM was not found to affect these enzymes' activity and stability (19). Immobilization of both fusion enzymes on functionalized and unmodified porous carriers was previously described and showed encouraging results (12, 13, 19), but up to the present point of time no studies exploring the long-term stability (exceeding an operation time of 5 h) were published.

2 Objectives

In this master thesis the potential of the polycationic linker peptide Z_{basic2} for immobilization of enzymes in the channel of a microreactor is investigated. Two industrially applied enzymes – *Lm*SPase and *Tv*DAAO – were selected as the fusion partners for this SBM within this work. *Lm*SPase was chosen in order to study the maximum loading, apparent bound activity and stability of attachment of a monomeric enzyme featuring a single SBM, as well as its catalytic effectiveness, for production of phosphorylated sugars by taking the example of glucose-1-phosphate. *Tv*DAAO was employed to determine the apparent loading and stability of attachment of a protein dimer. Since the catalyzed reaction is oxygen-dependent, the influence of flow on conversion and productivity was of special interest. Continuous operation was accomplished including both a single passage of the substrate and its recirculation to enhance product concentration by intermediary re-uptake of oxygen. Additionally, the oxygen concentration on the in- and outlet of the microreactor was monitored to gain information about oxygen supply and depletion as well as the impact on the reaction.

3 Material and methods

3.1 Microreactor and analytical devices

The glass microreactor (product code FC_R150.676.2) was purchased from Micronit Microfluidics (Enschede, Netherlands). Connections were established using Teflon tubings with an inner diameter of 250 µm from the same supplier. Flows were generated using either a Razel Scientific Instruments syringe pump purchased from Bioblock Scientific (Illkirch, France), a New Era NE-1000 syringe pump distributed by Next Advance (Averill Park, NY, USA), a Smartline 1000 HPLC pump from Knauer Advanced Scientific Instruments (Berlin, Germany) or a Bio-Rad 1350 HPLC pump. All spectroscopic measurements were performed using a Beckman Coulter DU 800 UV/Vis spectrophotometer or a Thermo Scientific Genesys 10S UV/Vis spectrophotometer.

3.2 Chemicals and reagents

D-Methionine (D-Met), N,N-Dimethylaniline (DMA), 2,4-Dinitrophenylhydrazine (DNP) and Horseradish Peroxidase (HRP) were purchased from Fluka Analytical/Sigma Aldrich (Steinheim, Germany). 4-Aminoantipyrene (4-AAP), Phosphoglucomutase from rabbit muscle (PGM), Glucose-6-phosphate Dehydrogenase from *Leuconostoc mesenteroides* (G6P-DH), Catalase from bovine liver and Glucose Oxidase from *Aspergillus niger* (GOX) were obtained from Sigma Aldrich (Steinheim, Germany). Glucose-1,6-biphosphate – in the form of a-D-Glucose-1,6-biphosphate tetra(cyclohexylammonium) salt hydrate – was purchased from Carbosynth (Compton, Berkshire, UK). Roti-Quant reagent for determination of protein concentration was acquired from Carl Roth (Karlsruhe, Germany). 3-(Trihydroxysilyl)-1-propanesulphonic acid (SPTHS) was obtained from ABCR (Karlsruhe, Germany). All other reagents were of analytical grade and were obtained elsewhere.

3.3 Culture and cell disruption

3.3.1 Recombinant Z$_{basic2}$_*Lm*SPase

100 µL aliquots of a resuspended cell pellet of *E. coli* strain BL21(DE3), bearing a plasmid with the gene coding for *Lm*SPase fused with the Z$_{basic2}$ peptide on its amino-terminal end, were streaked out on plates with LB agar (10 g/L peptone from casein, 5 g/L yeast extract,

5 g/L NaCl, 15 g/L Agar, pH set to 7.0) including Kanamycin (50 mg/mL, sterile filtrated). Upon incubation of the plates overnight at 37 °C, grown colonies were used for inoculation of 50 mL liquid precultures (LB medium containing 50 mg/L Kanamycin) which were subsequently shaken with 100 rpm at 37 °C overnight. 200 mL main cultures were inoculated with a suitable portion of the precultures to achieve an initial OD of 0.1 and incubated at 100 rpm and 37 °C, until an OD of 0.8-1.0 was reached. After cooling the culture to 25 °C and induction with 1 mM Isopropyl-β-D-thiogalactopyranoside (IPTG), the main cultures were incubated for 18 h at 100 rpm and 25 °C. Towards harvesting by centrifugation (Sorvall Evolution RC, 5000 rpm, 20 min, 4 °C), the cell pellets were stored at -20 °C until required for further processing. Whenever needed, the pellet was suspended in 50 mM KH_2PO_4 pH 7.0 and the cells were disrupted by passing through a French press (American Instruments Company, USA) at 150 bar. Following removal of the cell fragments via centrifugation (Eppendorf 5415R, 13200 rpm, 15 min, 4 °C), the crude cell extracts were stored at 4 °C until needed.

3.3.2 Recombinant Z_{basic2}_TvDAAO

Cell pellets containing recombinant Z_{basic2}_TvDAAO were kindly provided by Karin Longus and Sabine Schelch (Institute of Biotechnology and Biochemical Engineering, Graz University of Technology) and were obtained as follows: *E. coli* strain BL21(DE3) containing a plasmid with the gene coding for D-amino acid oxidase from *Trigonopsis variabilis* (*Tv*DAAO) linked to Z_{basic2} on its N-terminus was firstly cultivated in 150 mL precultures containing 50 mg/L Kanamycin at 130 rpm and 37 °C. Main culture was conducted in a 5 L fermenter. The different media compositions applied for pre- and main culture are shown in Table 1.

Table 1: Media composition applied in the TvDDAO pre- and main cultures

Solution*	Media component	Preculture	Main culture
A	Glucose x H_2O	5.5 g/L	22 g/L
B	Peptone from casein	10 g/L	10 g/L
	Yeast extract	5 g/L	5 g/L
	NaCl	5 g/L	5 g/L
	NH_4Cl	1 g/L	1 g/L
	$MgSO_4$ x 7 H_2O	0.25 g/L	0.25 g/L
	Micronutrients	1 mL/L	1 mL/L
	Polypropylene glycol	100 µL/L	100 µL/L
C	K_2HPO_4	3 g/L	3 g/L
	KH_2PO_4	6 g/L	6 g/L

*Solutions A, B and C were autoclaved separately

5mL of 50 mg/mL Kanamycin and 2 mg/mL Thiamin (both sterile filtrated) were supplemented before a suitable volume of the precultures to obtain an initial OD of 0.5 was added for inoculation. Cultivation was executed at 37 °C and a pO_2 of approximately 40%. When attaining an OD of ~2, the temperature was decreased to 25 °C prior to the addition of 0.25 mM IPTG for induction of Z_{basic2}_TvDAAO expression and Kanamycin for maintaining the selection pressure. 18 h after induction, the cells were harvested by centrifugation (Sorvall Evolution RC, 5000 rpm, 15 min, 4 °C) and the cell pellets were stored at -20 °C until required for further processing. Whenever needed, the cells were suspended in 50 mM KH_2PO_4 pH 7.0 and disrupted using a French press (American Instruments Company, USA) at 150 bar. Following removal of the cell fragments via centrifugation (Eppendorf 5415R, 13200 rpm, 45 min, 4 °C), the crude cell extracts were stored at 4 °C until needed.

3.4 Determination of Z_{basic2}_LmSPase activity

3.4.1 Continuous coupled assay

The activity of soluble Z_{basic2}_LmSPase was measured with a continuous coupled enzymatic assay as described in (20). At 30 °C, the generation of glucose-1-phosphate (G1P) from sucrose and inorganic phosphate catalyzed by sucrose phosphorylase (SPase) is coupled to the conversion to glucose-6-phosphate (G6P) using phosphoglucomutase (PGM) and reduction of NAD^+ by glucose-6-phosphate dehydrogenase (G6P-DH). The formation of NADH is detected spectrophotometrically at 340 nm.

$$\text{Sucrose + phosphate} \xrightarrow{SPase} \text{Glucose-1-phosphate + D-Fructose} \qquad \textbf{Equation 1}$$

$$\text{Glucose-1-phosphate} \xrightarrow{PGM} \text{Glucose-6-phosphate} \qquad \textbf{Equation 2}$$

$$\text{Glucose-6-phosphate + NAD}^+ \xrightarrow{G6P-DH} \text{Gluconolactone-6-phosphate + NADH + H}^+ \qquad \textbf{Equation 3}$$
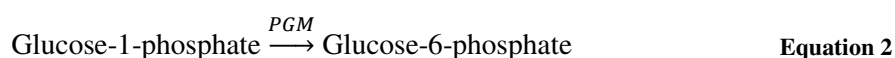
The test buffer used contained 50 mM KH_2PO_4, 10 mM $MgCl_2$, 10 mM EDTA (as sodium salt) and 5 µM glucose-1,6-biphosphate; pH was adjusted to 7.0. The assay mix comprised 380 µL test buffer, 40 µL NAD^+ solution (20 mg/mL), 2 µL PGM (945 U/mL in 3.2 M $(NH_4)_2SO_4$ containing 0.01% EDTA, pH 6.0), 2 µL G6P-DH (317 U/mL in 3.2 M $(NH_4)_2SO_4$ containing 50 mM Tris and 1 mM $MgCl_2$, pH 7.5) and 10 µL of the enzyme in appropriate dilution. Reaction was started by addition of 130 µL sucrose solution (1.1 M in test buffer).

The activity was calculated according to Equation 4. One unit of activity corresponds to the amount of Z_{basic2}_LmSPase which causes the reduction of 1 µmol NAD^+ per minute under the conditions described above.

$$\text{vol. act.} = \frac{\frac{dAbs}{min} \cdot V_{tot} \cdot df}{\varepsilon \cdot V_{sample} \cdot d}$$

Equation 4

vol.act.	volumetric activity (in U/mL)
dAbs/min	slope of absorbance increase per minute (in linear range)
V_{tot}	total volume of assay mix (=564 µL)
df	dilution factor of sample
ε	molar extinction coefficient of NADH at 340 nm (=5.216 $mM^{-1}cm^{-1}$)
V_{sample}	sample volume (=10 µL)
d	path length in cuvette (=1 cm)

3.4.2 Discontinuous coupled assay

The activity of immobilized Z_{basic2}_LmSPase was assessed by determination of the G1P concentration using a variation of the continuous coupled assay described above. According to Equation 1 in 3.4.1, G1P is produced using the Z_{basic2}_LmSPase immobilized in the microreactor at room temperature.

$$\text{Glucose-1-phosphate} \xrightarrow{PGM} \text{Glucose-6-phosphate}$$

Equation 5

$$\text{Glucose-6-phosphate} + NAD^+ \xrightarrow{G6P-DH} \text{Gluconolactone-6-phosphate} + NADH + H^+$$

Equation 6
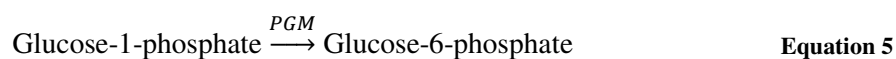
The employed test buffer contained 50 mM TRIS, 10 mM $MgCl_2$, 10 mM EDTA (as sodium salt) and 5 µM Glucose-1,6-biphosphate; pH was adjusted to 7.7 using concentrated HCl. The assay mix comprised 400 µL test buffer, 10 µL NAD^+ solution (20 mg/mL), 2 µL G6P-DH (317 U/mL in 3.2 M $(NH_4)_2SO_4$ containing 50 mM Tris and 1 mM $MgCl_2$, pH 7.5) and 10-100 µL of the enzyme in an appropriate dilution as necessary. After mixing and incubation for 3-5 min absorbance (A1) at 340 nm was read. 2 µL PGM (945 U/mL in 3.2 M $(NH_4)_2SO_4$, pH 6.0 containing 0.01% EDTA) were added and after mixing and incubation for 5-15 min the absorbance A2 at 340 nm was measured.

The concentration of G1P was calculated using Equation 7.

$$c(G1P) = \frac{\Delta Abs \cdot V_{tot} \cdot df}{\varepsilon \cdot V_{sample} \cdot d}$$

Equation 7

c(G1P)   G1P concentration in sample (in mM)
ΔAbs   difference in absorbance after addition of PGM (A2-A1)
V_{tot} total volume of assay (=424-514 µL, depending on V_{sample})
df   eventual dilution factor of sample
ε   molar extinction coefficient of NADH at 340 nm (=5.216 $mM^{-1}cm^{-1}$)
V_{sample} sample volume (=10-100 µL)
d   path length in cuvette (=1 cm)

The G1P concentration was converted to the apparent volumetric activity (in the microreactor) in accordance with Equation 8.

$$vol.\,act. = \frac{c(G1P) \cdot F}{V_{MR}}$$

Equation 8

vol.act.   volumetric activity (in U/mL)
F   flow (in µL/min)
V_{MR} volume of microreactor (=13 µL)

Subsequently the apparent total activity can be calculated as follows:

$$tot.\,act. = V_{MR} \cdot vol.\,act.$$

Equation 9

tot.act.   total activity (in mU)

In order to determine the range, in which the absorbance responds linearly to the concentration of G1P, various dilutions of a 0.3 mM G1P concentration were used as samples. The assay mixture was similar to that mentioned above, but with the volume of test buffer increased to 422.5 µL and sample volume set to 13.5 µL, which leads to V_{tot}=450 µL. The determinations were repeated after 2 h using the previously prepared dilutions.

3.5   Determination of Z_{basic2}_*Tv*DAAO activity

3.5.1   Coupled peroxidase assay

The activity of soluble and immobilized Z_{basic2}_*Tv*DAAO was measured using an assay similar to the method described in (19, 23). D-Methionine is oxidized at 25 °C by the

soluble/immobilized D-amino acid oxidase producing the corresponding α-keto acid and hydrogen peroxide. Upon conversion of hydrogen peroxide by HRP in presence of 4-AAP and DMA, a quinonediimine dye is formed and detected photometrically at 565 nm.

$$\text{D-Methionine} + O_2 \xrightarrow{TvDAAO} \text{α-keto acid} + H_2O_2 \qquad \textbf{Equation 10}$$

$$2\,H_2O_2 + \text{4-AAP} + \text{DMA} \xrightarrow{HRP} \text{Quinonediimine dye} + H_2O \qquad \textbf{Equation 11}$$
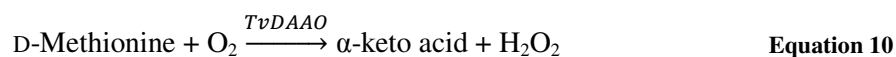
The assay mix for soluble or eluted Z_{basic2}_TvDAAO was composed of 350 µL KH_2PO_4 50 mM pH 8.0, 50 µL D-Met 100 mM, 50 µL 4-AAP 15 mM, 50 µL DMA 0.2 % (v/v), 10 µL HRP (0.5 mg/mL) and 25 µl of sample containing the Z_{basic2}_TvDAAO activity to be determined. Blanks were prepared adding additional 25 µL of KH_2PO_4 50 mM pH 8.0 instead of the sample.

Z_{basic2}_TvDAAO activity was calculated according to the following formula:

$$\text{vol. act.} = \frac{\frac{\text{dAbs}}{\text{min}} \cdot V_{tot} \cdot df}{\varepsilon \cdot cf \cdot V_{sample} \cdot d} \qquad \textbf{Equation 12}$$

vol.act.	volumetric activity (in U/mL)
dAbs/min	slope of absorbance increase per minute (in linear range)
V_{tot}	total volume of assay (=1070 µL)
df	dilution factor of sample
ε	molar extinction coefficient of quinonediime dye at 565 nm (=35.33 mM^{-1}cm^{-1})
cf	conversion factor based on one mole of H_2O_2 producing 0.5 mole of dye (=0.5)
V_{sample}	sample volume (=50 µL)
d	path length in cuvette (=1 cm)

In an approach to determine the activity of the immobilized Z_{basic2}_TvDAAO – which is also denoted as "continuous coupled peroxidase assay" in the following – a mixture with the same composition (but certainly lacking the sample volume) was passed through the loaded microreactor and the resulting absorbance was measured.

To gain an appropriate window of operation regarding the flows to be suitable at each potential v_{max}, calculations were performed using Equation 13. Noticeable is the linear relationship between the desired final absorbance and the resulting flow at constant v_{max}. The

desired absorbance was chosen to lie in between 0.1 and 1.0, since the assay showed reliability in this range.

$$F = \frac{v_{max} \cdot V_{MR} \cdot \varepsilon}{Abs}$$

<div align="right">**Equation 13**</div>

F   flow (µL/min)
v_{max} maximum volumetric activity (U/mL)
V_{MR} total volume of the microreactor (=13 µL)
ε molar extinction coefficient of quinonediime dye at 565 nm (=35.33 $mM^{-1}cm^{-1}$)
Abs   absorbance at 565 nm

3.5.2   Keto acid assay

Apparent activity of immobilized Z_{basic2}_TvDAAO was also assessed via determination of the produced α-keto acid using an assay modified from (24–27). 150 µL of the sample (diluted with 50 mM KH_2PO_4 pH 8.0 where necessary) were mixed with 150 µL of DNP solution (1 M DNP in 2 M HCl) in a 1.5 mL reaction tube. Upon incubation for 10 min in a lab rotator (20 rpm) at room temperature, 600 µL of 2.5 M NaOH were added and the mixture was again placed in a lab rotator (20 rpm) for 10 min. Afterwards 400 µL of the assay mix were transferred to a cuvette, diluted with 400 µL of 50 mM KH_2PO_4 pH 8.0 and absorbance was measured at 440 nm.

The keto acid concentration was reckoned using Equation 14.

$$c(\text{keto acid}) = \frac{Abs \cdot df}{\varepsilon}$$

<div align="right">**Equation 14**</div>

c(keto acid)   concentration of α-keto acid (in mM)
dAbs   absorbance at 440 nm
df   dilution factor of sample
ε molar extinction coefficient of quinonediime dye at 440 nm
              (=1.0353 $mM^{-1}cm^{-1}$ when determining α-Keto-γ-(methylthio)butyric acid, the corresponding α-keto acid of D-Methionine; valid up to a maximum absorbance of 0.4055)

The apparent volumetric and total activities were calculated according to Equation 8 and Equation 9 shown in 3.4.2, respectively, with c(keto acid) replacing c(G1P).

3.6 Determination of protein concentration

Protein concentrations in the used crude extracts were quantified based on the method of Bradford (28), using Roti-Quant dye solution and BSA as the standard. The reagent was prepared by dilution according to the manufacturer's instructions and samples were diluted 1:20, 1:50 and 1:100, respectively. 500 µL of the dye solution were mixed with 10 µL of sample and incubated for at least 5 min at room temperature. The blank was prepared with dH$_2$O replacing the sample. Finally the absorbance was measured at 595 nm.

3.7 Immobilization in the microreactor

3.7.1 Calculation of ideal loading

Theoretical maximum loading which can be achieved when assuming formation of a monolayer of bound enzyme was estimated considering the geometrical dimensions of microreactor and enzyme. Starting from the microreactor dimensions given in the technical drawing (29) the inner surface area of the channel was calculated.

For gaining an estimation of the maximum enzyme loading possible, three different models were utilized. The models 1 and 2 make use of the cross sectional area derived by calculation of the mean diameter of a rigid "enzyme sphere" comprising of the monomeric *Lm*SPase and the linked Z$_{basic2}$ peptide, or the *Tv*DAAO homodimer and the two corresponding Z$_{basic2}$ chains, respectively.

For model 1 the particular enzyme masses were derived from UniprotKB (*Lm*SPase: entry code Q59495, mass 55743 Da; *Tv*DAAO: entry code Q09942; mass 39301 Da for each subunit), while the mass for a single Z$_{basic2}$ peptide chain was found in the literature [7 kDa as given in (13)]. The summarized masses were converted into volumes for the rigid enzyme spheres assuming a density of 1.41 g/mL (30), followed by calculation of the cross sectional areas (Figure 1).

Regarding model 2, the masses and diameters for the enzymes and the tethered Z$_{basic2}$ chain(s) were calculated using the CalcTool protein mass calculator (31). Given the amino acid quantities for *Lm*SPase, *Tv*DAAO and the Z$_{basic2}$ peptide with 490, 356 and 58 amino acids, respectively, the total numbers of amino acids were calculated for each Z$_{basic2}$ enzyme variant. Starting with the gained total number of 548 amino acids for the *Lm*SPase (monomeric enzyme plus one Z$_{basic2}$ module connected to its amino-terminal end), the tool calculated a

mass of 65760 Da and a diameter of 5.65 nm. Regarding the *Tv*DAAO (a homodimer, thus featuring two Z_{basic2} linkers) the total value of 828 amino acids was converted to a total mass of 99360 Da and a diameter of ~6.48 nm by CalcTool. The obtained diameter values were deployed for calculation of the required footprint.

In contrast to the aforementioned, the required area for model 3 is not derived based on the mass, but instead gained by measurement of the 3D structure's dimensions using PyMol. Lacking a structure for the monomeric *Lm*SPase_Z_{basic2}, the structure of the dimeric SPase from *Bifidobacterium adolescentis* (PDB code 1R7A) was used, whereas one subunit was removed prior to determining the dimensions of the remaining subunit. As a Z_{basic2}_*Tv*DAAO structure was also not available, a structure of the native *Tv*DAAO was employed. The largest possible footprint was chosen for further calculations. A possible contribution of the Z_{basic2} linker(s) to the areas required by the enzymes was ignored in this estimation model.
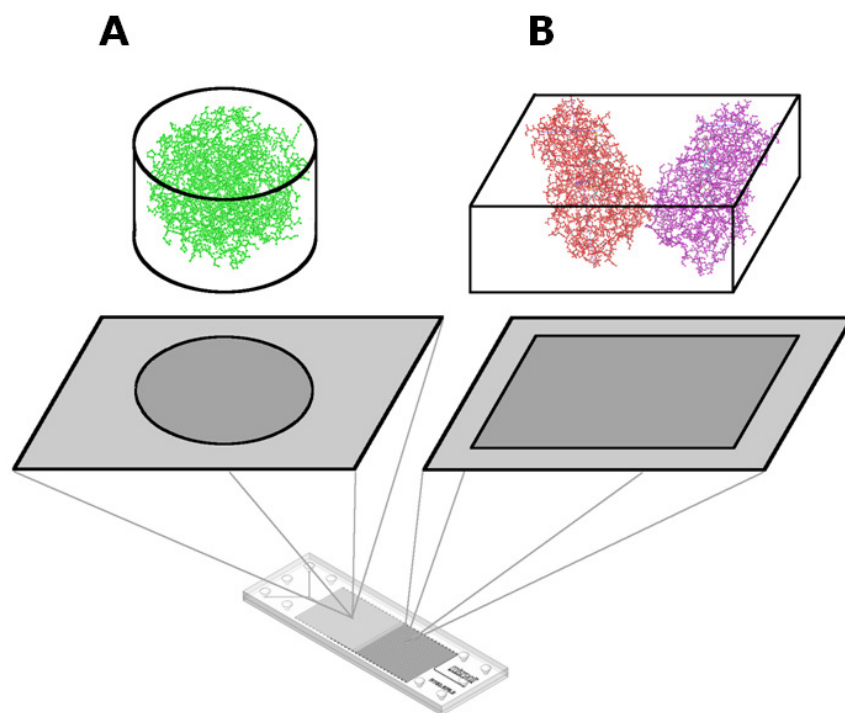
Figure 1: Models for estimation of the theoretical maximum loading

Estimation of the footprint as employed in Models 1 and 2 (A) or in Model 3 (B) shown for the example of *Tv*DAAO

Dividing the microreactor's inner surface by the enzyme's footprint gives information about the quantity of enzyme molecules which can be theoretically immobilized when generation of a monolayer is desired. This quantity can be converted into the theoretical maximum activity

loading using Avogadro's number and the specific activity of the enzymes [*Lm*SPase: 110 U/mg, *Tv*DAAO: 71 U/mg (19)].

3.7.2 Pretreatment of the microreactor

During the initial immobilization experiments, the cleaning procedure at the forefront of immobilization was a sequence of consecutive washing steps with ethanol, deionized water and 50 mM KH_2PO_4 pH 8.0. In the subsequent experiments, the microreactor was subjected to an extended cleaning procedure prior to the immobilization process in order to study any effect in increase of the loading. An effective removal of organic molecules and other contaminants as well as – at least partial – (re-)activation of the silanol groups on the surface was seen as particularly important, as the microreactor chip was reused during the course of the experiments.

The extended cleaning procedure started with rinsing with deionized water to remove possible salt residues from foregoing elution experiments, followed by 30 min incubation with MeOH/HCl (1:1) to remove contaminants. Towards rinsing with deionized water the surface was incubated with NaOH 1 M for 20 min. NaOH is a known etchant of glass (32) and might also be adjuvant to raise the amount of available silanol groups available on the surface. A comparison of different cleaning methods for glass can be found in (32). After another rinsing step with deionized water, the microreactor was washed with KH_2PO_4 50 mM pH 8.0. During the initial experiments with Z_{basic2}_*Lm*SPase, incubation with either MeOH/HCl or NaOH was in some cases skipped for reasons of comparison. When using a microreactor chip functionalized with sulfonate groups, the treatment with NaOH was omitted in any case.

3.7.3 Functionalization of the microreactor with sulfonate groups

The inner surface of the glass microreactor chip was also activated with sulfonate groups according to a method presented in (12). The microreactor chip was washed with 1 M NaOH for 20 min at room temperature at a flow of 20 µL/min. Towards rinsing with dH_2O, it was filled with 10% (v/v) SPTHS adjusted to pH 8.0. All entry holes of the chip were sealed with snippets of disposable gloves (made of acrylonitrile-buradien-rubber). The chip was kept in an oven at 80 °C for 19 h. Subsequently the microreactor was extensively rinsed with water and filled with 50 mM KH_2PO_4 pH 7.0 until further use.

3.7.4 Immobilization of Z_{basic2}_LmSPase and Z_{basic2}_TvDAAO

A "static approach" was chosen for immobilization of the enzyme in the microreactor, which means that the microreactor was completely filled with the immobilization mixture and incubated for a certain time at room temperature.

Z_{basic2}_LmSPase was applied in a suitable concentration (preferably with a small excess) to reach the maximum loading capacity estimated as described in 4.1.1, or in total excess (6- to 8-fold of the ideal loading) to favor complete saturation of the available surface.

The concentration of Z_{basic2}_TvDAAO present in the immobilization mixture was matching the calculated ideal loading (see 4.2.1), again with an intermittently small excess.

When deploying a non-functionalized microreactor chip, immobilization mix composition was defined in accordance with the findings presented in (13). The mix contained 0.5% (v/v) Tween 20, the respective activity of enzyme and a NaCl concentration of 0.25 M (LmSPase$\_Z_{basic2}$) or 1 M (Z_{basic2}_TvDAAO), in KH_2PO_4 50 mM pH 8.0. As the addition of NaCl causes a pH drop, the pH was adjusted to 8.0 using a saturated solution of $NaHCO_3$.

Using a microreactor chip functionalized with sulfonate groups, the respective activity was prepared in KH_2PO_4 50 mM pH 7.0. NaCl in a concentration of 0.25 M was included in the immobilization mix for Z_{basic2}_TvDAAO compliant with the results shown in (12), but was missing in the mix for immobilizing Z_{basic2}_LmSPase.

After incubation the either unbound or weakly bound enzyme fraction was collected by rinsing with KH_2PO_4 50 mM pH 7.0 and activity was determined. A small portion of the deployed immobilization mix was not brought into contact with the microreactor to serve as an "immobilization blank". In order to identify the decrease of activity during the respective incubation time, the retained activity in this blank was also determined. The activity of immobilized Z_{basic2}_LmSPase and Z_{basic2}_TvDAAO was measured using the assays described in 3.4 and 3.5, respectively.

At the end of each immobilization experiment, the bound enzyme was eluted from the non-functionalized microreactor using solutions of 0.5% Tween 20 in KH_2PO_4 50 mM pH 7.0, containing NaCl in increasing concentrations of 2 M and 3 M or 2 M and 4.75 M, respectively. Elution from the functionalized surface was achieved using 5 M NaCl in KH_2PO_4 50 mM pH 7.0. Towards elution, the activity of the detached enzyme was determined.

3.7.5 Immobilization balances

For evaluation of the immobilization efficacy, the immobilization balance showing the total activities entering and leaving the system were prepared. In this case the term offered total activity is referring to the residual activity of the *immobilization blank* at the end of the respective incubation time, multiplied with the system volume. The system includes the volumes of the glass microreactor chip and all connected capillaries. The design of the chip (29) provides 2 inlets and 1 outlet – or vice versa, if operated in the opposite direction as done in the experiments within this thesis. So, besides the connections pump→inlet and outlet→specimen cup, the design of the chip demands an additional capillary at the second in- or outlet to gain control over this dead volume, raising the total system volume to 61.6 µL. Subtracting the non-bound activity from the total activity applied to the system allows for the calculation of the amount of theoretically bound enzyme. The occurrence of unspecific binding of the enzyme to the capillary material was checked and could be excluded in advance, since the calculation would certainly be compromised by this possibility.

3.7.6 Study of the stability of soluble enzyme under elution conditions

In order to investigate whether the activity of eluted enzyme is impaired under elution conditions, defined activities of Z_{basic2}_LmSPase were added to an elution mixture comprising 2 M NaCl and 0.5% Tween 20 in 50 mM KH_2PO_4 pH 7.0. After 5, 10, 20, 30, 45 and 60 min the activity was determined spectrophotometrically as described in 3.4.1 and compared with the initial activity. Regarding the Z_{basic2}_TvDAAO this data was already available from former studies for up to 30 minutes (33). However, to assess the stability of Z_{basic2}_TvDAAO when eluting it from the surface functionalized with sulfonate groups, certain activities were prepared in a mix containing a higher NaCl concentration of 5 M in 50 mM KH_2PO_4 pH 7.0 and measured at the identical time points already mentioned for Z_{basic2}_LmSPase.

3.8 Flow conditions

To estimate to flow conditions, the Reynolds number (Re) was calculated as given in Equation 15.

$$Re = \frac{u \cdot D \cdot \rho}{\mu}$$

Equation 15

whereas u is the flow speed, D is the hydraulic diameter of the microreactor channel, and ρ and μ are the density and dynamic viscosity of the fluid at 25 °C, respectively.

3.9   Monitoring of oxygen concentration

When performing oxygen-dependent reactions deploying Z_{basic2}_TvDAAO in the microreactor, the oxygen concentration at the in- and outlet was monitored using the phase-modulation technique. By excitation of the luminophore using a sinusoidally modulated high frequency light, the emitted light has the same frequency, but shows a phase shift Φ which is a manifestation of the lifetime τ (34). The correlation between phase shift and lifetime is defined according to Equation 16, whereas f_{mod} is the modulation frequency.

$$\tan \phi = 2 \cdot \Pi \cdot f_{mod} \cdot \tau$$

Equation 16

Molecular oxygen is a well-known quencher of luminophores, affecting the intensity and the lifetime of the luminescent response (35). The dependency can be described using the Stern-Volmer equation (Equation 17) (34).

$$\frac{\tan \phi_0}{\tan \phi} = \frac{\tau_0}{\tau} = 1 + K_{SV} \cdot c(O_2)$$

Equation 17

Φ_0 and τ_0 are phase shift and lifetime in absence of the quencher, respectively, while K_{SV} is the Stern-Volmer quenching constant and $c(O_2)$ is the oxygen concentration.

Magnetic particles covered with platinum(II)-tetraphenyltetrabenzoporphyrin (kindly provided by Assoc. Prof. Dr. Torsten Mayr from the Institute of Analytical Chemistry and Food Chemistry, Graz University of Technology) were immobilized in the form of small spots inside the Teflon capillaries connected to the microreactor chip. The used sensor material is a metal-ligand complex exhibiting a (unquenched) lifetime of 47 µs (36) and therefore allowing for a lifetime-based sensing of oxygen (35). 1 mm optical fibers were positioned directly above the sensor spots on the outside of the capillary. Excitation at 620 nm and detection of the emitted wavelength at 760 nm was realized using a Firesting O_2 optical

oxygen meter (Aachen, Germany). Firesting Logger software V2.18 was deployed for data acquisition. For calibration purposes O_2 was depleted by passing a solution containing glucose and GOX in ample amounts.

3.10 SDS-PAGE

SDS-PAGE was performed using the Novex NuPAGE system with BisTris gels 4-12% (Carlsbad, CA, USA). For sample preparation 2.5 µL of the LDS sample buffer and 1.0 µL of the reducing agent (500 mM Dithiothreitol) were mixed with the sample to obtain a total volume of 10 µL. If necessary, sample was diluted with dH_2O to adjust to a protein concentration of 10-20 µg. Following incubation on a thermomixer at 70 °C for 10 min at 600 rpm, the samples were loaded onto the precast gel along with 5 µL of PageRuler Prestained Protein Ladder from Thermo Scientific (Waltham, MA, USA). Separation was performed in MOPS SDS running buffer (50 mM MOPS, 50 mM Tris Base, 0.1% SDS, 1 mM EDTA, pH 7.7) applying 200 V for 50 min. Subsequently the protein bands were dyed by treatment with staining solution (2.5 g Coomassie Brilliant Blue G250 in 75 mL acetic acid plus 500 mL ethanol, filled up to 1 L with dH_2O) for 30 min on a lab rocker. To remove excess dye, the gel was incubated in destaining solution (75 mL acetic acid mixed with 200 mL ethanol, filled up to 1 L with dH_2O) while being placed on a lab rocker again. The destaining step was repeated using fresh solution until the result was satisfactory.

3.11 Z_{basic2}_LmSPase purification and concentration

Purification of Z_{basic2}-tagged LmSPase was achieved employing Fractogel EMD SO_3^- (M) resin purchased from Merck Millipore (Darmstadt, Germany). The resin was washed 3x with dH_2O and 1x with 50 mM KH_2PO_4 pH 7.0 using a Schott Duran 3 filter. Filtration was sped up with a water-jet vacuum pump. The resin was weighed when containing residual moisture. An appropriate dilution of the Z_{basic2}_LmSPase crude extract was incubated with a suitable amount of carrier in a lab rotator at 20 rpm and room temperature for 30 min. Afterwards the carrier was washed for 30-45 min at room temperature with 50 mM KH_2PO_4 pH 7.0 three times, whereas in the last step 100 mM NaCl were supplemented. Activity in the supernatant was determined after each washing step. The bound enzyme was eluted from the carrier using 50 mM KH_2PO_4 pH 7.0 containing 2 M NaCl and subsequently activity was measured.

For enhancing the volumetric activity the solution containing purified Z_{basic2}_LmSPase was concentrated employing Vivaspin 2 tubes from Sartorius Stedim (Göttingen, Germany). The tubes were washed with dH_2O twice at 4000 rpm in a benchtop centrifuge. 1 mL of the Z_{basic2}_LmSPase solution was transferred to the tubes, followed by centrifugation at 4000 rpm. After reaching a proper reduction of the volume, the activity of the Z_{basic2}_LmSPase solution was quantified.

3.12 Microflow Imaging (MFI)

In order to identify potential formation of aggregates, Z_{basic2}_LmSPase immobilization mixtures containing 0.25 M NaCl, 0.5% (v/v) Tween 20 and crude extracts prepared during different phases of the experimental course were analyzed employing the ProteinSimple Microflow Imaging system (San Jose, CA, USA) aided by the MFI View System software. At the forefront the measurement chamber was rinsed with 1 mL of 50 mM KH_2PO_4 pH 8.0 and blanking was performed using an immobilization mixture lacking crude extract. For measurement the amount of added Z_{basic2}_LmSPase crude extract was complying with the activity desired for conduct of an immobilization experiment.

3.13 Confocal laser scanning microscopy (CLSM)

Z_{basic2}_TvDAAO immobilized on the walls of the microreactor channel was visualized by detecting the autofluorescence of its cofactor $FAD_{oxidized}$ via CLSM. Leica DM5500Q microscope system (Mannheim, Germany) was used in combination with the Leica Application Suite Advanced Fluorescence (version 3.2.1.9702). The spectra of FAD show absorption and emission maxima at 450 nm and 530 nm, respectively (37). As the CLSM system on hand did not feature a laser exhibiting a wavelength closer to the absorption maximum, fluorescence was induced at 405 nm, while the emitted light was gathered in the range of 480-650 nm. A 20x/0.5 water immersion objective and a 40x/1.15 oil immersion objective were used for detection of fluorescence in the microreactor channel or on microscopy slides, respectively. Bright field images were acquired using a Leica DFC360FX CCD camera connected to the CLSM system. The microreactor chip was filled with 20 mM KH_2PO_4 pH 7.0 during CLSM imaging.

4 Results and discussion

4.1 Immobilization of Z_{basic2}_LmSPase

4.1.1 Calculation of ideal loading

Having regard to the dimensions provided in the technical drawing (29), the surface of the microreactor channel was calculated to be 374.25 mm². The enzyme footprints and ideal loadings considering the different estimation models are shown in Table 2.

Table 2: Calculated footprints and ideal loading capacities

	Footprint (nm^2)	Quantity (mol/microreactor)	Mass (µg/microreactor)	Total activity (U/microreactor)	Volumetric activity (U/mL/microreactor)
Model 1	21.3	2.92×10^{-11}	1.83	2.01×10^{-1}	15.5
Model 2	25.0	2.48×10^{-11}	1.63	1.80×10^{-1}	13.8
Model 3	40.5	1.54×10^{-11}	0.962	1.06×10^{-1}	8.15

Since model 3 is more closely related to the experimentally found dimensions of the enzyme, it was regarded to meet the realistic situations better than the other models. Therefore the volumetric activity of 8.15 U/mL was chosen as the lower limit for the prepared immobilization mixes. When assuming the desired formation of a monolayer during the immobilization process, this volumetric activity is corresponding to an ideal loading of 106 mU of Z_{basic2}_LmSPase.

It should be noted here that the calculation was based on the assumption that the channel walls are absolutely smooth. Thus, the actually available surface might be higher than calculated. According to additional data provided by the manufacturer, the surface area was specified with 0.024 m^2, which exceeds the calculated value by a factor of ~64. Although this large discrepancy might be a basis for discussion, the high surface roughness of Ra=2.45 µm will contribute to an enhancement of the area. The concentration of silanols on the purchased chip without further modification (like the used pretreatment or the functionalization with sulfonate groups) was stated to be 5×10^{14} cm^{-2} (data from manufacturer).

4.1.2 Calibration for continuous and discontinuous coupled assay

In order to determine the linear range of the continuous and discontinuous coupled assay, the discontinuous assay was performed adding several dilutions of a 0.3 mM G1P solution instead of samples.
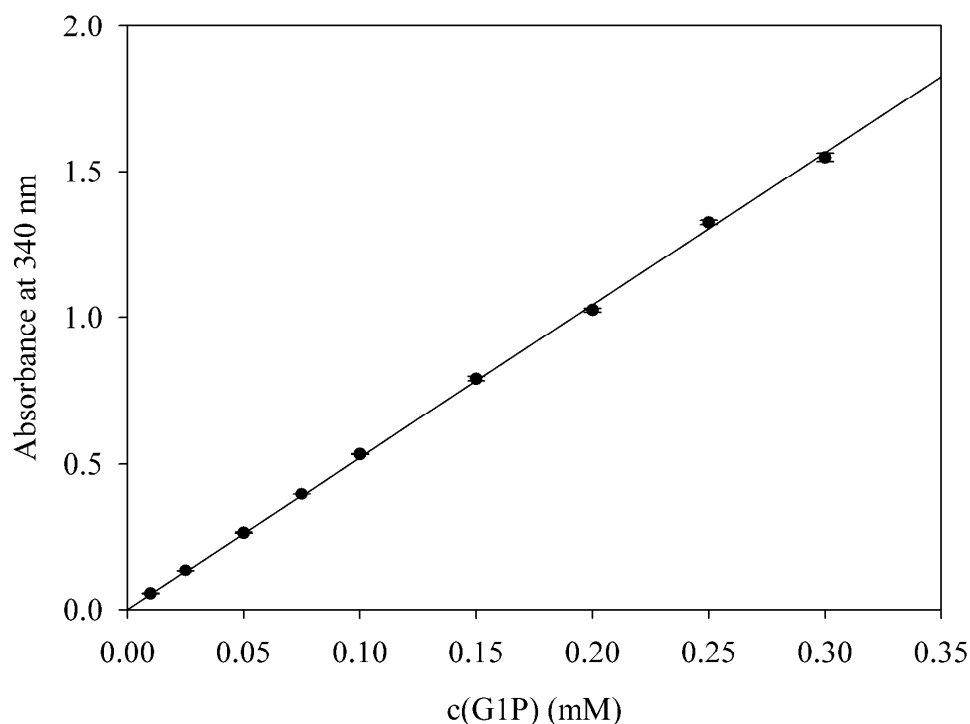
Figure 2: Calibration for G1P concentrations ranging from 10 to 300 μM

As shown in Figure 2, the linear range extends over the whole range of applied G1P concentrations up to an absorbance of higher than 1.5. The slope is equating to the extinction coefficient ε which according to that exhibits a value of 5.216 mM^{-1}cm^{-1}.

4.1.3 Expression level of Z$_{basic2}$_*Lm*SPase and selectivity of immobilization

To evaluate the expression of recombinant Z$_{basic2}$_*Lm*SPase, crude extracts were separated via SDS-PAGE. Furthermore, Z$_{basic2}$_*Lm*SPase immobilized in the microreactor was eluted and the thereby obtained fraction was also loaded onto the SDS gel to examine whether the immobilization strategy is selective for enzymes fused with the Z$_{basic2}$ linker peptide (Figure 3). Because they showed the highest activity when being assayed, the respective first elution fractions of 3 different immobilization experiments were chosen for separation.
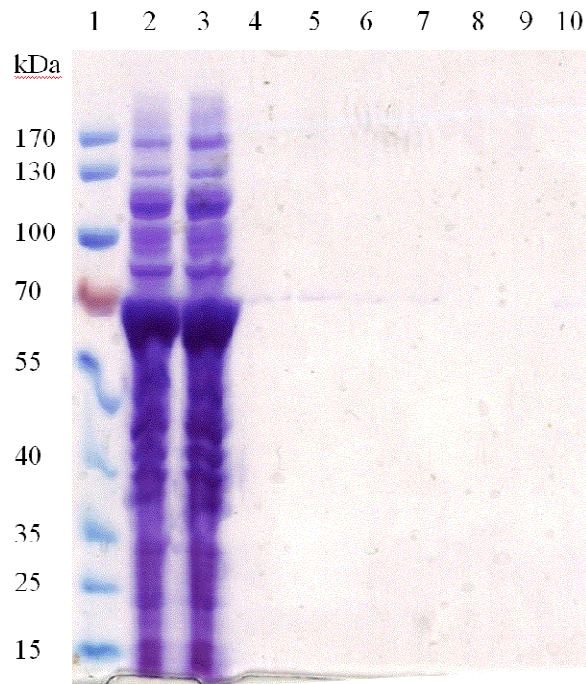
Figure 3: SDS-PAGE for assessing the expression level of Z_{basic2}_LmSPase and the selectivity of the immobilization

Lane 1: PageRuler Prestained Protein Ladder; Lane 2: Z_{basic2}_LmSPase crude extract 1A; Lane 3: Z_{basic2}_LmSPase crude extract 1B; Lane 4: empty; Lane 5: elution fraction of immobilization experiment 2; Lane 6: empty; Lane 7: elution fraction of immobilization experiment 3; Lanes 8 and 9: empty; Lane 10: elution fraction of immobilization experiment 4

Lanes 2 and 3 both show a prominent band between 55 and 70 kDa which is remarkably stronger than the remaining bands. As the estimated size of Z_{basic2}_LmSPase is around 63 kDa, this indicates that the protein of interest is intensely overexpressed. Faint bands of approximately the same size can be seen on the lanes 4, 5, 6, 7 and 10. This faintness is not surprising, as the anticipated protein quantity correlating with the activity seen in the elution fractions was generally very low. However, as the lanes were lacking bands of any other size, this might be an indication that the immobilization method is selective for molecules featuring the Z_{basic2} linker. Unexpected is the presence of bands on the lanes 4 and 6, were no sample was loaded, suggesting that samples loaded on the lanes 5 and 7 were partially relocated to the empty lanes. This might be a result of the very high NaCl concentration, since the respective first elution fractions were obtained by application of 2 M NaCl (as well as 0.5% Tween 20). In order to evaluate the usefulness of the Z_{basic2} peptide for direct purification and immobilization, the sensitivity of the employed protein determination method has to be increased. An immediate approach might be to use a more sensitive staining method when performing SDS-PAGE. Quantification of the eluted enzyme might be enabled by application of standards (e.g. containing BSA).

As the bands of the ladder on lane 1 were distorted in the range from 55 to 35 kDa (an effect also seen for the non-shown samples left to the ladder), crude extracts were separated again (Figure 4). The destaining process of the SDS-Gel was prolonged by an additional incubation in dH_2O overnight. The crude extracts used herein were originating from cells cultivated in different shaking flasks and the interval between the respective disruptions was 3 months, whereas crude extract 2 was the fresher one.
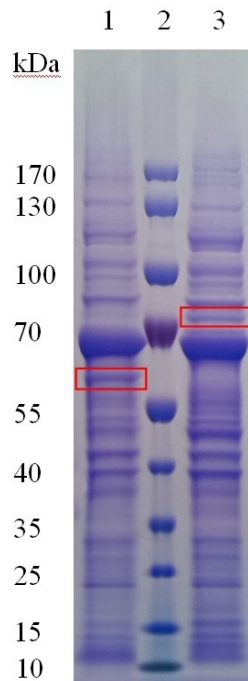
Figure 4: SDS-PAGE for assessing the expression level of Z$_{basic2}$_*Lm*SPase in crude extracts

Lane 1: Z$_{basic2}$_*Lm*SPase crude extract 1B; Lane 2: PageRuler Prestained Protein Ladder; Lane 3: Z$_{basic2}$_*Lm*SPase crude extract 2

Again the bold bands at approximately 63 kDa can be observed, strengthening the assumption that Z$_{basic2}$_*Lm*SPase is intensively expressed. The banding patterns are largely comparable with generally only small differences in intensity, with the exception of a band with a size just above 70 kDa which is present in lane 3 (crude extract 2), but can be barely seen on lane 1 (crude extract 1). In contrast lane 1 shows a band between 55 and 70 kDa which is completely missing on lane 3. Whether this differences are manifestations of actually distinct expression patterns or are a result of proteolytic / aggregation processes, was not further studied within this thesis in view of the presumption that the immobilization itself should not be affected by small disparities regarding the protein composition of the crude extract.

4.1.4 Immobilization without pretreatment

Preceding studies dealing with the immobilization of Z_{basic2}_TvDAAO in an identical microreactor setup showed that the amount of immobilized enzyme could be considerably enhanced when applying a pretreatment procedure as described in 3.7.2 (33). When deploying Z_{basic2}_LmSPase, initial experiments (denoted as B1-B5 in Figure 5) were lacking a pretreatment in order to examine whether this beneficial effect can also be observed for this monomeric enzyme. Also based on the results presented in (13, 33), an incubation time of 1.5 h was chosen for the immobilization. The crude extract used for preparation of the immobilization mixtures showed an activity of 436-573 U/mL and a protein content of 17.1 mg/mL, determined with the assays presented in 3.4.1 and 3.6, respectively.

For evaluation of the immobilization efficacy, the immobilization balance showing the total activities entering and leaving the system was prepared (Figure 5).
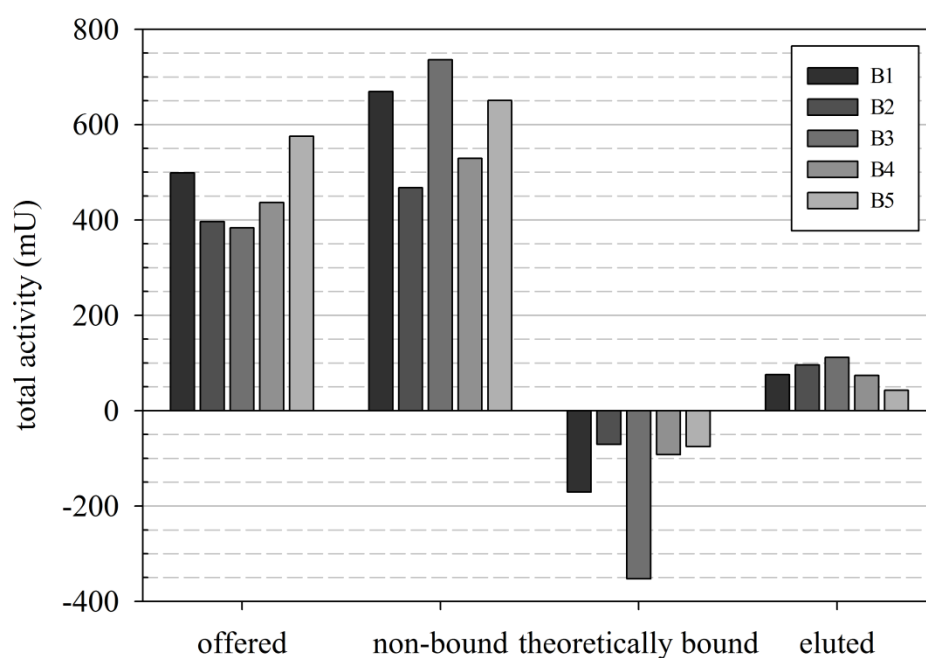
Figure 5: Immobilization balances for experiments without pretreatment

B1-B5: experiments without pretreatment of the microreactor;
offered total activity is referring to total enzymatic activity provided to the whole volume of the microreactor and all connected capillaries and was 3.6-5.4 fold higher than the ideal loading; non-bound activity was determined after washing the microreactor with 50 mM KH_2PO_4 pH 7.0 subsequent to the immobilization step; theoretically bound activity was calculated by subtracting non-bound from offered activity; eluted activity is the total activity which was detected in the elution fractions

It can be concluded from the balance that the immobilization failed in all cases, as the non-bound activity was higher than the offered activity in each experiment. In B3 the non-bound activity was almost twice as high which also implies errors during activity measurement. In the other experiments non-bound activity was in the range from 113 to 134% of the offered activity. As a direct result the theoretically bound activities – which are solely calculated values – are certainly negative.

Despite the findings indicating apparently failed immobilization, activity could be found in the eluted fractions. Having in mind again that the ideal loading was calculated to be 106 mU (according to Table 2 in 4.1.1), the observed values were in an appealing order of magnitude considering this early stage of experiments.

For determination of the apparent immobilized activity a substrate solution composed of 1.1 M sucrose in the test buffer also used in the continuous coupled assay (see 3.4.1) was passed through the microreactor applying various flows. The observed values are summarized in Table 3.

Table 3: Apparent total activities immobilized in the microreactor without pretreatment

F (in µL/min)	apparent total activity (in mU)				
	B1	B2	B3	B4	B5
5	-	**30.6**	-	-	-
10	**48.5**	-	**57.6**	*59.2*	**62.2**
25	*38.9*	*24.2*	42.4	**73.5**	-
50	34.9	22.9	*46*	49.8	-

The bold values are the initial activities which were determined first in the respective experiment. Values in italics are associated with the respective second flow applied, whereas non-bold/non-italic values are the activities observed for the remaining flow. Remembering the ideal loading of 106 mU the initial values were promising – although in need of improvement – but showed large deviations ranging from 30.6 to 73.5 mU. In comparison with the values of the detached enzyme after subsequent elution, the bound values were lower in any case, suggesting that the immobilization affects the activity of Z_{basic2}_LmSPase.

It can also be perceived that for each experiment the apparent activity is decreasing along the sequence of applied flows. After performing B1 to B3 this was interpreted to be an indication for a flow-dependency of the apparent activity, an impression which was questioned when obtaining the data from B4. In order to investigate whether activity is also dropping without

flow variations, experiment B5 was conducted, where flow was kept constant and samples were taken spread over 3 days. The course of the apparent activity is depicted in Figure 6. Plainly visible is the fast declination on the first day, reducing the activity to less than a quarter of its initial value.
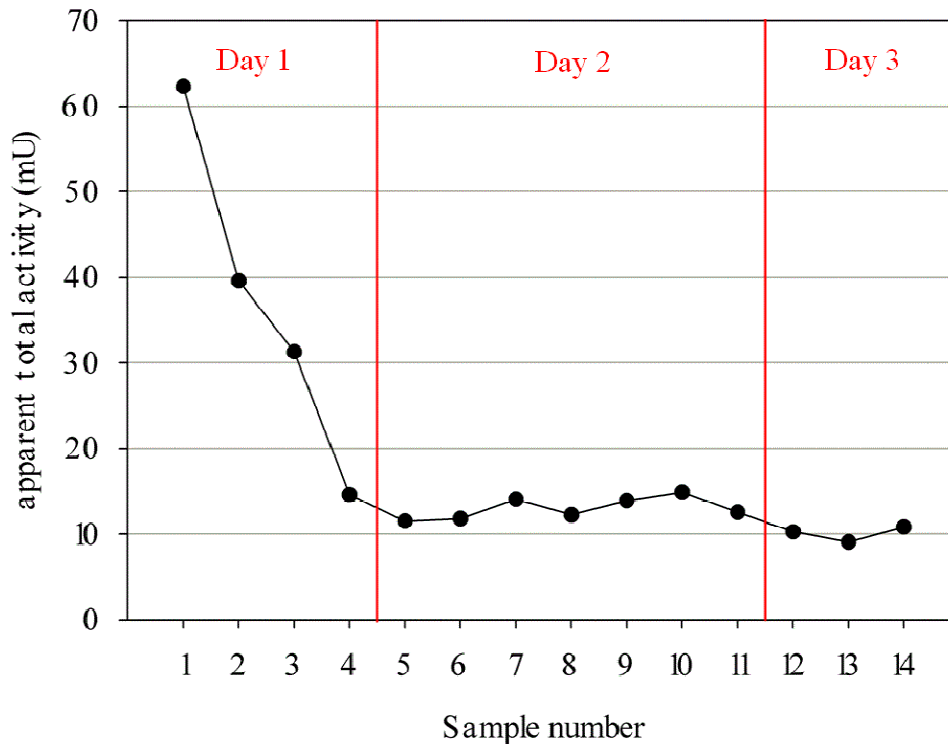
Figure 6: Course of apparent activity during experiment B5

After this pronounced initial reduction the activity is fairly stable during the remaining period under observation. This is particularly interesting as there were 2 days of storage between day 2 and day 3. Between the measurement phases the loaded microreactor was filled with 50 mM KH_2PO_4 and stored at 4 °C.

As soluble *Lm*SPase is generally quite stable under the applied reaction conditions (T=22 °C, pH 7.0) as presented in (20) and under storage conditions (T=22 °C, in phosphate buffer at pH 7.0 and pH 8.0), as verified in a control experiment (see Appendix), the initial decrease is not regarded as a result of inactivation, but rather a consequence of weak adsorption to the microreactor surface and therefore washout. Since the microreactor was reused, a pretreatment for removing residues from preceding immobilizations and (re-)activation of the surface was not only considered an opportunity for ensuring reproducibility of immobilization, but also for increasing the strength of adsorption and therefore stability.

4.1.5 Immobilization with pretreatment

Crude extracts exhibiting a volumetric activity of 270-899 U/mL and protein contents in the range of 14.6-32.0 mg/mL were employed for preparation of the immobilization mixes. When using purified enzyme, the available solution showed a activity of 149 U/mL and a protein content of 1.04 mg/mL (see also 6.1.2). Apart from that, the immobilization conditions were kept the same as described for the experiments without pretreatment.

First means to evaluate the benefit of the pretreatment was the construction of an immobilization balance. Figure 7 shows a selection of experiments, where either incubation with MeOH/HCl (M1), with 1 M NaOH (N1, P1, LS1) or a combination of both (SLS2) was applied. At first glance it is conspicuous that the balances were improved, as the non-bound activities are not exceeding the offered amounts.
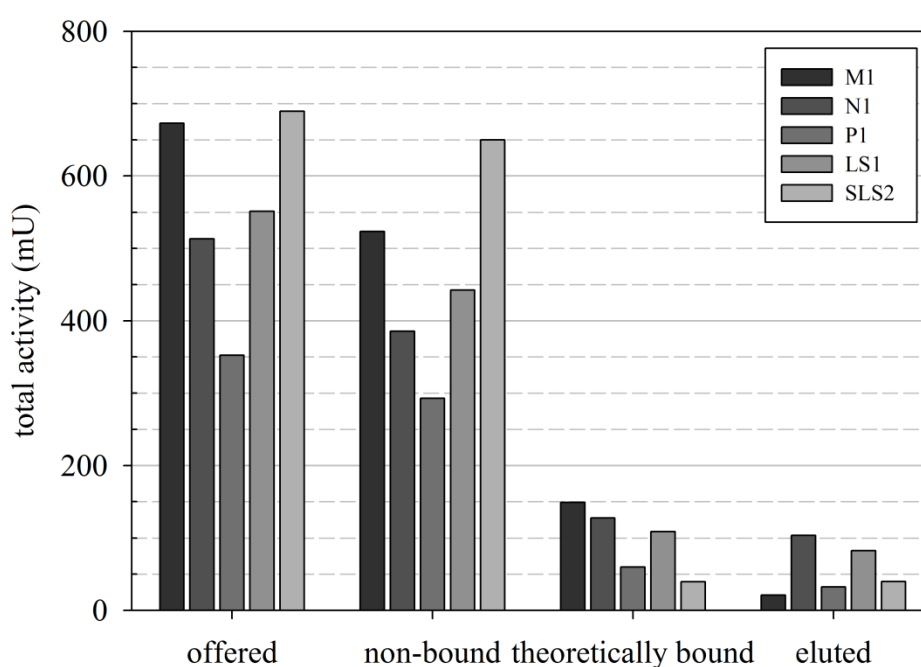
Figure 7: Immobilization balances for experiments without pretreatment

M1: incubation with MeOH/HCl (1:1) for 30 min; N1: incubation with 1M NaOH for 20 min; P1: like N1 using purified enzyme; LS1: like N1 using deviating substrate mix during operation; SLS2: sequence of both incubation steps, using deviating substrate mix during operation;
offered total activity is referring to total enzymatic activity provided to the whole volume of the microreactor and all connected capillaries and was 3.3-6.5 fold higher than the ideal loading; non-bound activity was determined after washing the microreactor with 50 mM KH_2PO_4 pH 7.0 subsequent to the immobilization step; theoretically bound activity was calculated by subtracting non-bound from offered activity; eluted activity is the total activity which was detected in the elution fractions

Each of the pretreatment strategies were found to decrease the quantity of non-bound enzyme, even when only one of them was employed. Nevertheless the sequence of both treatments was

considered reasonable for removal of contaminants, since they are complementing each other. Incubation with the MeOH/HCl mixture establishes highly acidic conditions involving protonation of the surface, while MeOH assists by affecting hydrophobic interactions of any biomolecule with the surface. Subsequent exposure to NaOH causes deprotonation of the surface resulting in the repulsion of anionic compounds. When comparing the theoretically bound with the eluted activity, it is plainly visible that the latter is generally lower – especially when viewing the values for M1. One explanation for this is that the pretreatment was beneficial for the immobilization process *per se*, but apparently did not show the desired effect on the stability – a situation raising doubts on the significance of eluted activity values. For evaluation the activity was monitored over the time of operation and the initial drop already seen in the experiments without pretreatment (Figure 6 in 4.1.4) could be observed again, followed by a phase of decelerated declination. During M1 the enzyme was eluted at a later stage, thus resulting in a lower eluted activity.

Contrary to expectations, deployment of purified $Z_{basic2\_}Lm$SPase (in P1) did not result in a noticeable improvement. According to Figure 7, the non-bound fraction seems to be slightly higher in SLS2, resulting in a lower value for the theoretically bound activity. Nevertheless the initial apparent immobilized activity found for this experiment was higher than anticipated, as shown in the following section.

4.1.6 Performance of immobilized $Z_{basic2\_}Lm$SPase

As for the experiments without pretreatment, the applied substrate solution for determination of the immobilized activity in the initial experiments was composed of 1.1 M sucrose in the test buffer also used in the continuous coupled assay (see 3.4.1). In contrast to B5, the microreactor setup was also operating overnight without relocation to a cooled environment for storage. To increase the possible G1P formation and to minimize the risk of favoring washout of the bound enzyme due to low binding forces, applied flow was kept in a low range (F≤10 µL/min). The activity courses for the experiments M1 (pretreatment with MeOH/HCl), N1 (pretreatment with NaOH) and P1 (use of purified $Z_{basic2\_}Lm$SPase) are displayed in Figure 8. Pretreatment with NaOH solely resulted in higher initial loading compared to pretreatment with MeOH/HCl, but this effect rapidly became negligible due to the fast initial decrease. After just 2 hours the respective activities were halved and activity kept decreasing. Use of purified enzyme also did not improve the stability. Initial activity was even lower

compared to M1 and N1, and the initial decrease was less pronounced, but after 4 hours the course was rather similar.
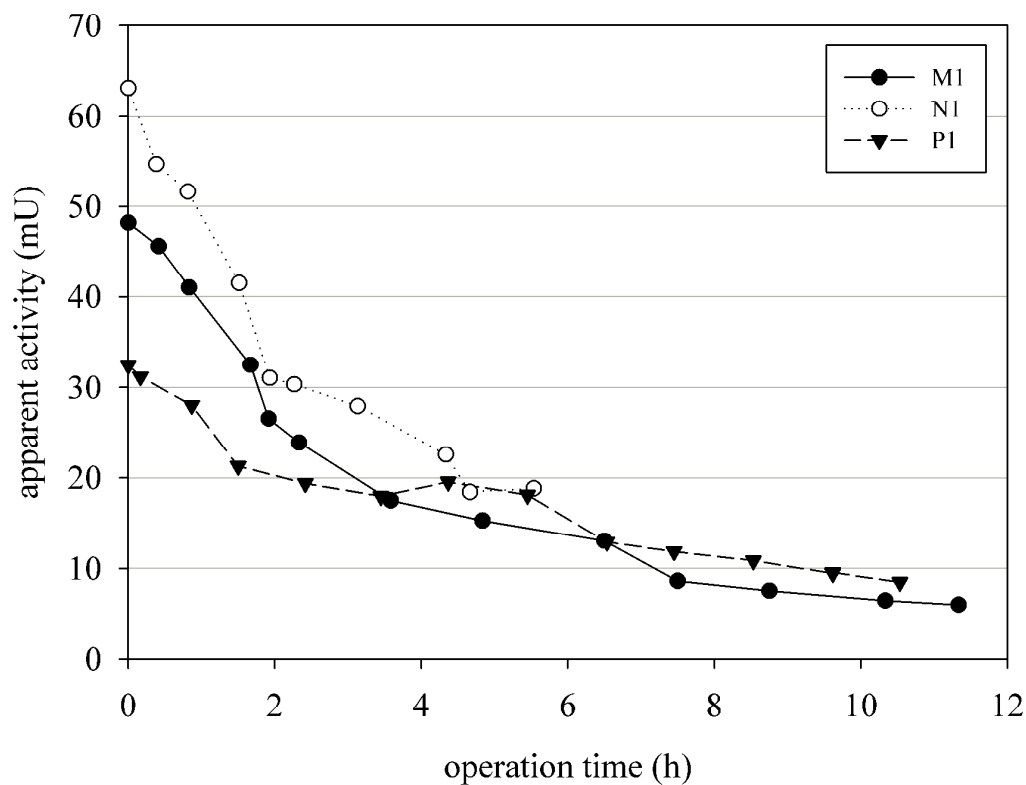
Figure 8: Stability of immobilized Z_{basic2}_LmSPase when introducing pretreatment/purified enzyme

M1: pretreatment with MeOH/HCl (1:1); N1: pretreatment with 1 M NaOH; P1: pretreatment with 1 M NaOH and use of purified Z_{basic2}_LmSPase

Aiming at the improvement of stability, the substrate mix composition and the reaction conditions were altered later on. A summary of all the parameters is shown in Table 4.

Table 4: Summary of studied parameters for increasing the stability of apparent *Lm*SPase activity

Experiment	Immobilization		Operation				Short description of main alterations
	Buffer	pH	$c_{sucrose}$ (mM)	Buffer	pH	F (µL/min)	
M1	50mM KH$_2$PO$_4$	8	1100	test buffer*	7	8	pretreatment with MeOH/HCl
N1	50mM KH$_2$PO$_4$	8	1100	test buffer*	7	10	pretreatment with NaOH
P1	50mM KH$_2$PO$_4$	8	1100	test buffer*	7	10	use of purified SPase
LS1	50mM KH$_2$PO$_4$	8	1100	50mM KH$_2$PO$_4$	7	10	decrease of ion concentration in substrate mix (90->50 mM)
LS2	50mM KH$_2$PO$_4$	8	1100	50mM KH$_2$PO$_4$	7	2	like LS1 applying lower flow
LS2_2	50mM KH$_2$PO$_4$	8	1100	50mM KH$_2$PO$_4$	7	2	like LS1 applying lower flow (repetition)
OLS1	50mM KH$_2$PO$_4$	8	1100	50mM KH$_2$PO$_4$	7	5	overloading experiment; substrate mix as in LS1
OLS2	50mM KH$_2$PO$_4$	8	1100	50mM KH$_2$PO$_4$/K$_2$HPO$_4$	8	5	like OLS1 lacking Na-ions in the substrate mix, pH 8 during operation
OLS2_2	50mM KH$_2$PO$_4$/K$_2$HPO$_4$	8	1100	50mM KH$_2$PO$_4$/K$_2$HPO$_4$	8	5	like OLS2 with Na-ions strongly reduced in the immobilization mix
SLS1	50mM KH$_2$PO$_4$/K$_2$HPO$_4$	8	50	50mM KH$_2$PO$_4$/K$_2$HPO$_4$	7	5	lowered sucrose concentration in the substrate mix; lacking Na-ions in the immobilization and substrate mix
SLS2	50mM KH$_2$PO$_4$	8	50 (switch to 1100 after 43 h)	50mM KH$_2$PO$_4$	7	5/2	lowered sucrose concentration in the substrate mix
SLS2_2	50mM KH$_2$PO$_4$	8	50	50mM KH$_2$PO$_4$	7	5	lowered sucrose concentration in the substrate mix (repetition)
SLS2_3	50mM KH$_2$PO$_4$	8	50	50mM KH$_2$PO$_4$	7	5	lowered sucrose concentration in the substrate mix (repetition)
SLS2_4	50mM KH$_2$PO$_4$	8	50	50mM KH$_2$PO$_4$	7	5	lowered sucrose concentration in the substrate mix (repetition)
SLS2_5	50mM KH$_2$PO$_4$	8	50	50mM KH$_2$PO$_4$	7	5	lowered sucrose concentration in the substrate mix (repetition)
SLS2_6	50mM KH$_2$PO$_4$	8	50	50mM KH$_2$PO$_4$	7	5	lowered sucrose concentration in the substrate mix (repetition)
SLS3	50mM KH$_2$PO$_4$	8	50	50mM KH$_2$PO$_4$	8	5	lowered sucrose concentration in the substrate mix (repetition), pH 8 during operation
NSLS1	50mM KH$_2$PO$_4$	8	50	50mM NaH$_2$PO$_4$	7	5	lowered sucrose concentration in the substrate mix, only Na-ions in the substrate mix
FSLS1	50mM KH$_2$PO$_4$	7	50	50mM KH$_2$PO$_4$	7	5	lowered sucrose concentration in the substrate mix, functionalized plate
FSLS1_2	50mM KH$_2$PO$_4$	7	50	50mM KH$_2$PO$_4$	7	5	lowered sucrose concentration in the substrate mix, functionalized plate (repetition)

* 50 mM KH$_2$PO$_4$, 10 mM MgCl$_2$, 10 mM EDTA (as sodium salt), 5 µM glucose-1,6-biphosphate

Up to this point the substrate sucrose was prepared in test buffer which besides KH_2PO_4 also included $MgCl_2$ and EDTA (as described in 3.4.1 and Table 4). In order to decrease the concentration of present ions and to avoid a possible interference of these constituents, the reaction mixture was simplified to 1.1 M sucrose in 50 mM KH_2PO_4 and – as shown for experiment LS1 in Figure 9 – stability could be enhanced. A distinct initial decrease followed by a more stable phase could again be observed (compare Figure 6 in 4.1.4), suggesting that a particular fraction of enzyme was bound more weakly and is detached and washed off during the first hours of operation. LS1 was performed at an operational flow of 10 µL/min. When reducing the flow to 2 µL/min (LS2 and its repeat experiment LS2_2), the activity curiously showed a dramatic decrease within the first hours of operation.
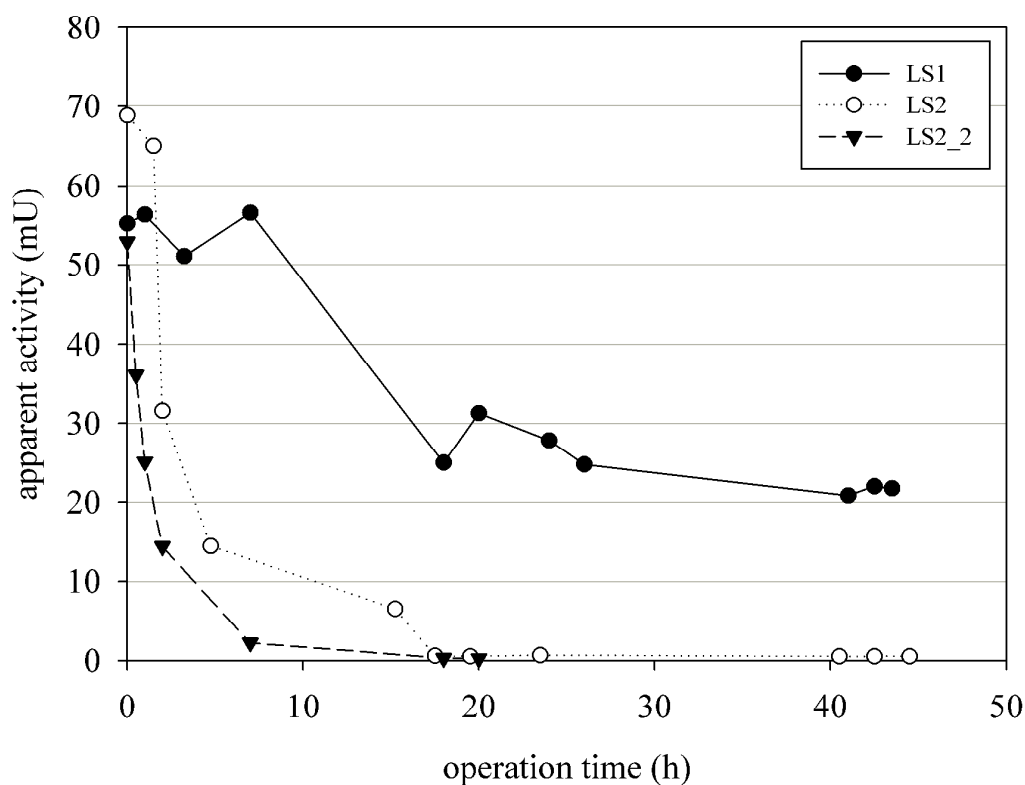
Figure 9: Stability of immobilized Z_{basic2}_LmSPase when decreasing ion concentration in substrate mix

LS1: F=10 µL/min; LS2 and LS2_2: F=2 µL/min

This behavior was considered to be a result of low adsorption strength which becomes particularly unfavorable if loading is inefficient, but can potentially be overcome by promotion of the binding by application of high enzyme concentrations. With the aim to achieve saturation of the channel surface, immobilization mixes offering a total activity

28-39 times higher than needed (according to the calculated ideal loading) were employed. A lower flow (implying a higher residence time) also corresponds with a higher G1P and D-fructose formation, whereby the latter is a reducing sugar which might interfere with the adsorption via Z_{basic2} tag. To diminish this risk while still enhancing the G1P production, the operating flow was set to 5 µL/min in the vast majority of the subsequent experiments deploying Z_{basic2}_LmSPase. Viewing the courses shown in Figure 10, it can be perceived that the course of OLS1 is resembling the course of LS1 (Figure 9), especially in the interval starting at 18h of operation until the end of the experiment. In contrast to expectations, the initial activity and stability were not enhanced.
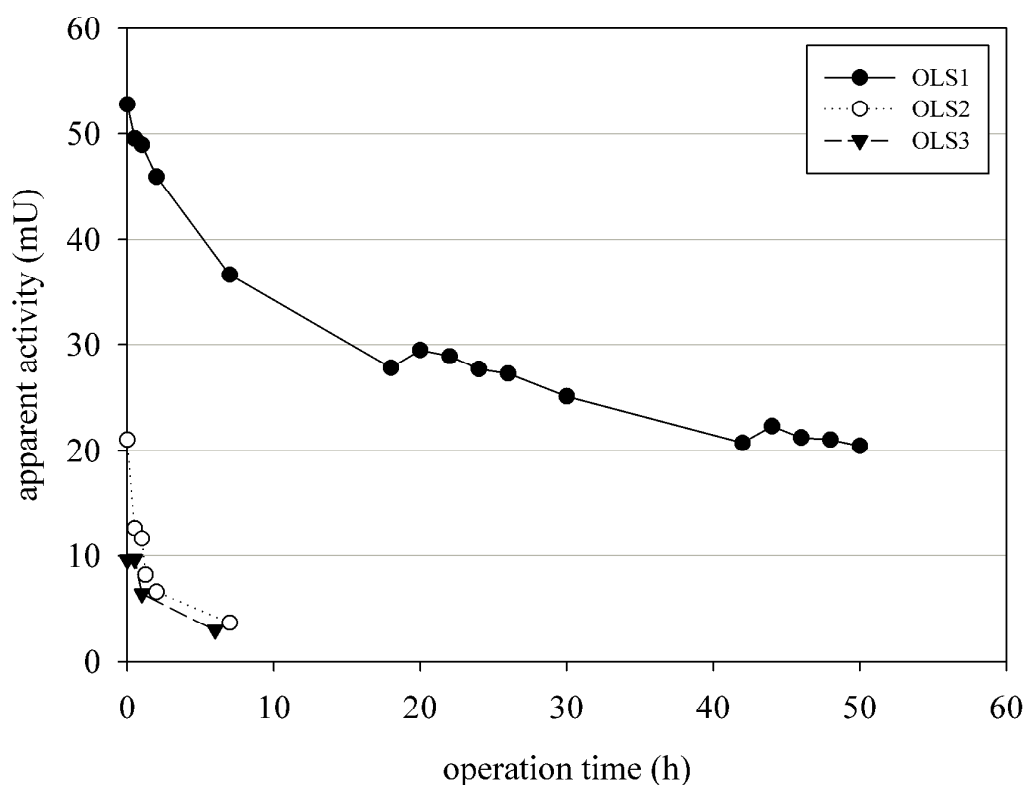
Figure 10: Stability of immobilized Z_{basic2}_LmSPase for "overloading" experiments

OLS1: F=5 µL/min, pH7.0; OLS2: F=5 µL/min, pH8.0, substrate mix lacking Na⁺ ions; OLS3: like OLS2 with additionally strongly reduced sodium concentration in immobilization mix

In OLS2 the overloading approach was combined with the removal of sodium ions (which are introduced when adjusting the pH of the 50 mM KH_2PO_4 buffer solution using NaOH) from the substrate mix and the increase of pH to 8.0. Sodium and potassium possess the same charge, but as the ion radius of sodium is smaller (38), its potential for binding to the silanol groups of the glass surface and thereby replacing the positive charges of the arginine side

chains of the Z_{basic2} linker peptide is considered higher. pH value was increased in order to extend deprotonation of the surface silanol groups. Impairment of enzymatic activity due to the higher pH could be excluded (for the period of observation) after a control experiment comparing activity of soluble Z_{basic2}_LmSPase incubated at pH 7.0 and pH 8.0 (see 6.1.1). Surprisingly this measure resulted in lower initial activity and stability. In a third overloading experiment, the immobilization mix was blended using 50 mM KH_2PO_4/K_2HPO_4 pH 8.0, too. However, it has to be noted that the available crude extract was prepared in 50 mM KH_2PO_4 (adjusted with NaOH according to the standard cell disruption method). Hence, the sodium concentration in the immobilization mix was not zero, but as the required volume of crude extract to gain the desired activity was very low (generally 1/75 of total mix volume), it was at least strongly reduced. Nevertheless the course was similar to OLS and offering Z_{basic2}_LmSPase in tremendous excess was again not beneficial.

Sucrose in a concentration higher than 30% (w/v) (complying with approximately 876 mM) was found to inhibit LmSPase (39). Up to and including OLS3 the substrate mix included 1.1 M sucrose, a value which showed a small but yet non-negligible effect on the activity. Since the second substrate phosphate (present as potassium phosphate) was limited to 50 mM, sucrose was also reduced to this concentration. Figure 11 shows the courses of activity after this further modification of the substrate mix. SLS1 was conducted lacking sodium ions as with OLS3, but with pH restored to 7.0, while in SLS3 the conventional buffer (50 mM KH_2PO_4) was used at pH 8.0. Both variations resulted in low activity and stability, closely resembling OLS2 and OLS3. When performing the reaction at pH 7.0 (SLS2), the initial activity was comparable to LS1 and OLS1. The initial drop was less pronounced and the apparent activity was observed to be stable at 31-34 mU in the period of 7 to 28 h after starting continuous operation. After 23 h of operation the flow was reduced to 2 µL/min to investigate whether stability is again affected as observed in experiment LS2. Surprisingly the activity was stable for the following 5 h and was only slightly reduced to 25 mU after 43 h. After 44 h the flow was restored to 5 µL/min while again introducing a substrate mix containing 1.1 m sucrose in order to assess its effect. As a result, apparent activity was decreasing from 19 to 11 mU in only 5 h. This development was supporting the premise that lowering the sucrose concentration might be beneficial for the stability.

In a subsequent experiment the substrate mix was prepared using Na_2HPO_4 (NSLS1) while maintaining the remaining parameters. The initial activity was lower than in SLS2 and

decreased steadily, resulting in a value of 17 mU after 23 h, which is approximately half of the value found in SLS2 at this respective point in time.
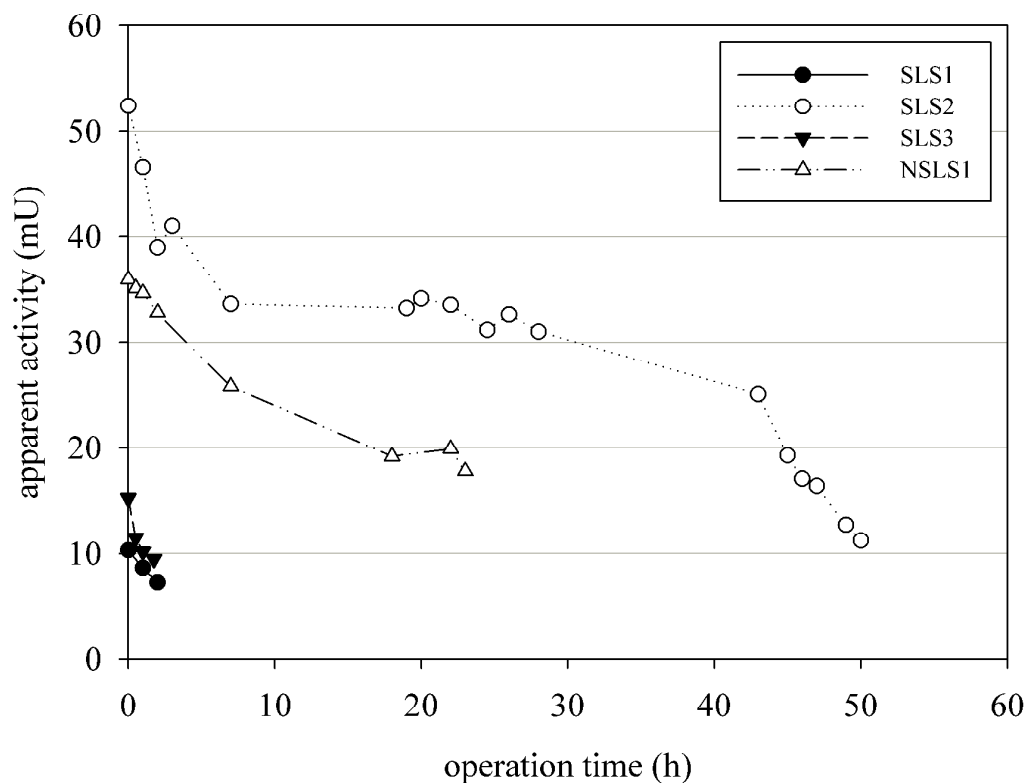
Figure 11: Stability of immobilized Z_{basic2}_LmSPase after reducing sucrose concentration

SLS1: F=5 µL/min, pH7.0, substrate mix lacking Na^+ ions; SLS2: F=5 and 2 µL/min, pH7.0, conventional buffer (50 mM KH_2PO_4); SLS3: like SLS2, but operation at pH8.0; NSLS1: like SLS2, but using 50 mM NaH_2PO_4 in the substrate mix

Although the performance seen during SLS2 was the most favorable in the series of experiments, attempts to reproduce the results failed. As shown in Figure 12, initial activity and stability were worsening over the five repeat experiments SLS2_2 to SLS2_6.
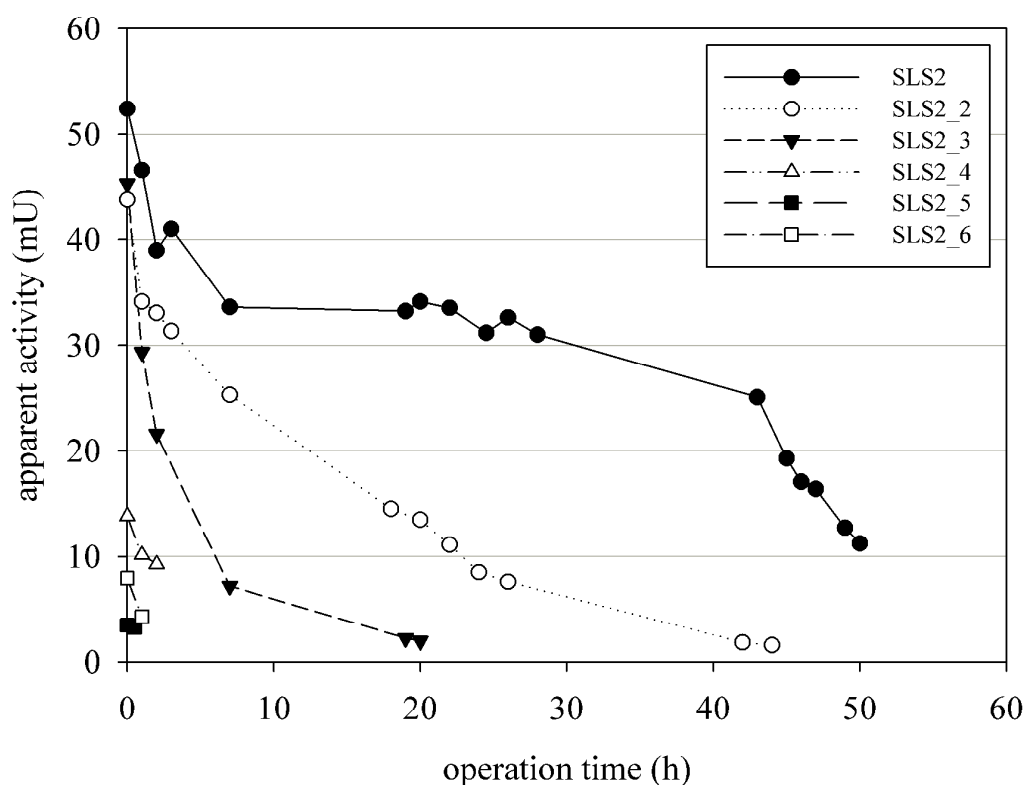
Figure 12: Stability of immobilized Z$_{basic2}$_*Lm*SPase in repeat experiments of SLS2

SLS2_x: F=5 µL/min, pH7, conventional buffer (50 mM KH$_2$PO$_4$)

Both usage of a fresh microreactor plate and preparation of fresh crude extract did not allow for a successful replication. Finally it had to be concluded that although progress was achieved regarding the operational stabilization, the immobilization process itself is controlled by a factor (or several factors) which are not yet identified and understood.

In order to raise the probability of an effective immobilization, a microreactor chip functionalized with sulfonate groups was employed (Figure 13).
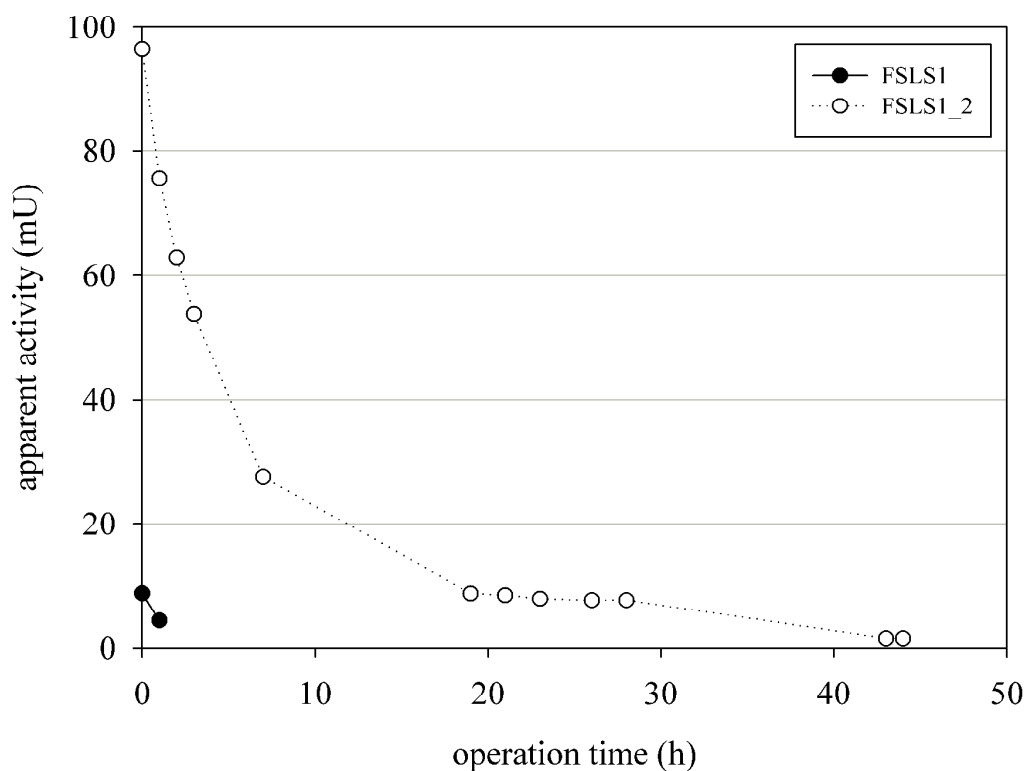
Figure 13: Stability of immobilized Z$_{basic2}$_*Lm*SPase when using a functionalized microreactor

FSLS1 and FSLS1_2: F=5 µL/min, pH7, conventional buffer (50 mM KH$_2$PO$_4$)

First conduct failed and was therefore terminated after only 1 h of operation, but the repetition yielded a higher initial loading (96 mU) than seen in any experiment with a non-functionalized microreactor chip. However, the activity rapidly declined to 8 mU after 19 h and was stable at this value for at least another 10 h. Considering this course it is concluded that the binding affinity is increased when introducing sulfonate groups to the surface, but the immobilization process is still not satisfyingly controllable.

4.1.7 Dependence of G1P formation on residence time

For better comparison of G1P formation, the courses of the experiments showing the best performance (LS1, OLS1, SLS2) were plotted in Figure 14. Excluding a possible limitation of any kind whatsoever, the achievable c(G1P) should be linearly dependent on the residence time. The achievable concentration when considering ideal loading of the microreactor channel (106 mM) and the corresponding space-time yield (STY), as well as the residence times (τ) for the applied flows, are given in Table 5.

Table 5: Residence times, ideal G1P production and STY corresponding with applied flows

F (µL/min)	τ (sec)	$c(G1P)_{ideal}$ (mM)	STY_{ideal} (mM/min)
2	390	53	8.15
5	156	21.2	8.15
10	78	10.6	8.15

As it can be noted in view of Figure 14, c(G1P) indeed shows a linear dependence on the residence time. As mentioned above, the flow was decreased from 5 to 2µL/min after 23 h when conducting SLS2, causing a remarkable increase of c(G1P) from 6.7 to 15.6 mM. The ratio of the two concentrations is 2.33 and thus very close to the ratio of the corresponding residence times of 2.5. During the phase sharing the same flow of 5 µL/min with SLS2 (the first 23 h), the course of OLS1 was similar, but slightly lower, which might be related to the high sucrose concentration as discussed above. In LS1 – where a flow of 10 µL/min was used – the G1P concentration was approximately half of it which was also matching expectations as the residence time was halved.
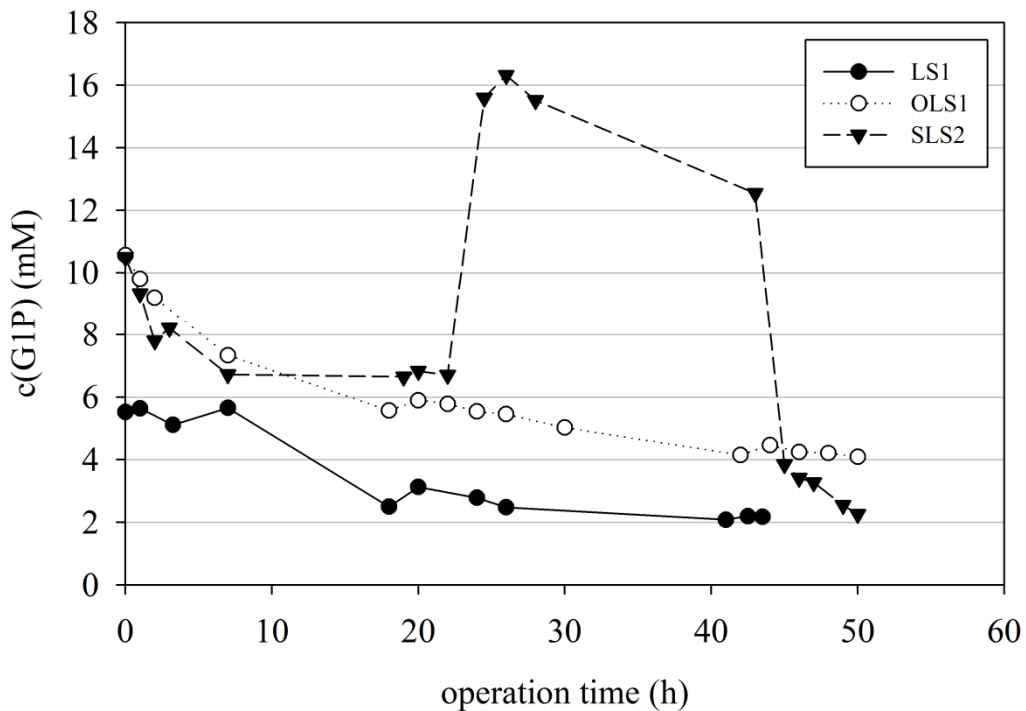
Figure 14: Course of c(G1P) production for selected experiments

LS1: F=10 µL/min, 1.1 M sucrose; OLS1: F=5 µL/min, 1.1 M sucrose; SLS2: F=5 and 2 µL/min, 50 mM sucrose; Substrate mix in all shown experiments was prepared using 50 mM KH_2PO_4, pH 7.0

The average STY's for certain hours of operation are displayed in Table 6. For calculation the phases of operation following the intial decrease were considered.

Table 6: Average STY for LS1, OLS1 and SLS2

Experiment	Operation phase (h)	$STY_{average}$ (mM/min)
LS1	18-43.5	1.98
OLS1	18-50	1.90
SLS2	7-43	2.44

All three experiments showed comparable initial loadings (Table 7), indicating that the immobilization process worked similarly efficient.

Table 7: Apparent initial loadings and operating flows for experiments LS1, OLS1 and SLS2

Experiment	Initial loading (mU)	Applied flow (µL/min)
LS1	55.2	10
OLS1	52.8	5
SLS2	52.4	5+2

Aiming at a more obvious illustration of the linear dependence c(G1P) vs. τ, data of these 3 experiments was gathered and combined in one graph (Figure 15). Respective values after 20 h of continuous operation were chosen, because at that point of time the experiments reached a phase, where activity was quite stable and merely decreasing very slowly. The values for OLS1 and SLS2 at 156 sec (F=5 µL/min) show only a small deviation, while the SLS2 value when switching to τ=390 sec (F=2 µL/min) is completing the relation in the expected manner.
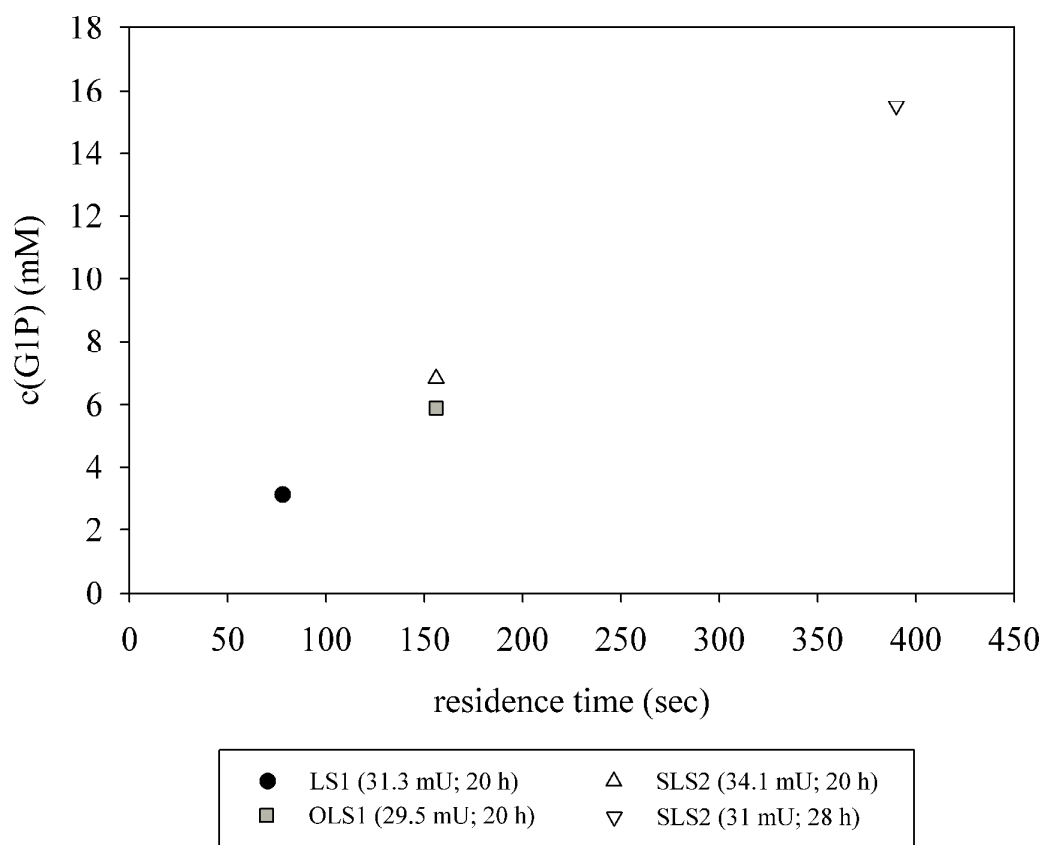
Figure 15: Comparison of c(G1P) obtained at different residence times (summarized from data of immobilization experiments LS1, OLS1 and SLS2)

Values shown in brackets in the legend are signifying the apparent total activity at the corresponding operation time

4.1.8 Stabiliy of soluble Z_{basic2}_LmSPase under elution conditions

To investigate whether activity is impaired under elution conditions, defined activities of soluble enzyme were added to an elution mix and reassessed after certain time intervals (Figure 16). In view of the higher activity it is remarkable that the determined activities were in any case massively exceeding the estimated value of 135.5 mU/mL, indicating an error during preparation of the mixture, when using a crude extract showing very high activity. Regarding the lower value (26.5 mU/mL) the preparation was working slightly better. However, no decrease was noted for the given period of time, which suggests that the enzyme is not affected by the presence of NaCl and the detergent Tween 20 in their respective concentrations.
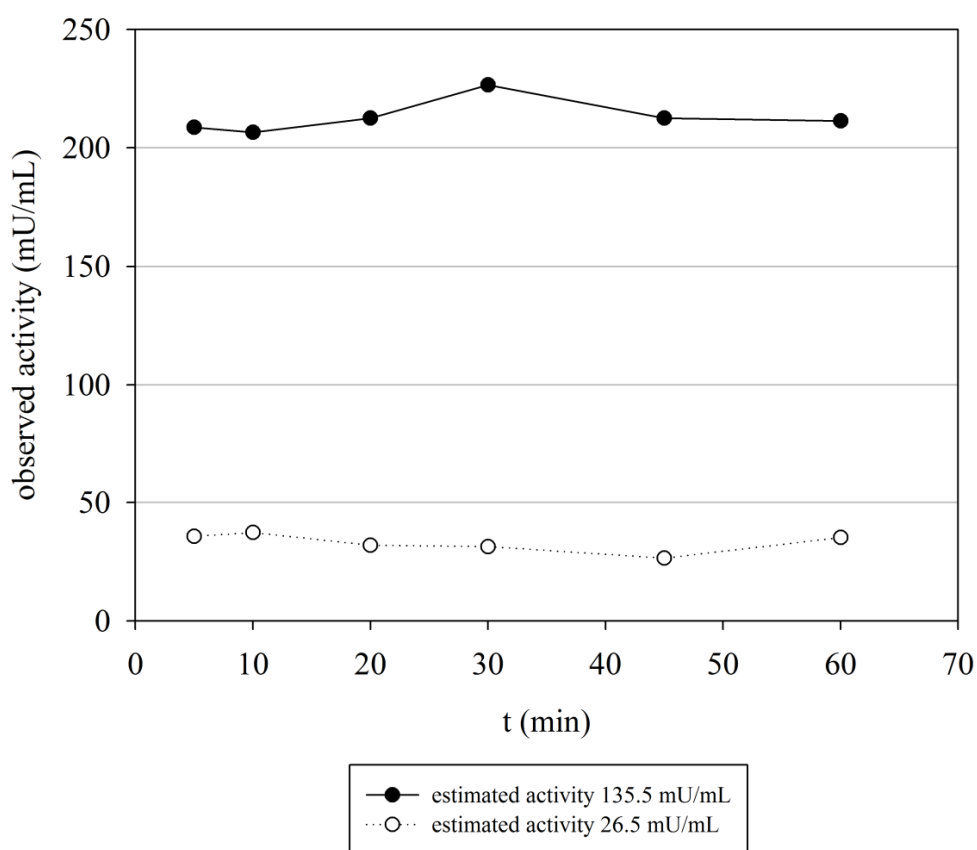
Figure 16: Activity of Z$_{basic2}$_*Lm*SPase when simulating elution conditions

Activities were prepared in 50 mM KH$_2$PO$_4$ containing 2 M NaCl and 0.5% Tween 20 at pH 7.0

4.1.9 Catalytic effectiveness

In order to determine whether the applied immobilization strategy affects the activity of Z$_{basic2}$_*Lm*SPase, the catalytic effectiveness η was determined. In the manifestation used herein, the apparent total activity when being immobilized in the microreactor was compared to the activity of the detached enzyme after an immediately following elution. In order to obtain significant results by diminishing the measurement error, this evaluation is preferentially performed regarding experiments showing sufficiently high immobilized activity at the respective end of continuous operation. Thus, the experiments LS1, OLS1, SLS2 and NSLS1 were selected, which showed final apparent activities in the range from 11.3 to 21.7 mU. The results shown in Table 8 suggest that Z$_{basic2}$_*Lm*SPase shows only 26-34% of its activity when being attached to the microreactor channel. This is significantly lower than η found when immobilizing Z$_{basic2}$_*Lm*SPase on anionic resins (offering sulfopropyl or sulfoisopropyl surface groups), where the catalytic effectiveness was around

the ideal value of 100% (19). However, it has to be mentioned that η in those studies was defined to be the ratio of apparent activity and theoretical activity (calculated by subtracting the non-bound from the offered activity), a strategy which was not transferable to this investigation due to low stability.

Table 8: Catalytic effectiveness for selected experiments

Experiment	η (%)
LS1	26.4
OLS1	30.6
SLS2	28.2
NSLS1	34.4

Certainly this raises questions about potential reasons for this low η, e.g. a possible interference of the Z_{basic2} peptide with the *Lm*SPase. Mixing and distribution of reactants in the microreactor is solely achieved by diffusion. Diffusional limitation might therefore be imaginable, but would be absolutely contradictory to the alleged benefits of microfluidic systems. Besides this kind of limitation could not be identified when comparing c(G1P) attained for different τ (Figure 15), but admittedly the studied range of flows was very limited. Diffusive mass transfer is described by the Einstein-Smoluhovski equation (Equation 18), where x is the diffusion length, D is the diffusion constant (10^{-9} to 10^{-10} m^2/s for liquids with low viscosity) and t is the diffusion time (40).

$$x^2 = 2 \cdot D \cdot t$$

Equation 18

Having x=75 µm [half of the microreactor channel width and height which is 150 µm according to (29)] and assuming D with 10^{-9} m^2/s, t is estimated with 2.8 seconds. The residence times corresponding to 2, 5 and 10 µL/min are 390, 156 and 78 seconds, respectively. An impact of mass transfer limitation on the reaction is therefore considered absolutely negligible.

The obtained numbers for the catalytic effectiveness also allow for another reasoning: If the apparent activity is only around 30% of the "true" activity, this would imply that the initial activity was actually higher than the suggested ideal loading (106 mU), in some cases raised by 70%. Furthermore, when considering the values found during the more stable phase of the

courses, the theoretical true activities would be close to the ideal loading, indicating that the estimation was matching the real situation quite well.

4.1.10 Conclusions

When immobilizing Z_{basic2}_LmSPase in the non-functionalized channel of a microreactor, the initial apparent activities were in the range between 50 and 60 mU considering the experiments with the best performance (LS1, OLS1, SLS2). These values are approximately the half of the ideal loading expected from the calculation (4.1.1). Overall the reproducibility was found to be low, as the values were varying within 4 and 68 mU in the remaining experiments with worse performance. The quick declination observed in the first hours of operation is not considered a result of inactivation, since data from literature for soluble His-tagged LmSPase (20) and a control storage experiment using soluble Z_{basic2}_LmSPase suggest high or at least sufficient stability under the applied operational conditions, namely T=22 °C in combination with pH 7.0 or pH 8.0. Therefore it is deduced that the attachment of the monomeric LmSPase featuring only one Z_{basic2} linker peptide on its aminoterminal end is weaker than expected. Whether this can be improved by introduction of either a dimeric SPase having two Z_{basic2} tags is currently an object of investigation in a follow-up study. Alternatively the fusion protein could be modified by addition of further Z_{basic2} sections, maybe on both N- and C-terminal ends. The immobilization process itself appeared to be under control of one or several factors which are not clearly identified and understood, but strongly affect the reproducibility of immobilization.

However, it can be stated that the reaction conditions could be optimized in terms of stability. In the case of LS1, OLS1 and SLS2 the course of activity entered a "plateau phase" after the initial decrease, where the apparent activity was decreased by no more than 15-25% within 25 to 36 h. When increasing flow and sucrose concentration after a total operation time of 44 h, apparent activity in SLS2 showed a considerable decrease within a few hours. This observation was supporting the premise that lowering the sucrose concentration has a beneficial impact on the stability.

Assuming ideal loading of the microchannel, the ideal STY (identical to the ideal volumetric activity) would be 8.15 mM/min. During the plateau phases of the experiments LS1, OLS1 and SLS2 the average STY was found to be 1.98, 1.90 and 2.44 mM/min, respectively.

Fearing that high flow favors the detachment of the enzyme and aiming at a higher G1P production, flows higher than $10\,\mu L/min$ were excluded after revealing of the low stability. In the studied range of $2\,\mu L/min$ to $10\,\mu L/min$ no flow dependency of the apparent activity could be found for the described model reaction, suggesting that mass transfer limitations are negligible. This assumption is also supported by the fact that the residence times are multiple times higher than the diffusion time. Nevertheless the low effectiveness factor of 26-34% indicates an impact on the activity by a yet unknown factor.

Employment of surface functionalization with sulfonate groups did not result in a higher stability of Z_{basic2}_LmSPase. However, besides variations in the design of the Z_{basic2} fusion protein (as mentioned above), different surface modifications may be studied in order to increase loading and operational stability. Moreover, modifications of the immobilization conditions like altered incubation times and immobilization in flow are currently under investigation.

4.2 Immobilization of Z_{basic2}_TvDAAO

4.2.1 Calculation of ideal loading

Considering the dimensions provided in the technical drawing (29), the surface of the microreactor channel was calculated to be 374.25 mm². The footprints and ideal loadings considering the different estimation models are shown in Table 9.

<div align="center">

Table 9: Calculated footprints and ideal loading capacities

</div>

	Footprint (nm^2)	Quantity (mol/microreactor)	Mass (µg/microreactor)	Total activity (U/microreactor)	Volumetric activity (U/mL/microreactor)
Model 1	27.6	$2.25x10^{-11}$	2.09	$1.48x10^{-1}$	11.4
Model 2	33.0	$1.89x10^{-11}$	1.87	$1.33x10^{-1}$	10.2
Model 3	70.0	$8.88x10^{-12}$	0.822	$5.84x10^{-2}$	4.49

Model 3 was regarded to meet the real situation better than the other models and therefore the volumetric activity of 4.49 U/mL was chosen as the lower limit for the prepared immobilization mixes. When assuming the desired formation of a monolayer during the immobilization process, this volumetric activity is corresponding with an ideal loading of 58.4 mU of Z_{basic2}_TvDAAO.

It should be noted here that the calculation was based on the assumption that the channel walls are absolutely smooth. Thus, the actually available surface might be higher than calculated. According to additional data provided by the manufacturer, the surface area was specified with 0.024 m^2 which exceeds the calculated value by a factor of ~64. Although this large discrepancy might be a basis for discussion, the high surface roughness of Ra=2.45 µm will contribute to an enhancement of the area. The concentration of silanols on the purchased chip without further modification (like the used pretreatment or the functionalization with sulfonate groups) was stated to be $5x10^{14}$ cm^{-2} (data from manufacturer).

4.2.2 Immobilization with pretreatment

The crude extracts deployed for the preparation of the respective immobilization mixes showed volumetric activities ranging from 11.5 to 36.5 U/mL and protein contents from 11.0 to 17.8 mg/mL as determined using the assays described in 3.5.1 and 3.6.

It is emphasized that the activity offered to the microreactor was adjusted to enable a total covering of the calculated surface (=ideal loading). In contrast to that, the enzyme concentration offered to porous carriers is often not aiming at the maximum loading. Catalytic effectiveness thereby found was decreased at higher loadings which was supposed to be a result of diffusional limitation of the cosubstrate O_2 (12, 13, 41).

Available data from preceding studies on immobilization of Z_{basic2}_TvDAAO in a non-functionalized microreactor already demonstrated that application of the complete pretreatment as described in 3.7.2 assisted an increase of both the theoretically bound and the apparent immobilized activity, which is why further experiments without pretreatment were omitted (33). First Z_{basic2}_TvDAAO immobilization pretrials performed within in this present work aimed at exceeding the values found during the mentioned initial studies, but immobilization balances showed to be highly unstable and immobilized activities were lower than desired. In order to gain more confidence about the immobilization efficiency, a combination of countermeasures was introduced. Studies conducted using an unmodified silica carrier (controlled pore glass) showed that the adsorption process reached an equilibrium state after 1.5 h (13). Since the microchannel surface was considered to feature a lower porosity and thus better accessibility of the silanols than this porous carrier, adsorption equilibrium is regarded to occur faster. However, to ensure completion of the process, incubation time was slightly enhanced to 2 h. Additionally, immobilization was performed in several steps as depicted in Figure 17. Consecutive steps to remove weakly bound enzyme of any foregoing step and to fill potential gaps were considered adjuvant in generating a layer of stably immobilized enzyme.
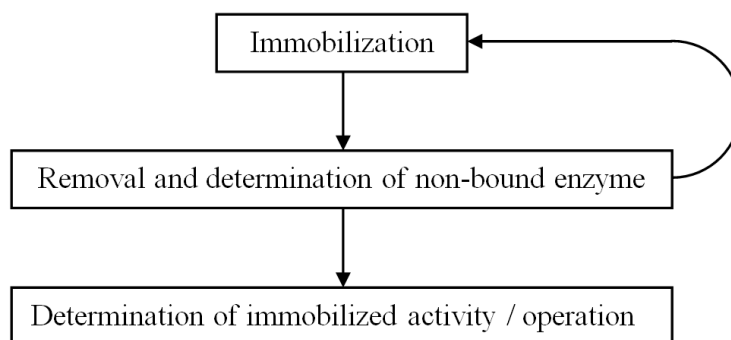
Figure 17: Sketch of the workflow when conducting several immobilization steps

To further increase the probability of a high and stable loading, a microreactor chip functionalized with sulfonate groups was employed. While 2-step immobilization did not result in a sufficient improvement (data not shown), a subsequent raise to 3 steps yielded better balances and increased initial bound activities. The data on each immobilization step of a set of 5 experiments were collected in Figure 18. As it can be perceived in view of the error bars, the deviations are quite high, but on average the first and third immobilization steps seemed to be working well.
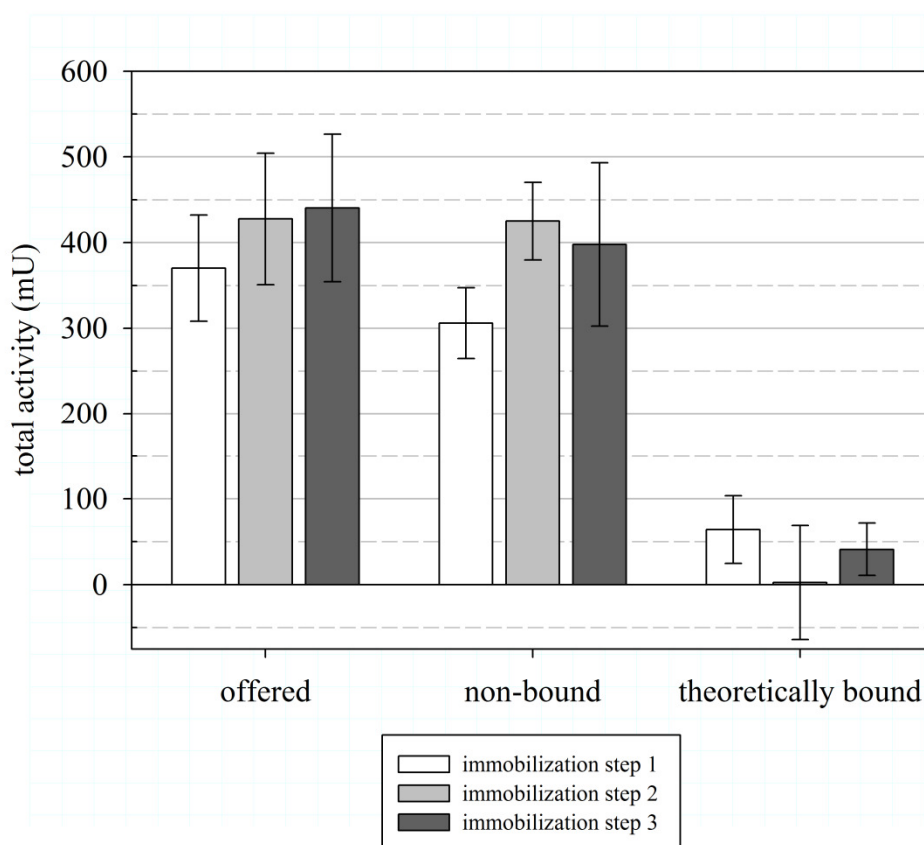
Figure 18: Immobilization balances using a microreactor chip functionalized with sulfonate groups

Bars signify mean values of 5 immobilization experiments; error bars indicate standard deviations; offered total activity is referring to total enzymatic activity provided to the whole volume of the microreactor and all connected capillaries and was 5.0-9.5 fold higher than the ideal loading; non-bound activity was determined after washing the microreactor with 50 mM KH_2PO_4 pH 7.0 following the immobilization step; theoretically bound activity was calculated by subtracting non-bound from offered activity

After gaining confidence about the reproducibility of the immobilization process, these results were opposed with 3 comparative experiments on a non-functionalized chip while keeping the remaining immobilization conditions constant to evaluate the impact of the functionalized surface. In view of the balance in Figure 19 only the first immobilization step was working reliably, while the remaining two failed, leading to an overall negative value for the

theoretically bound activity. It can therefore be deduced that the affinity of the Z_{basic2} tag for the functionalized surface is stronger than for the non-derivatized surface.
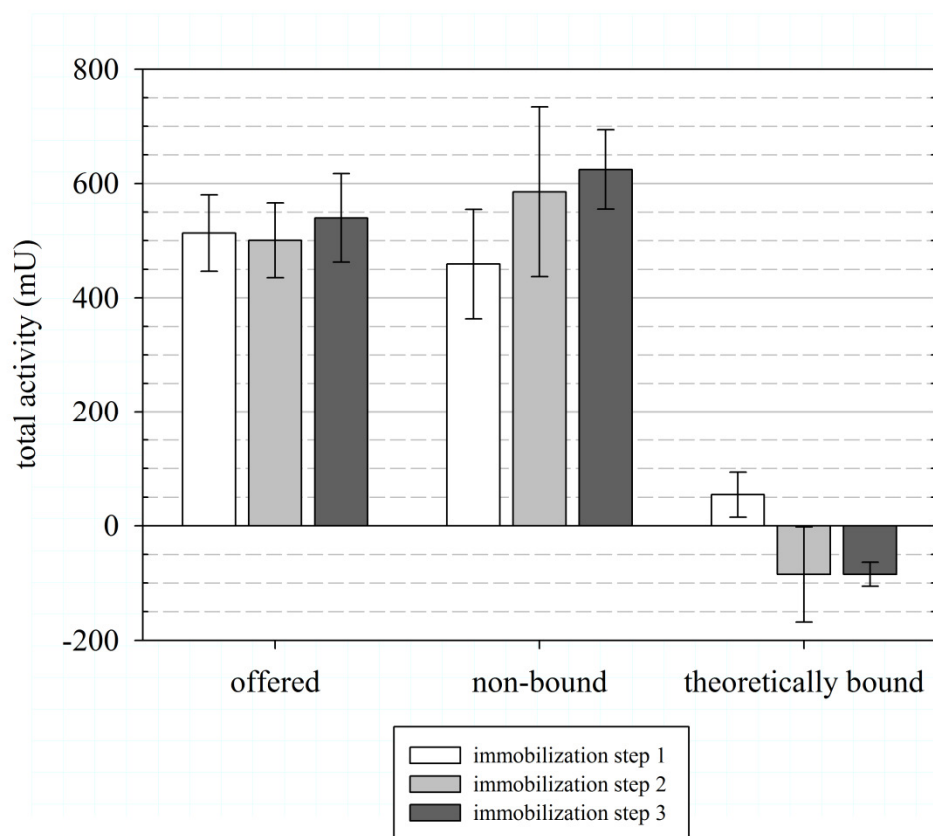
Figure 19: Immobilization balances using a non-functionalized microreactor chip

Bars signify mean values of 3 immobilization experiments; error bars indicate standard deviations; offered total activity is referring to total enzymatic activity provided to the whole volume of the microreactor and all connected capillaries and was 7.3-10.0 fold higher than the ideal loading; non-bound activity was determined after washing the microreactor with 50 mM KH_2PO_4 pH 7.0 following the immobilization step; theoretically bound activity was calculated by subtracting non-bound from offered activity

Although the results indicate that the immobilizations failed, no substantial differences in loading could be noticed between the experiments deploying functionalized and non-functionalized chips when determining the initial apparent activities and their respective stability (see next section).

4.2.3 Performance of immobilized Z_{basic2}_TvDAAO

As stated above, data on Z_{basic2}_TvDAAO immobilized in an underivatized glass microreactor was available from foregoing investigations. Apparent immobilized activities between 13.5 and 15.7 mU were measured at a flow of 90 µL/min. However, a flow dependency was

observed, resulting in activities of 6.8-9.6 mU and 28.3-34.4 mU at F=44-48 µL/min and F=173-184 µL/min, respectively (33). The minor deviations between applied flows were caused by an imperfectly working syringe pump. It also has to be noted here that the stability and performance of immobilized Z_{basic2}_TvDAAO over a longer period of continuous operation were not assessed during the course of these early studies. As also already mentioned, the pretrials within this work were geared towards a confirmation or – preferentially – a surpassing of the results obtained in (33). Immobilized activity was initially measured using the same continuous variant of the coupled peroxidase assay described in 3.5.1. First results of initial activity were 3.2-3.5 mU (F=50 µL/min), 4.6 mU (F=100 µL/min) and 15.0 mU (F=200 µL/min) and therefore well below the previously achieved values. In a further preliminary test initial values determined at flows of 50 and 100 µL/min were 8.0 and 14.9 mU, respectively, which was matching the expected minimum loading, but unfortunately they were decreasing quickly. When changing the conditions of immobilization as described above (3 steps of 2 h incubation using a functionalized microreactor chip), these values could be slightly overtopped (9.4, 18.7 and 36.1 mU at 50, 100 and 200 µL/min, respectively), while showing promising stability.

However, while the standard coupled peroxidase assay has proven reliability for assessing the activity of soluble TvDAAO, the applicability of its continuous variant was increasingly questioned. Control experiments revealed a high dependency of the response on the HRP concentration in the assay mix passing the microreactor channel (data not shown). Another factor that was raising concerns was the reflection on the possible consequences when using an assay with a high extinction coefficient (in this case 25.12 $mM^{-1}cm^{-1}$) for determination of an enzyme with uncertain stability of attachment. This would imply that already small amounts of detached Z_{basic2}_TvDAAO might continue the assay reaction and provoke a considerable increase of the color formation in the sample introduced to the spectrophotometric measurement. To minimize this risk, the time period between obtaining and measuring the sample was usually kept as short as possible, but a noteworthy degree of insecurity was still remaining.

As an alternative the keto acid assay was introduced, which is based on direct measurement of the product of the reaction catalyzed by TvDAAO. In the case described herein, this product is α-Keto-γ-(methylthio)butyric acid, the corresponding α-keto acid of the employed substrate D-Methionine. According to the obtained calibration, the response was linear between 0.01 and 0.4 mmol of α-Keto-γ-(methylthio)butyric acid and hence limited, but absolutely

sufficient for the given demands. The extinction coefficient in this range was 1.0353 mM^{-1}cm^{-1}, often allowing the samples to fit into the linear range without need for dilution. The ratio between values derived from keto acid assay and continuous coupled peroxidase assay was found to be 2.11±0.20. It has to be noted that the reaction was performed in presence of Catalase which continuously degrades the H_2O_2 and thus partially recycles the oxygen introduced with the substrate mix. This results in an increase of the product formation rate and consequently the product concentration. Depending on whether the oxygen is depleted during the reaction or not, oxygen recycling is affected and the stated ratio will be altered.

Table 10 shows the initial activities detected with the keto acid assay after implementation of the 3-step immobilization. All values were measured applying a flow of 100 µL/min. The substrate mix fed to the microreactor comprised 10 mM D-Met in 50 mM KH_2PO_4 pH 8.0. 10 µg/mL Catalase were added to minimize the risk of inactivation of Z_{basic2}_TvDAAO by H_2O_2 formed during the reaction.

Table 10: Initial activities of Z_{basic2}_TvDAAO detected after performing 3-step immobilization

microreactor chip	initial activity (mU)*
functionalized	33.65±1.21
non-functionalized	35.50±1.64

* determined at F=100 µL/min

In view of these figures, initial loadings on non-functionalized and functionalized surface were comparable. In combination with the corresponding results of the balances shown in 4.2.2 this evokes the impression that the balances only exhibit a limited significance when applying several steps of immobilization. However, they were considered suitable for predicting the success of a particular immobilization experiment because as far as only one step was considered effective, the apparent immobilized activity was satisfying, too.

As stated above, TvDAAO activity showed a high reliance on the applied flow, which was suggested to originate from the oxygen-dependent nature of the catalyzed reaction (33). Except for the in- and outlet the deployed microreactor chip is a closed system and the required oxygen is fed to the system dissolved in the substrate mix. Since oxygen solubility is low in aqueous solutions, only a limited amount is available for performing the desired reaction.

The activity of Z_{basic2}_TvDAAO immobilized in a functionalized microreactor chip was monitored at different flows (Figure 20). Working flow was chosen to be 100 µL/min, while at given points of time it was altered to 50 and 200 µL/min to get comparative values. Flow dependency is clearly cognizable and confirms the previous observations.
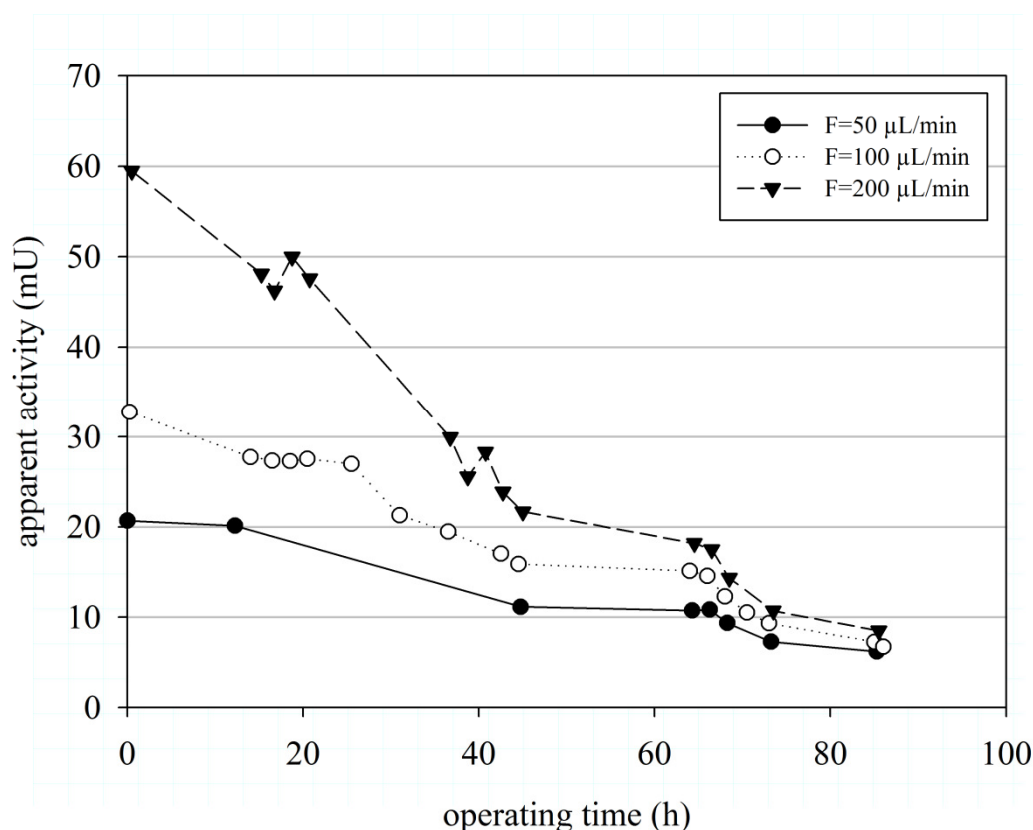
Figure 20: Stability of Z_{basic2}_TvDAAO immobilized in a microreactor functionalized with sulfonate groups

Working flow was 100 µL/min; at certain points the flow was altered as indicated for determination of the respective activity

Activity values were distinctly raised at higher flows, with the highest initial value seen at 200 µL/min. However, activities decreased with similar velocity and showed only ~50% of their respective initial values after ~40 h. Certainly the strongest declination when considering discrete numbers was seen for the highest applied flow. Noteworthy is that the courses of activity are converging during long term operation, indicating that the oxygen limitation is progressively losing importance.

In order to evaluate the impact of the functionalization, the used approach of continuous operation was also performed employing a non-functionalized microreactor chip. The

respective courses determined at F=100 µL/min are confronted in Figure 21. Corresponding keto acid concentrations are shown on the right y-axis.
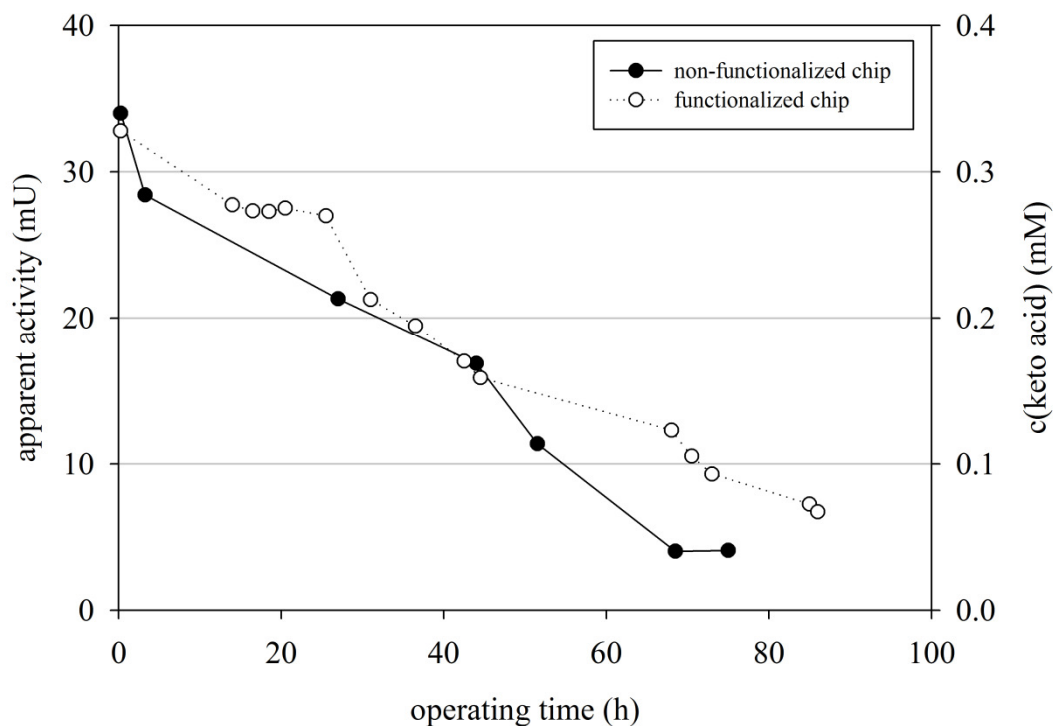
Figure 21: Stability of Z_{basic2}_TvDAAO immobilized in microreactors featuring or lacking surface functionalization at F=100 µL/min

It can be perceived that they show quite similar behavior in the first phase until their initial activities were halved at ~44 h, but subsequently the reduction on the non-funtionalized chip was speeding up. This might be an indication that surface functionalization has a slightly beneficial impact on the stability of the enzymatic activity.

Up to this point, the microreactor system was used to study the intrinsic activity, apparent immobilized activity and stability by analysis of the keto acid production rates. Subsequently a recycling setup was designed as illustrated in Figure 22, which allowed for evaluation of the stability of Z_{basic2}_TvDAAO while enhancing the concentration of keto acid. Reoxygenation of the substrate mix leaving the microreactor was solely realized by dropping it back into a collection vessel, where it was taken up by the inlet capillary again. The collection vessel was placed in ice to minimize evaporation of the substrate mix over the course of recycling.
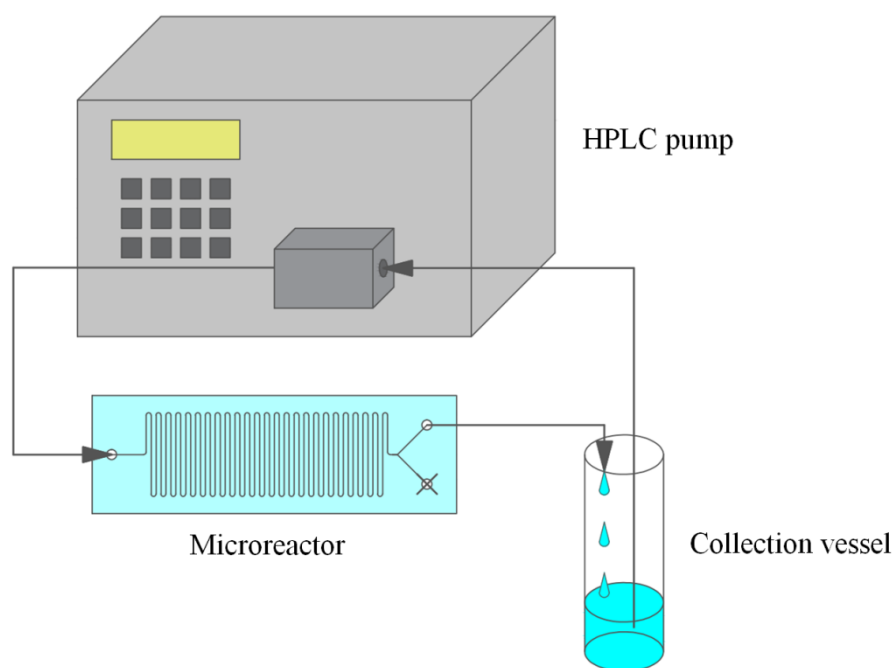
Figure 22: Scheme of the recycling setup

Working flow was adjusted to $F=100\,\mu L/min$ and not altered during operation to avoid unnecessary perturbation of the system. Working volumes – i.e. the total volume of substrate mix circulating through the system – were 3.75 and 5 mL, respectively. The appropriate initial concentration of D-Met was estimated based on the performance data attained during the single passage experiment using the functionalized chip. Linear regression of the course of the apparent volumetric activity yielded a function (y=-0.023x+2.47) which was subsequently used to calculate the mean volumetric activity in the observed period of operation (75 h). In view of the thereby obtained value of 1.48 U/mL, the concentration of α-Keto-γ-(methylthio)butyric acid to be expected after the priorly defined 80 h of operation was figured to be 18.5 mM. Initial c(D-Met) was set to 20 mM, with the option to supply additional D-Met if depletion becomes conceivable. As long-term stability of Catalase was questionable, a fresh portion equivalent with $10\,\mu g/mL$ was added twice a day. To perpetuate the respective working volume, those small fractions lost due to sampling were replaced by addition of the appropriate amount of 50 mM KH_2PO_4 pH 8.0 which was in due time supplemented with fresh Catalase.

The courses of keto acid production are combined in Figure 23. Achieved end concentrations observed for experiments with working volumes of 5 and 3.75 mL were ~12 and ~15 mM, respectively. It has to be noted that even if the end value was higher, when having a smaller

working volume, the total quantities of formed keto acid – when normalized based on the volume – were quite similar in the range of 54.9 to 62.4 µmol. After a fairly linear increase all courses show stagnation beginning after 38-45 h which is in compliance with the points of time where the activity was halved during the single passage experiments (Figure 21). Addition of fresh D-Met did not entail a further raise of the product concentration, implying that the stagnation is not caused by low substrate availability. The distinct resemblance of the 5 mL experiments performed on microreactor chips with or without functionalization indicate that the applied surface modification did not result in a notable improvement of the stability.
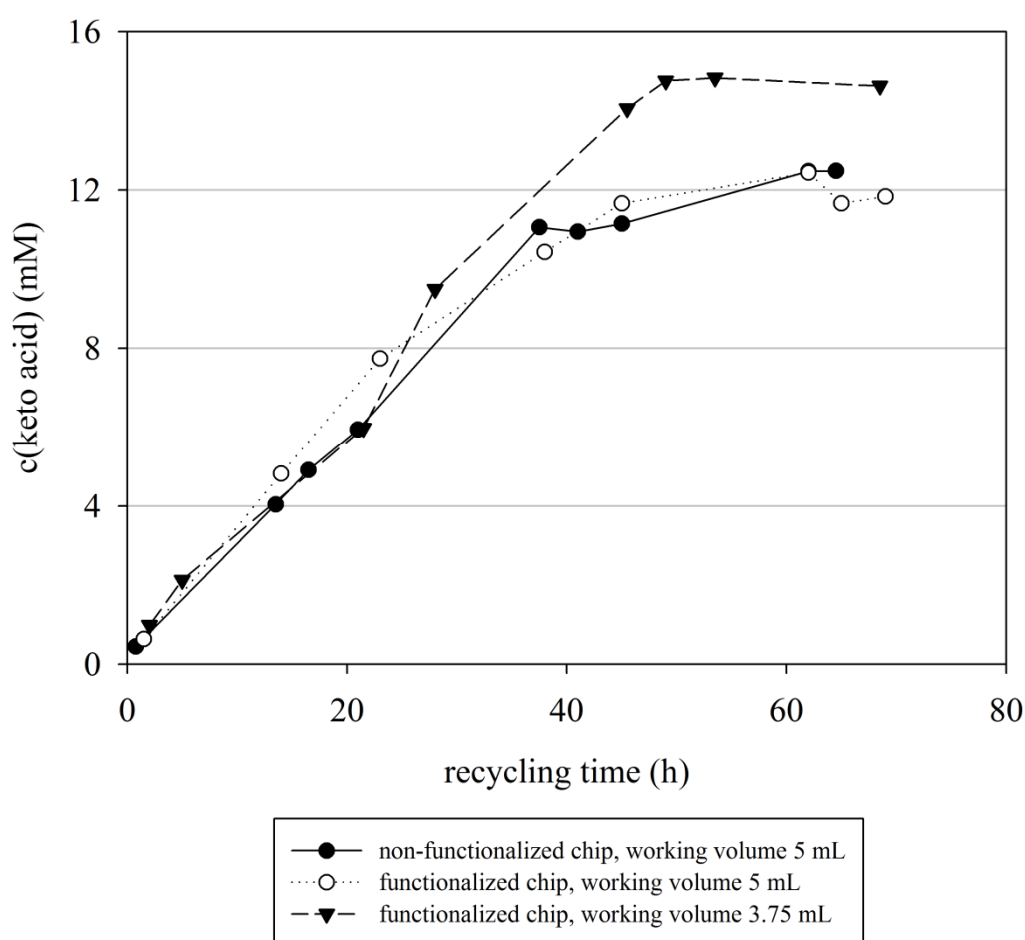
Figure 23: Formation of α-Keto-γ-(methylthio)butyric acid when using a recycling setup

Z_{basic2}_TvDAAO immobilized in different microreactors; F=100 µL/min

For a better comparison of the recycling experiments the productivities were calculated and depicted in Figure 24. Although displaying differences at beginning, they are soon becoming similar and show a common trend. In accordance with the higher end concentration, the

productivity was also higher when using a smaller working volume of 3.75 mL. Given an ideal loading of 57 mU, the maximum productivity regarding a working volume of 3.75 and 5 mL would have been 11.7 and 15.2 µM/min, respectively.
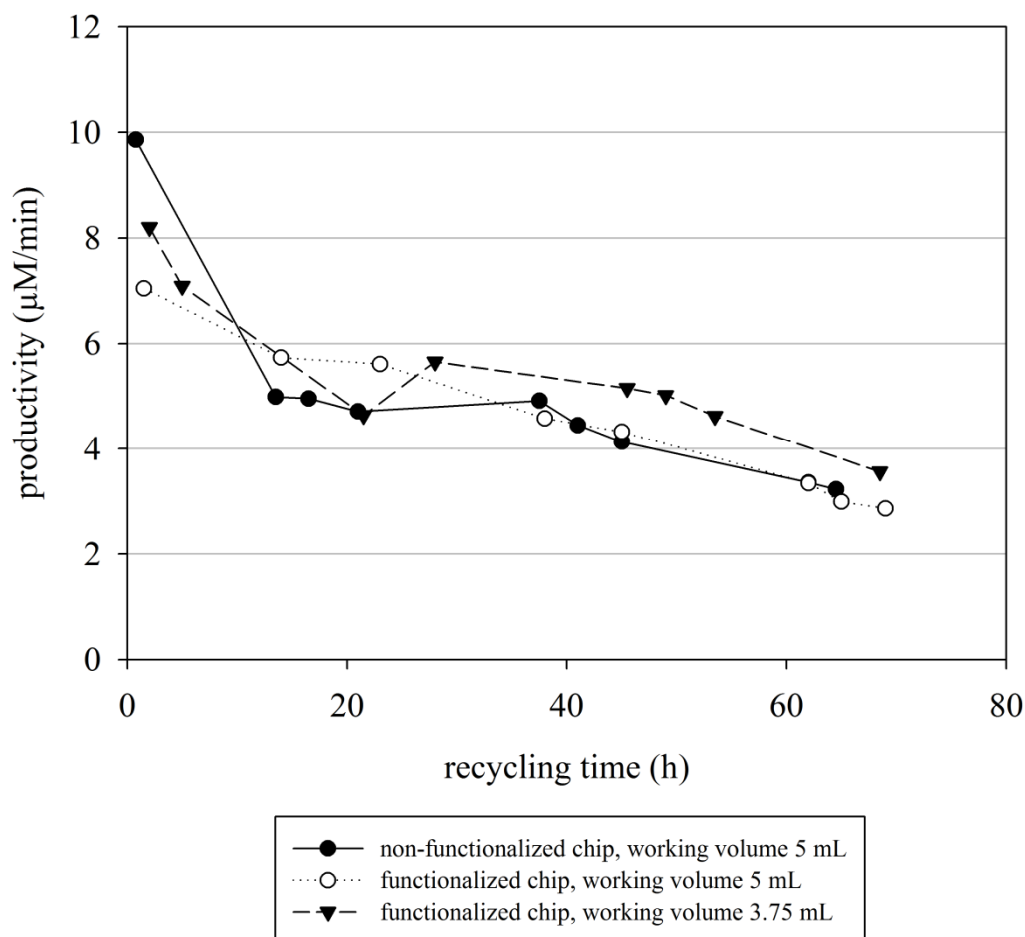
Figure 24: Productivities calculated for recycling experiments

In order to provide comparative values the initial activities of the continuous experiments without recycling were also translated to the working volume of 5 mL and were found to be 6.8 and 6.6 µM/min deploying the non-functionalized and functionalized microreactor chip, respectively.

Furthermore, the reaction rates of recycling experiments were compared with those when conducting single passage continuous operation (Figure 25). The values were calculated for each individual time phase which corresponds to the time between 2 particular samplings. Although this mode of calculation generates high deviations if the keto acid production is just slightly altered, a common trend can be observed. With the exception of the recycling

experiment without functionalization (49.3 nmol/min), all initial conversion rates were ranging from 30.8 to 35.2 nmol/min. Assuming ideal loading without limitations of any kind whatsoever, the total immobilized activity expected would be 58.4 mU (corresponding to a conversion rate of 58.4 nmol/min). As far as the available data allows for a reliable assessment, the most stable course was perceived when running single passage continuous operation on a functionalized microreactor chip. It has to be noted that the higher quality of the corresponding values was also promoted by the thereby higher sampling frequency.
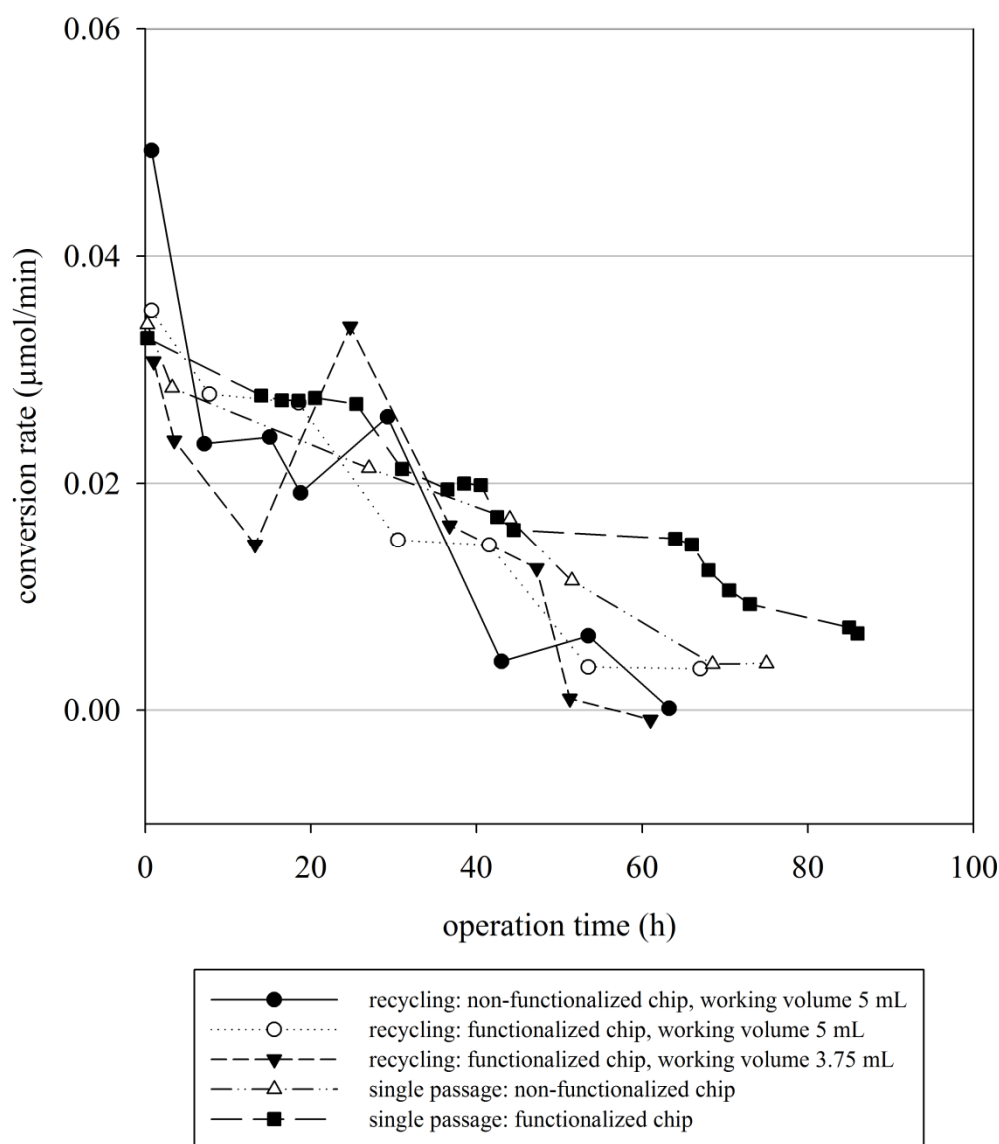
Figure 25: Comparison of calculated conversion rates

Values were calculated for each individual phase (time between two samplings) for recycling and single passage experiments

4.2.4 Oxygen consumption during the course of reaction

The different observed levels of keto acid production and thus varying apparent activities when changing the flow are considered to be a result of limited availability of oxygen. Hence, the oxygen concentration at the in- and outlet capillary of the microreactor was monitored in order to gain more information. Figure 26 shows the oxygen consumption during the course of the single passage operation using a functionalized chip. Working flow was 100 μL/min, intermitted by alterations of the flow to 50 and 200 μL/min.
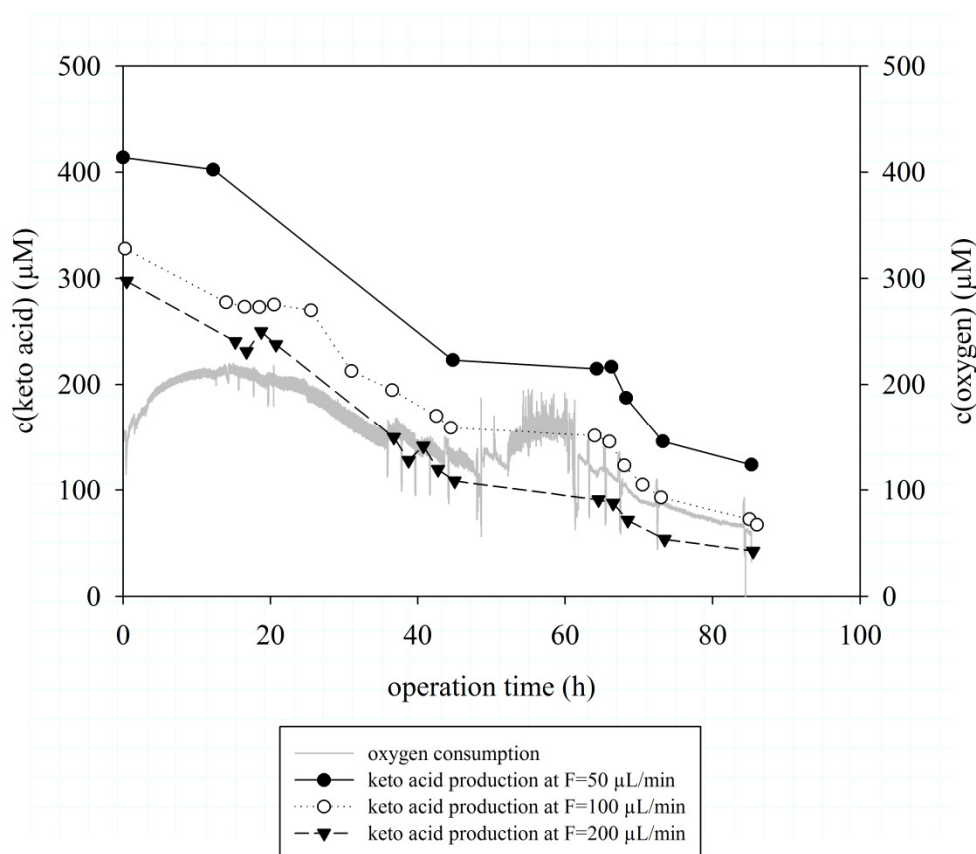
Figure 26: Oxygen consumption in comparison to keto acid production at different flows

Experiment performed in single passage continuous mode on a functionalized microreactor chip

Although the course of consumption is inconclusive during the first hours of operation, it can be stated that it is basically suitable for following the course of reaction. Furthermore, the consumption is correlating well with the keto acid production at F=100 μL/min in the second half of the operation time, almost enabling the generation of a decent mass balance.

Selecting data from the same experiment, c(keto acid) at the outlet was used in order to take a closer look at the situation during variations of flow. As it can be observed in Figure 27, the response is overall quite immediate. Oxygen concentration increases with flow, which is consistent with a decreasing consumption.
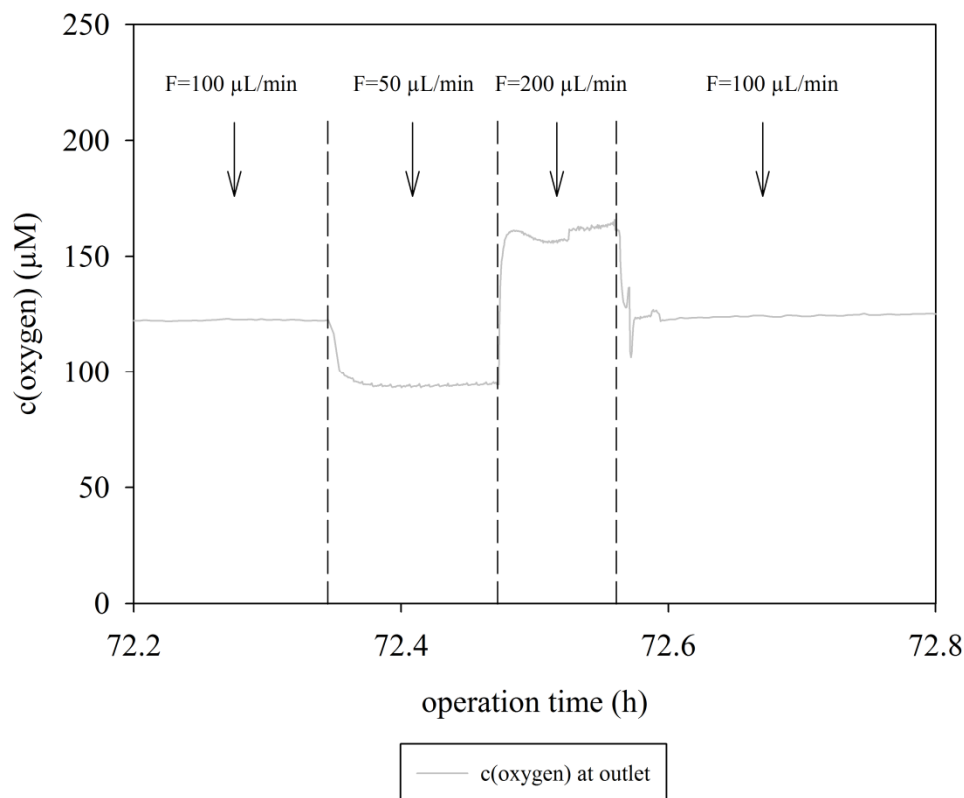
Figure 27: Response of oxygen concentration at the outlet to alterations of the flow

As it can be perceived from the x axis, the signal was recorded at a late phase of the experiment, where apparent activity was already strongly reduced and oxygen depletion is off the cards. Nevertheless the oxygen concentration is reliant on the flow, which raises questions about the impact of mass transfer. Mixing and distribution of reactants is solely achieved by diffusion in the microreactor. Using the Einstein-Smoluhovski equation, the diffusion time is estimated with 2.8 seconds as shown in 4.1.9. The residence times corresponding to 50, 100 and 200 µL/min are 15.6, 7.8 and 3.9 seconds, respectively. In order to estimate the impact of mass transport on the conversion, the reaction time was also calculated. Information about available oxygen concentration at the inlet was obtained by taking data of the online monitoring of this particular experiment and calculating the mean value between 16.5 to 20.5 h of operation (~240 µM). Accordingly the mean reaction rate (=volumetric activity of

the microchannel) at F=100 µL/min in the same period of time was calculated (~2.1 U/mL). Considering these values the reaction time during this early phase of operation is 6.9 seconds. An impact of mass transfer limitation on the turnover of oxygen is therefore considered very reasonable.

Oxygen consumption during recycling experiments was also compared with the course of keto acid production (Figure 28). Despite the improvable signal quality it can be easily observed that the consumption is decreasing as c(keto acid) approaches the phase of stagnation.
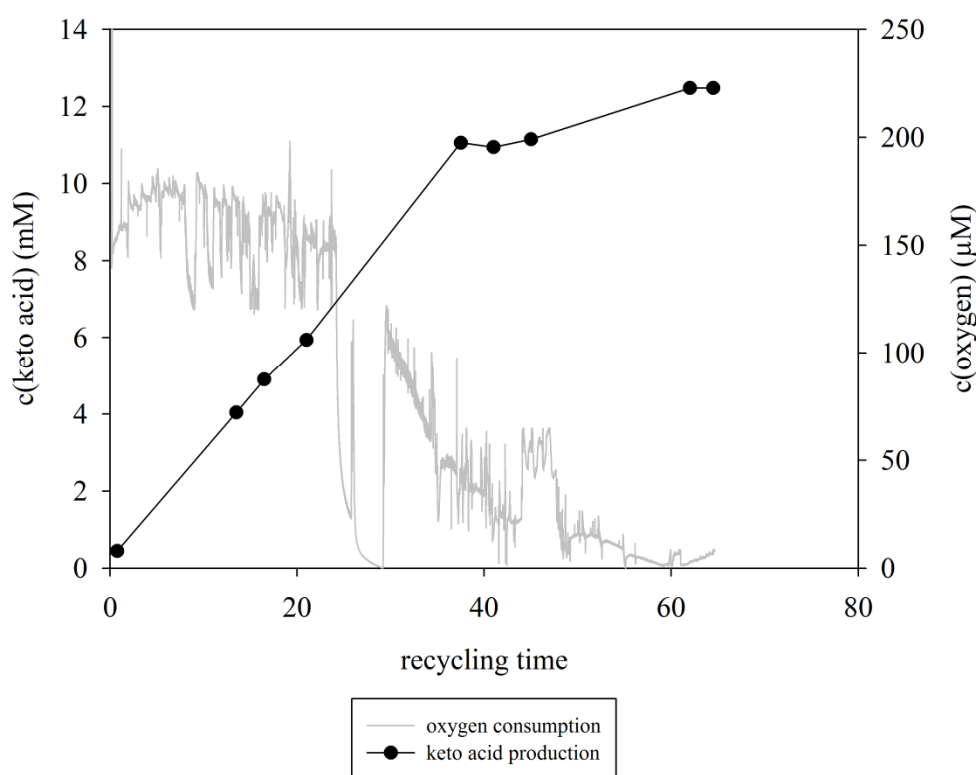
Figure 28: Oxygen consumption in comparison to keto acid production in a recycling experiment

Experiment performed in recycling mode (working volume 5 mL) on a non-functionalized microreactor chip

In Figure 29 the keto acid formation during a recycling experiment (functionalized chip, working volume 5 mL) was confronted with the oxygen concentration at the microreactor outlet. In the beginning c(oxygen) is low, but not depleted, which might be a further indication for a minor impact of mass transfer limitation. As the keto acid production approaches the phase of stagnation, the oxygen concentration undergoes an increase.
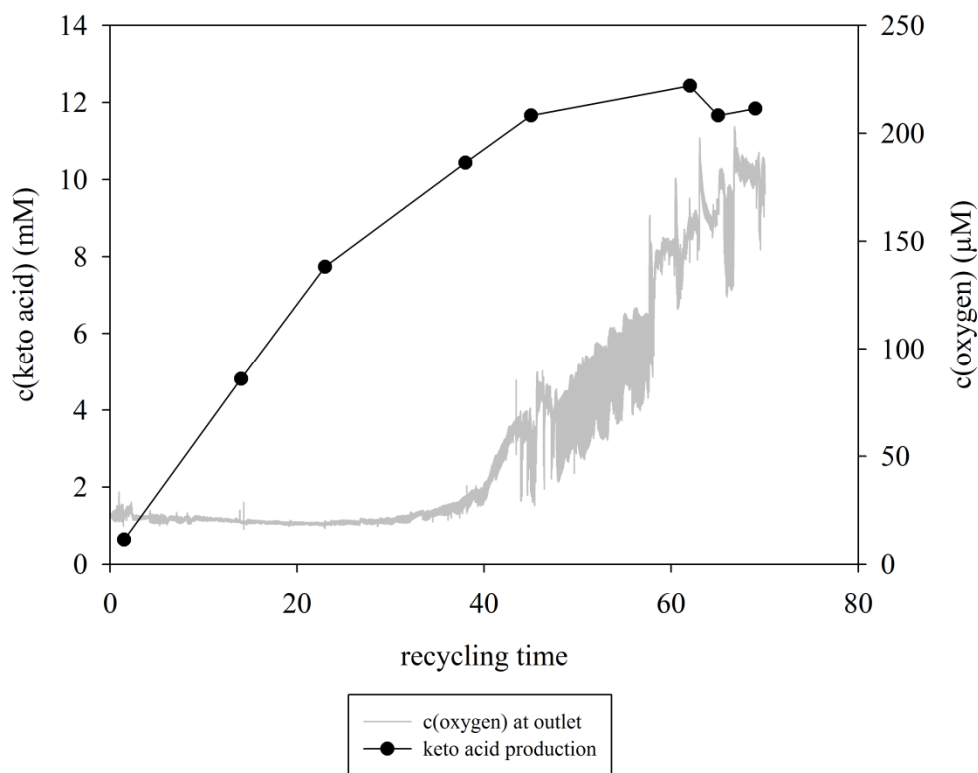
Figure 29: Oxygen concentration at the outlet in comparison to keto acid production in a recycling experiment

Experiment performed in recycling mode (working volume 5 mL) on a functionalized microreactor chip

Figure 30 shows the respective data for the corresponding experiment with the lower working volume of 3.75 mL.
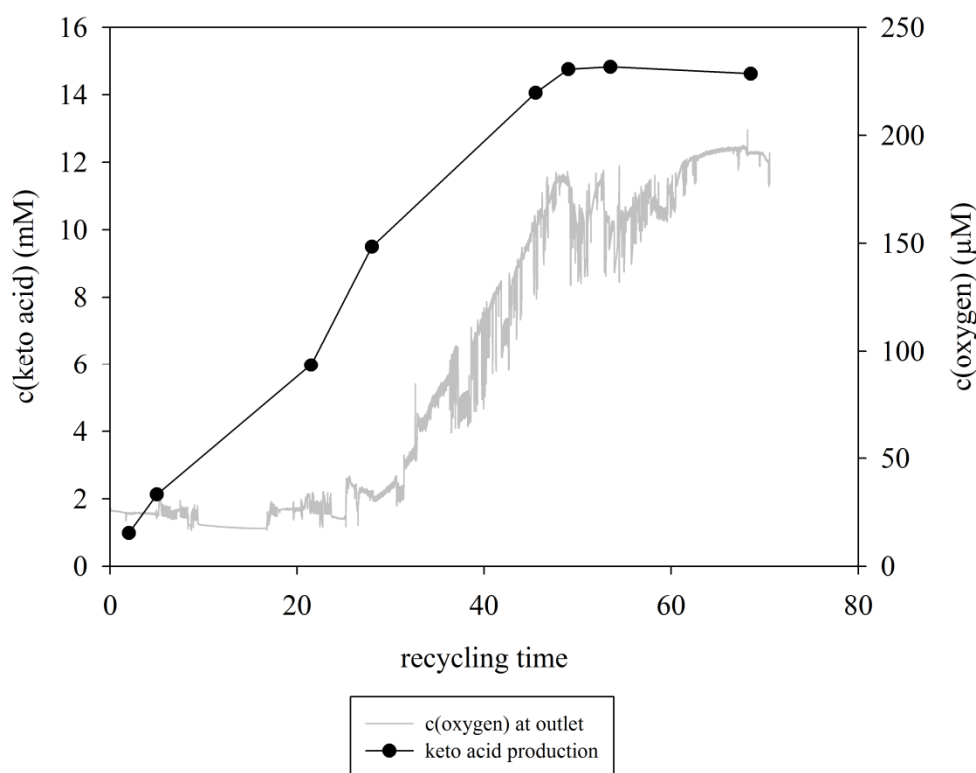
Figure 30: Oxygen concentration at the outlet in comparison to keto acid production in a recycling experiment

Experiment performed in recycling mode (working volume 3.75 mL) on a functionalized microreactor chip

The low, but noteworthy, remaining oxygen content during the first phase is again strengthening the suggestion of a mass transfer limitation. The mean values for the first 20 h of recycling were rather similar and around 22 µM for both experiments observed. The product courses in Figure 29 and Figure 30 indicate that the keto acid formation stagnates at approximately the same time (~45 h). It is therefore remarkable that the oxygen concentration at the outlet increases earlier in the experiment with the lower working volume. When having a closer look, it can be noted that both oxygen courses increase after a product concentration of ~10 mM is reached. This behavior was also sensed when performing the recycling approach on a non-functionalized microreactor chip (data not shown). It is therefore assumed that this shift of the oxygen increase might be a result of the higher productivity when deploying a lower working volume. When leveling off, the production could not be promoted by the addition of more D-Met to the reaction mix, suggesting that the stagnation is rather caused by the lack of active Z_{basic2}_TvDAAO than falling below a critical D-Met concentration.

4.2.5 Identification of the critical flow

In order to determine whether Z_{basic2}_TvDAAO is detached from the surface by exceeding a certain flow, the enzyme was subjected to a sequence of flows in ascending order.

After immobilizing the enzyme using the 3-step immobilization strategy on a non-functionalized chip, bound activity was determined at 100 µL/min and found to be comparable with the results of the remaining experiments (35.3 mU). The flows were applied in the sequence specified in Table 11, each for a duration corresponding to 10 volume changes (130 µL) using 50 mM KH_2PO_4 pH 8.0.

Table 11: Summary of parameters for high flows

F (µL/min)	t (s)	u (mm/s)	Re (-)
50	15.60	123	0.013
100	7.80	247	0.026
200	3.90	494	0.051
300	2.60	741	0.077
400	1.95	988	0.102
500	1.56	1235	0.128
600	1.30	1482	0.154
800	0.98	1975	0.205
1000	0.78	2469	0.256
1200	0.65	2963	0.307
1500	0.52	3704	0.384
2000	0.39	4938	0.512

All collected fractions were analyzed, but no notable activity could be detected. After deploying the highest flow of 2000 µL/min the immobilized activity was again measured and was only slightly decreased (30.8 mU).

As shown in Table 11, flow speed (u) and Reynolds number (Re) were also calculated based on a cross sectional area of $1.125*10^{-2}$ mm², a hydraulic diameter of $9.27*10^{-2}$ mm and consulting the density and dynamic viscosity of water at 25 °C with values of 997.04 kg/m^3 and 0.891 kg/(m·s), respectively. In view of these low Re values laminar flow is maintained over the whole series of examined flows.

4.2.6 Stability of soluble Z_{basic2}_*Tv*DAAO under elution conditions

In order to examine whether the activity of Z_{basic2}_*Tv*DAAO is compromised under the applied elution conditions, defined activities were added to an elution mixture and redetermined after particular times of incubation. As data regarding the elution of Z_{basic2}_*Tv*DAAO from a non-functionalized chip was already available from former studies for up to 30 minutes (33), only elution from a functionalized surface was simulated. The values shown in Table 12 are mean values of duplicate measurements.

Table 12: Activity of Z_{basic2}_*Tv*DAAO when simulating elution conditions

estimated vol. act. (mU/mL)	incubation time (min)	observed vol. act. (mU/mL)
	5	294.2
	10	298.5
	20	419.5
600	30	418.2
	45	315.6
	60	407.4
	5	53.5
	10	51.5
	20	51.8
60	30	51.7
	45	51.0
	60	49.7
	5	1.8
	10	1.9
	20	1.8
2	30	1.8
	45	1.8
	60	1.7

Regarding the highest estimated activity of 600 mU/mL it is noticed that the determined activities were in each case well below the desired value, implying an error during preparation of the mixture. Regarding the lower values (60 and 2 mU/mL) the preparations were working slightly better. However, no distinct decrease was found for the given period of time, which suggests that the enzyme is not affected by the presence of 5 M NaCl (Figure 31).
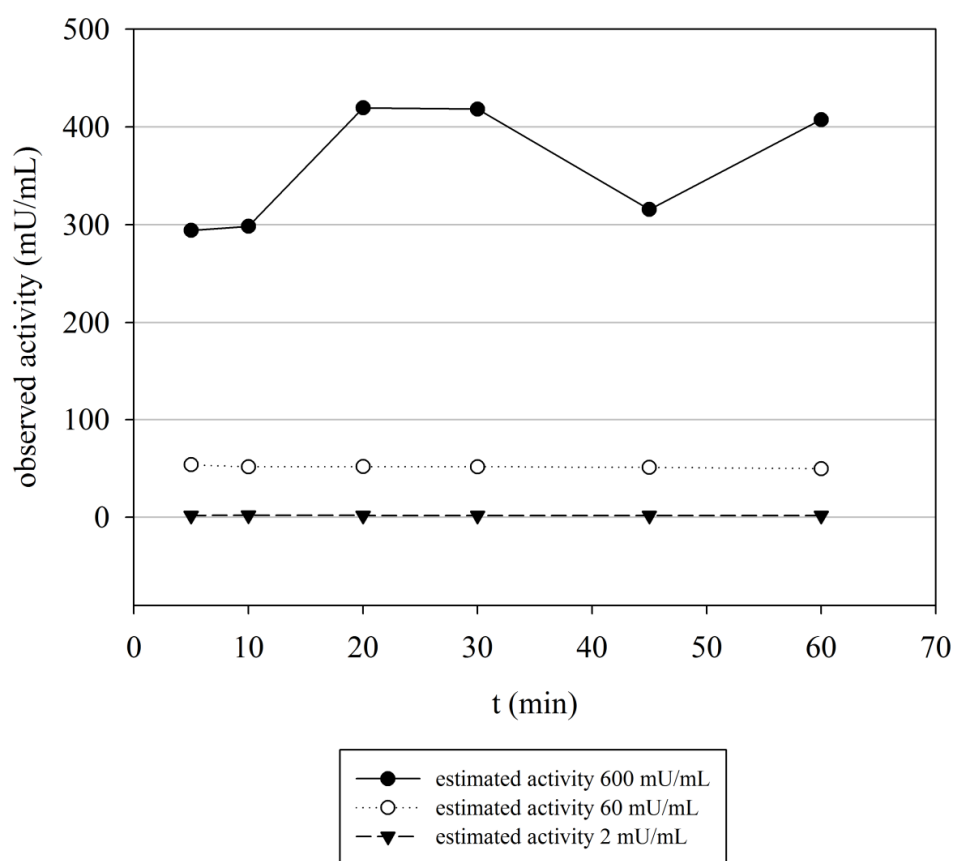
Figure 31: Activity of $Z_{basic2\_}Tv$DAAO when simulating elution conditions

Activities were prepared in 50 mM KH_2PO_4 containing 2 M NaCl and 0.5% Tween 20 at pH 7.0

4.2.7 Visualization of immobilized $Z_{basic2\_}Tv$DAAO

The immobilized enzyme was made visible by utilizing the autofluorescence of oxidized FAD which serves as the cofactor of TvDAAO, and detection via CLSM. In order to identify the minimum FAD concentration required for detection, different solutions were applied onto a microscope slide. Deduced from the ideal loading, the volumetric concentration of FAD in the microreactor should be ~1.4 nM. As shown in

Figure 32, half of this concentration (B) is not enough to be distinguished from pure buffer (A). An approximately 700 times higher concentration of 1 µM was also applied and exhibited a notable distinction (C).
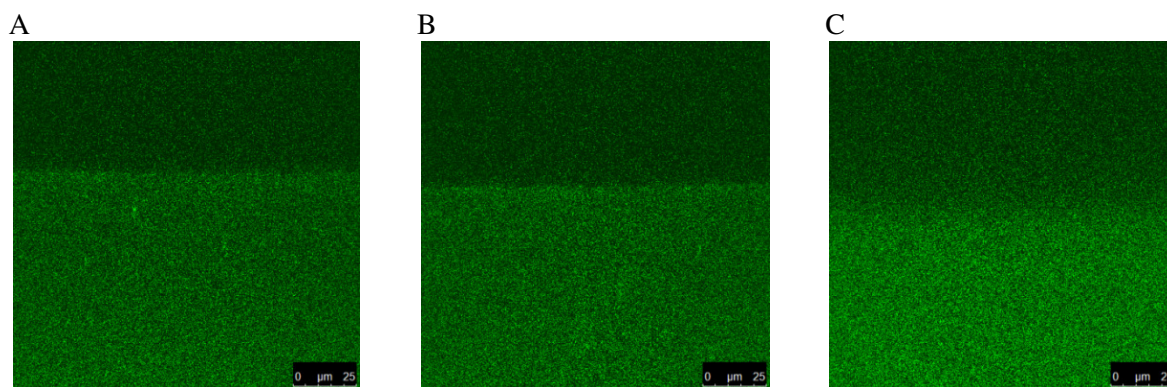
Figure 32: CLSM images of solutions on a glass microscope slide

A: 50 mM KH$_2$PO$_4$ pH7.0; B: 700 pM FAD in 50 mM KH$_2$PO$_4$ pH7.0; C: 1µM FAD in 50 mM KH$_2$PO$_4$ pH7.0
All images show cross sections at the border to the microscope slide; Contrast was set to the range of 0-70 for better visibility

As FAD bound to Z$_{basic2}$_TvDAAO should not be distributed in the whole volume, but rather concentrated at the microreactor walls, and regarding the possible dimensions when assuming formation of a monolayer of the enzyme, the factor of concentration would be at least 5000. Therefore it was assumed that FAD would clearly outshine the observed fluorescence signal of pure buffer.

Figure 33 shows microscopic pictures of a microreactor channel which was not subjected to any immobilization process, whereas the CLSM image (A) was complemented with a bright field picture (B). Without any enzyme or FAD added, the channel walls can be weakly perceived by detection of fluorescence. Regarding the bright field image, the surface seems to exhibit a considerable degree of roughness which is assumed to be a result of the manufacturing process employing wet etching with hydrofluoric acid (information given on the manufacturer's homepage), but may also be maintained by the subjection to NaOH during the pretreatment described in 3.7.2.
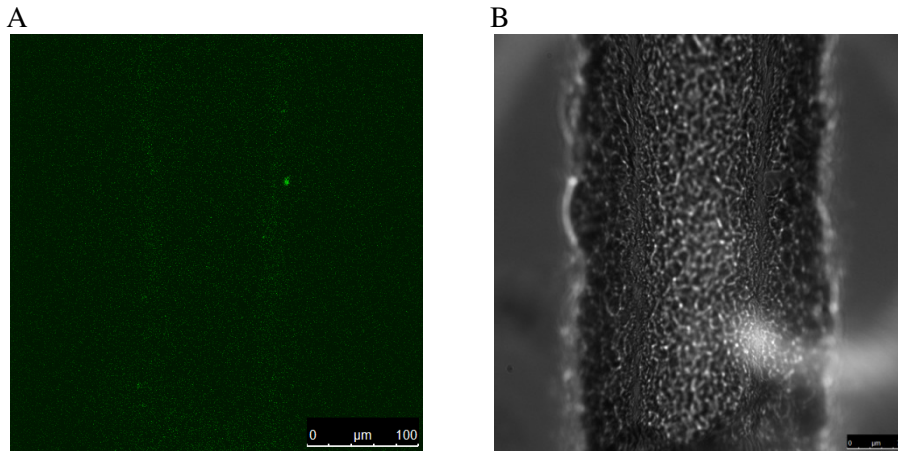
Figure 33: Images of a microreactor channel before immobilization of Z$_{basic2}$_*Tv*DAAO using CLSM (A) and bright field microscopy (B)

After immobilizing Z$_{basic2}$_*Tv*DAAO, the imaging was repeated. Horizontal and cross sections of two different segments of the microreactor channel are displayed in Figure 34. The images reveal a rather uniform fluorescent response on the channel walls, which indicates that the enzyme is homogeneously distributed on the available surface.
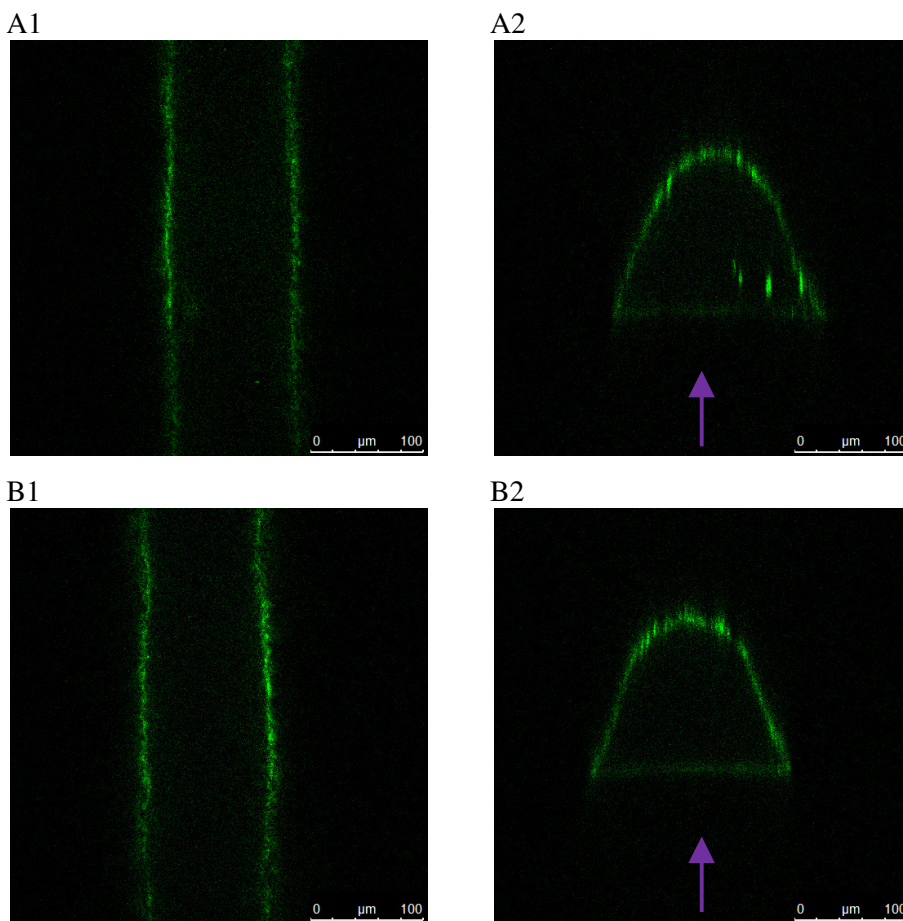
Figure 34: CLSM images of two microeactor channels (A, B) after immobilization of Z$_{basic2}$_*Tv*DAAO

A1 and B1 show horizontal sections, while A2 and B2 show the respective cross section; arrows indicate direction of light inducing autofluorescence of FAD

For generating the images in Figure 35, the chip was turned around and thus fluorescence provoked from the other side. These sections do not exhibit fluorescence on the flat side of the channel due to optical constraints which are accompanied by technical limitations. Although the CLSM system allows for detection of the signal within a narrow Z range (focusing), this range is still higher than the thickness of the protein layer itself. This results in an accumulation of the signal when moving in Z-direction and therefore a higher intensity of the channel sides in comparison with the flat top (or bottom, depending on the point of view) of the channel.
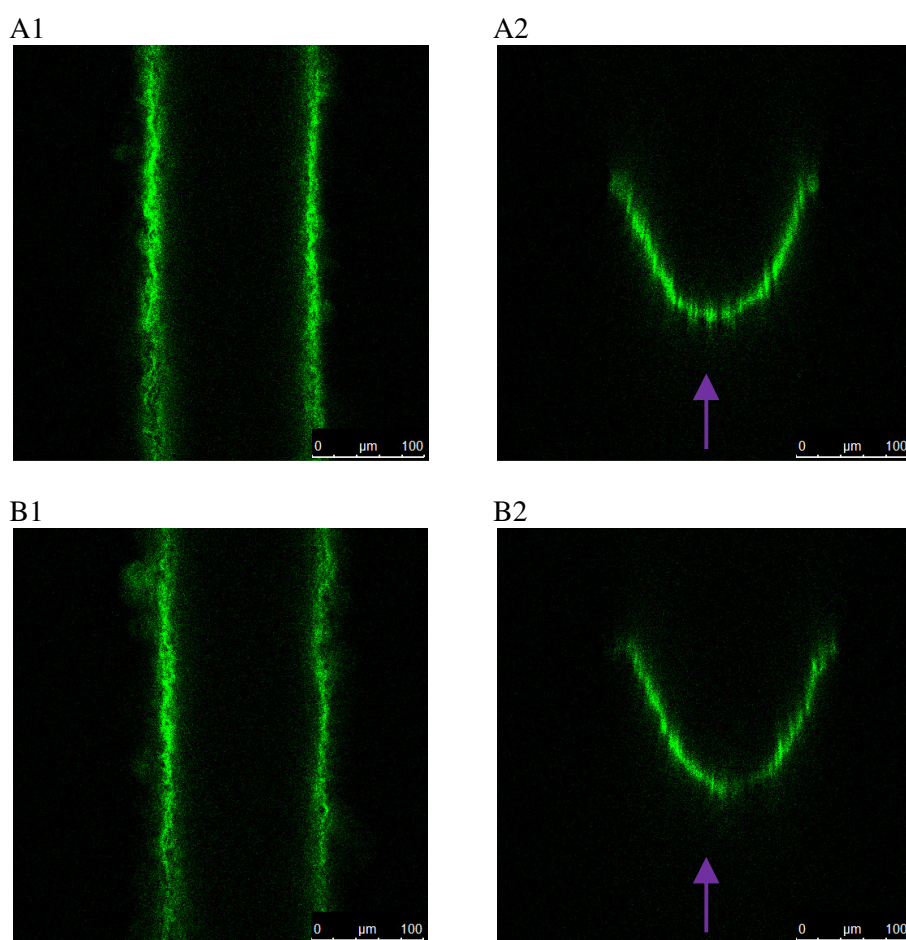
Figure 35: CLSM images of two microeactor channels (A, B) after immobilization of Z$_{basic2}$_TvDAAO

A1 and B1 show horizontal sections, while A2 and B2 show the respective cross section; arrows indicate direction of light inducing autofluorescence of FAD

The notable higher brightness is not a result of increased laser intensity, but rather a consequence of the chip's structure consisting of two glass plates of different thickness. The thinner plate harbors the etched channel and is bonded with the thicker one featuring the

powderblasted connection holes. Thus, the path length of the signal is shorter and the light itself appears brighter, depending on the side of the microreactor chip.

Subsequently Z_{basic2}_TvDAAO was eluted from the microreactor and the autofluorescence of FAD was detected anew (Figure 36). Surprisingly fluorescence was still present without considerable loss of intensity. Since the elution fractions of preceding experiments always exhibited TvDAAO activity, the elution conditions were regarded as effective. Assuming this, FAD (assumingly dissociated from Z_{basic2}_TvDAAO) or any other autofluorescent biomolecule featuring a very similar emission spectrum might be persisting on the surface.
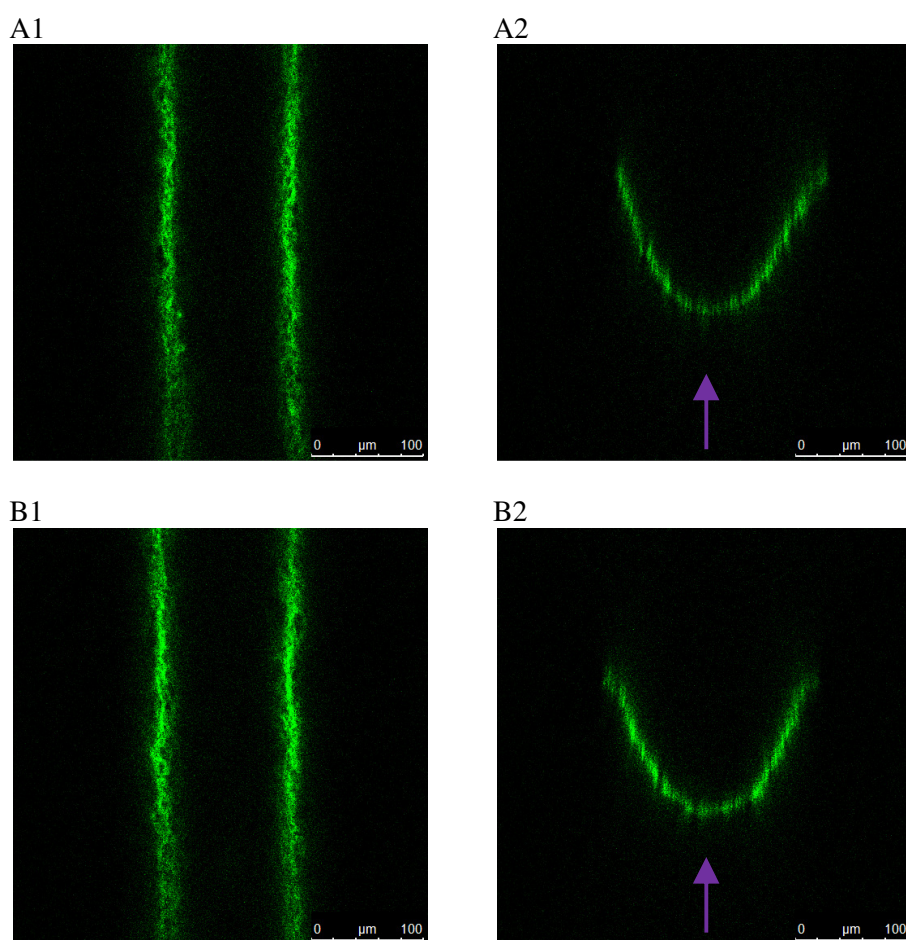
Figure 36: CLSM images of two microeactor channels (A, B) after elution of Z_{basic2}_TvDAAO

A1 and B1 show horizontal sections, while A2 and B2 show the respective cross section; arrows indicate direction of light inducing autofluorescence of FAD

Finally the microreactor chip was subjected to the pretreatment procedure in order to remove any organic contamination and CLSM was performed again. As it can be observed in Figure 37, fluorescence was still present, however with a lower intensity.
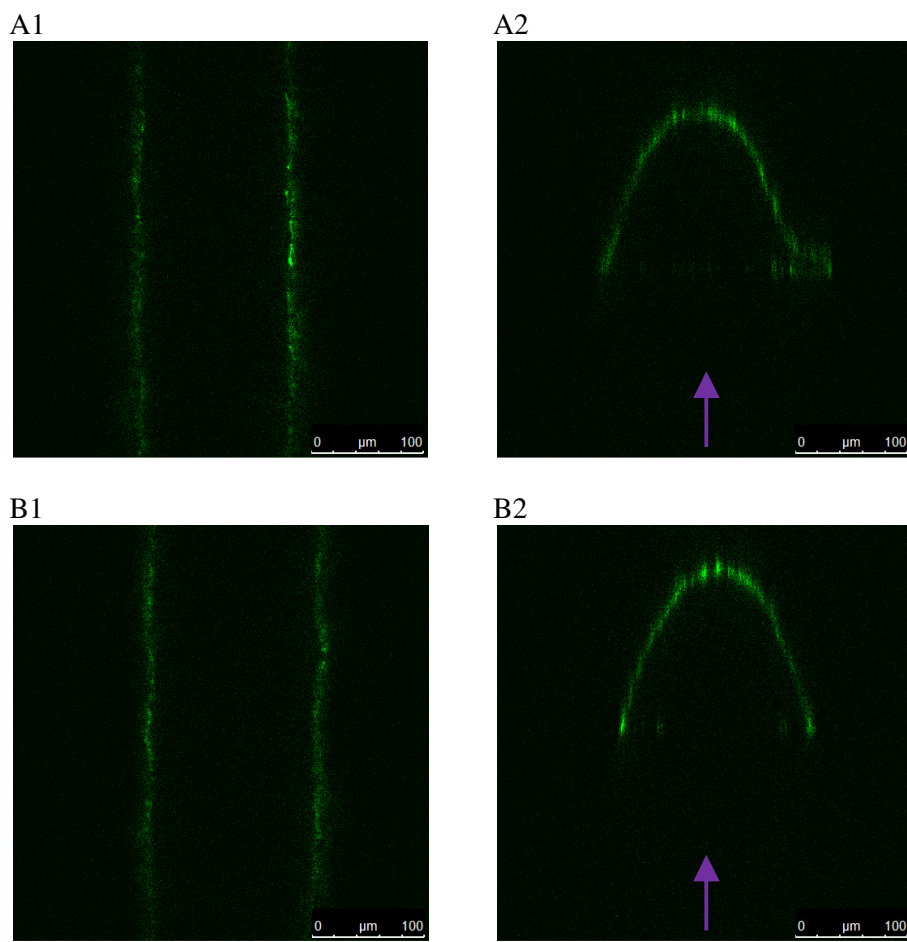
Figure 37: CLSM images of two microeactor channels (A, B) after pretreatment

A1 and B1 show horizontal sections, while A2 and B2 show the respective cross section; arrows indicate direction of light inducing autofluorescence of FAD

Images acquired from the other side of the chip show a similar result. Whether the weaker absorbance is a consequence of the pretreatment or the process of photobleaching, remains a subject of speculation.
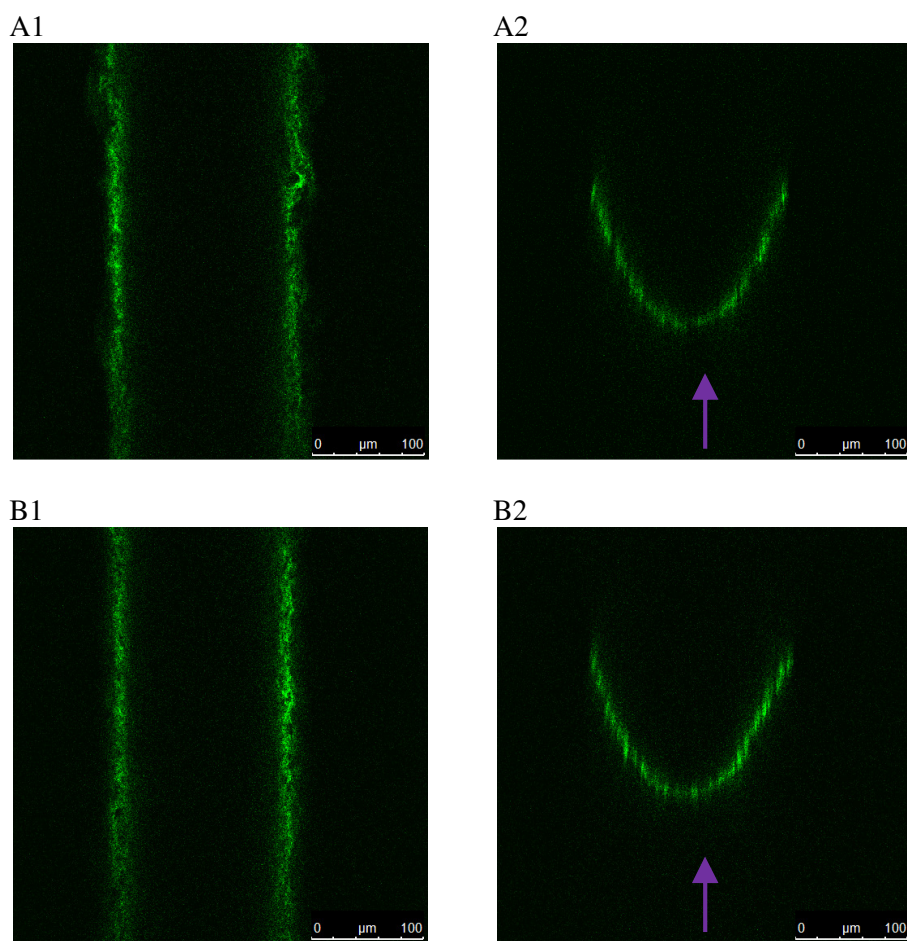
Figure 38: CLSM images of two microeactor channels (A, B) after pretreatment

A1 and B1 show horizontal sections, while A2 and B2 show the respective cross section; arrows indicate direction of light inducing autofluorescence of FAD

To ascertain whether this fluorescence persisting in the microchannel is a result of FAD – released from Z_{basic2}_TvDAAO and subsequently bound to the surface – or any other biomolecule introduced to the microchannel with the immobilization mix, further experiments are required. A first recommendation might be to subject the microreactor to an immobilization mixture containing crude extract from *E. coli* strain BL21(DE3) without recombinant Z_{basic2}_TvDAAO and to check fluorescence via CLSM after incubation times equal to those applied when performing an immobilization experiment. Alternatively the immobilization could be performed using purified Z_{basic2}_TvDAAO.

4.2.8 Conclusions

When immobilizing Z_{basic2}_TvDAAO in a non-functionalized glass microreactor chip, a single immobilization step did not result in the desired high loading. Conducting several steps with slightly increased incubation time was considered an opportunity to increase the probability of a total covering of the microchannel surface. In addition the potential benefit of surface functionalization with sulfonate groups was investigated. When performing three steps, high and reproducible loading was achieved on both the non-functionalized and functionalized surface. Values of apparent immobilized activity (measured at F=100 µL/min) were around 35.5 and 33.7 mU, respectively, which is roughly 60% of the calculated ideal loading. Disregarding potential mass transport limitations, implementation of additional steps might result in even higher apparent loading. However, in case of generally sensitive enzymes like D-amino acid oxidase, the higher demand of labor and time spent for preparation of the immobilizate has to be confronted with the expected operational lifetime of the enzyme. The three steps applied herein involve one working day of preparation, while the half-life time during single passage experiments was ~40 h.

Long term performance of Z_{basic2}_TvDAAO immobilized at both surface conditions was determined using continuous experimental setups. In the first configuration the substrate mix passed the microreactor a single time and apparent activity was calculated from the product concentration found at the outlet. Up to an operation time of 44 h – which also marks half-life time of the enzyme – the courses of apparent activity were similar. After this phase apparent activity was decreasing slightly quicker in the non-functionalized microreactor chip, indicating that derivatization of the surface with sulfonate groups is slightly assisting in stabilization of enzymatic activity. As expected in view of former studies (33), the oxygen limitation results in a flow dependency of the apparent activity. For the second continuous configuration a recycling setup was designed, where reuptake of the essential substrate oxygen was accomplished by surface aeration in an intermediary collection vessel. After a recycling time of ~60 h keto acid concentrations of ~15 and ~12 mM were obtained in working volumes of 3.75 and 5 mL, respectively. However, when normalizing these concentrations based on the working volumes, the respective total amounts achieved were quite similar (54.9-62.4 µmol), implying that higher keto acid concentration was mainly a result of the lower working volume. A contribution of surface functionalization to enhanced enzymatic stability could not be observed in this setup. Comparative data about the intrinsic long-term stability may be acquired by employment of Z_{basic2}_TvDAAO immobilized on beads for operation in a stirred tank reactor of mL-scale.

In order to assess the impact of enzyme detachment on the loss of activity, flow was raised stepwise up to 2 mL/min, a value which corresponds to a residence time of 0.39 seconds. Even at this high rate, the flow pattern was laminar according to the low Re value. No leaching of Z_{basic2}_TvDAAO from a non-functionalized microreactor surface could be identified, which indicates that the interaction of the dimeric enzyme featuring two SBM's with the non-functionalized microchannel surface is sufficiently strong for operation at higher flows. This finding supports the assumption made after the experiments using the monomeric Z_{basic2}_LmSPase that a higher number – or even multiple copies – of the SBM fused to a protein might result in a more stable attachment.

During continuous operation the oxygen concentration at the in- and outlet capillary of the microreactor was monitored in order to identify depletion and assess consumption of oxygen. Although the signal quality was in need of improvement in some cases, correlation of the measured oxygen concentration with the observed apparent activities was absolutely possible. It is therefore concluded that although the employed monitoring strategy did not allow for a fully quantitative observation during the entire operation times, it still provided valuable information in an at least semi-quantitative fashion. Increasing the productivity of an enzymatic microreactor for performance of an oxygen-dependent conversion does not only involve promotion of enzyme loading, but also elevated provision of the limiting substrate oxygen. Besides strategies for generation of oxygen *in situ* (realized in this study by supplementing the substrate mix with Catalase), the solubility of oxygen in the reaction medium might be elevated by conducting the reaction at high pressure (1).

The autofluorescence of oxidized FAD was exploited to visualize immobilized Z_{basic2}_TvDAAO and the thereby acquired CLSM images reveal a homogeneous covering of the microchannel surface. Strangely the fluorescent signal was persisting after applying elution conditions and even after subjecting the microreactor to the pretreatment procedure to remove remains of foregoing immobilizations, however with decreased intensity. In order to clarify whether this fluorescence is a result of FAD released from Z_{basic2}_TvDAAO – which was subsequently bound to the surface – or any other biomolecule introduced to the microchannel with the immobilization mix (containing crude extract), further experiments are essential. Immediate suggestions for verification include usage of crude extract of non-transformed *E. coli* BL21(DE3) lacking the recombinant Z_{basic2}_TvDAAO and/or deployment of previously purified Z_{basic2}_TvDAAO.

Despite the insecurity regarding the CLSM imaging, the employed system has otherwise exhibited promising performance. In view of the data derived by spectrophotometry and oxygen monitoring, the strategy presented here has shown to be a suitable means for preparation of an enzymatic microreactor harboring the dimeric Z_{basic2}_TvDAAO.

5 Literature

1. Wohlgemuth R, Plazl I, Žnidaršič-Plazl P, Gernaey KV, Woodley JM (2015) Microscale technology and biocatalytic processes: opportunities and challenges for synthesis. *Trends Biotechnol* 33(5):302–314.

2. Yao X, Zhang Y, Du L, Liu J, Yao J (2015) Review of the applications of microreactors. *Renew Sustain Energy Rev* 47:519–539.

3. Bolivar JM, Nidetzky B (2013) Smart enzyme immobilization in microstructured reactors. *Chim OggiChemistry Today* 31(3):50–54.

4. Bolivar JM, Wiesbauer J, Nidetzky B (2011) Biotransformations in microstructured reactors: more than flowing with the stream? *Trends Biotechnol* 29(7):333–342.

5. Yoshida J, Kim H, Nagaki A (2011) Green and Sustainable Chemical Synthesis Using Flow Microreactors. *ChemSusChem* 4(3):331–340.

6. Ehrfeld W, Hessel V, Löwe H (2000) State of the Art of Microreaction Technology. *Microreactors* (Wiley-VCH Verlag GmbH & Co. KGaA), pp 1–14.

7. Wirth T (2013) *Microreactors in Organic Chemistry and Catalysis* (John Wiley & Sons).

8. Žnidaršič-Plazl P, Plazl I (2009) Modelling and experimental studies on lipase-catalyzed isoamyl acetate synthesis in a microreactor. *Process Biochem* 44(10):1115–1121.

9. Matosevic S, Szita N, Baganz F (2011) Fundamentals and applications of immobilized microfluidic enzymatic reactors. *J Chem Technol Biotechnol* 86(3):325–334.

10. Sheldon RA, van Pelt S (2013) Enzyme immobilisation in biocatalysis: why, what and how. *Chem Soc Rev* 42(15):6223–6235.

11. Miyazaki M, Maeda H (2006) Microchannel enzyme reactors and their applications for processing. *Trends Biotechnol* 24(10):463–470.

12. Bolivar JM, Nidetzky B (2012) Oriented and selective enzyme immobilization on functionalized silica carrier using the cationic binding module Zbasic2: Design of a heterogeneous D-amino acid oxidase catalyst on porous glass. *Biotechnol Bioeng* 109(6):1490–1498.

13. Bolivar JM, Nidetzky B (2012) Positively charged mini-protein Zbasic2 as a highly efficient silica binding module: opportunities for enzyme immobilization on unmodified silica supports. *Langmuir ACS J Surf Colloids* 28(26):10040–10049.

14. Waugh DS (2005) Making the most of affinity tags. *Trends Biotechnol* 23(6):316–320.

15. Terpe K (2003) Overview of tag protein fusions: from molecular and biochemical fundamentals to commercial systems. *Appl Microbiol Biotechnol* 60(5):523–533.

16. Andersen KR, Leksa NC, Schwartz TU (2013) Optimized E. coli expression strain LOBSTR eliminates common contaminants from His-tag purification. *Proteins Struct Funct Bioinforma* 81(11):1857–1861.

17. Fuchs SM, Raines RT (2005) Polyarginine as a multifunctional fusion tag. *Protein Sci* 14(6):1538–1544.

18. Sassenfeld HM, Brewer SJ (1984) A Polypeptide Fusion Designed for the Purification of Recombinant Proteins. *Nat Biotechnol* 2(1):76–81.

19. Wiesbauer J, Bolivar JM, Mueller M, Schiller M, Nidetzky B (2011) Oriented Immobilization of Enzymes Made Fit for Applied Biocatalysis: Non-Covalent Attachment to Anionic Supports using Zbasic2 Module. *ChemCatChem* 3(8):1299–1303.

20. Goedl C, Schwarz A, Minani A, Nidetzky B (2007) Recombinant sucrose phosphorylase from Leuconostoc mesenteroides: Characterization, kinetic studies of transglucosylation, and application of immobilised enzyme for production of α-d-glucose 1-phosphate. *J Biotechnol* 129(1):77–86.

21. Dib I, Nidetzky B (2008) The stabilizing effects of immobilization in D-amino acid oxidase from Trigonopsis variabilis. *BMC Biotechnol* 8(1):1–11.

22. Buchholz K, Kasche V, Bornscheuer UT (2012) Case study 1: The enzymatic production of 7-ACA from cephalosporin C. *Biocatalysts and Enzyme Technology* (John Wiley & Sons), pp 381–392. 2nd Ed.

23. Maeda-Yorita K, Aki K, Sagai H, Misaki H, Massey V (1995) L-lactate oxidase and L-lactate monooxygenase: Mechanistic variations on a common structural theme. *Biochimie* 77(7–8):631–642.

24. D'Aniello A, et al. (1993) Biological role of D-amino acid oxidase and D-aspartate oxidase. Effects of D-amino acids. *J Biol Chem* 268(36):26941–26949.

25. Oguri S, Watanabe K, Nozu A, Kamiya A (2007) Screening of d-amino acid oxidase inhibitor by a new multi-assay method. *Food Chem* 100(2):616–622.

26. Nuutinen JT, Timonen S (2008) Identification of nitrogen mineralization enzymes, l-amino acid oxidases, from the ectomycorrhizal fungi Hebeloma spp. and Laccaria bicolor. *Mycol Res* 112(12):1453–1464.

27. Mesquita CS, et al. (2014) Simplified 2,4-dinitrophenylhydrazine spectrophotometric assay for quantification of carbonyls in oxidized proteins. *Anal Biochem* 458:69–71.

28. Bradford MM (1976) A rapid and sensitive method for the quantitation of microgram quantities of protein utilizing the principle of protein-dye binding. *Anal Biochem* 72(1–2):248–254.

29. Example Chip Drawing R150.676.2 (2008) *www.micronit.com*. Available at: http://www.micronit.com/wp-content/uploads/2014/08/R150.676.2-R1.1.pdf.

30. Fischer H, Polikarpov I, Craievich AF (2004) Average protein density is a molecular-weight-dependent function. *Protein Sci Publ Protein Soc* 13(10):2825–2828.

31. Shipway A, Shipway S (2008) Protein Size Calculator. *http://www.calctool.org*. Available at: http://www.calctool.org/CALC/prof/bio/protein_size [Accessed November 7, 2013].

32. Cras JJ, Rowe-Taitt CA, Nivens DA, Ligler FS (1999) Comparison of chemical cleaning methods of glass in preparation for silanization. *Biosens Bioelectron* 14(8–9):683–688.

33. Tribulato MA (2014) *Immobilization of D-amino acid oxidase in a glass microreactor* (Institute of Biotechnology and Biochemical Engineering, University of Technology Graz).

34. Valeur B, Berberan-Santos MN (2012) *Molecular Fluorescence: Principles and Applications, 2nd Edition* (Wiley-VCH Verlag GmbH).

35. Lakowicz JR (2011) *Principles of Fluorescence Spectroscopy* (Springer, New York). 3rd edition.

36. Borisov SM, et al. (2009) New NIR-emitting complexes of platinum(II) and palladium(II) with fluorinated benzoporphyrins. *J Photochem Photobiol Chem* 201(2–3):128–135.

37. Miller S, Hille R, Palfey B (2013) *FLAVINS and FLAVOPROTEINS 2011* (Lulu.com).

38. Riedel E, Janiak C (2007) *Anorganische Chemie* (Walter de Gruyter). 7th Ed.

39. Kitao S, Ariga T, Matsudo T, Sekine H (1993) The Syntheses of Catechin-glucosides by Transglycosylation with Leuconostoc mesenteroides Sucrose Phosphorylase. *Biosci Biotechnol Biochem* 57(12):2010–2015.

40. Néméthné-Sóvágó J, Benke M (2014) Microreactors: A new concept for chemical synthesis and technological feasibility. *Mater Sci Eng* 39(2):89–101.

41. Bolivar JM, Schelch S, Mayr T, Nidetzky B (2014) Dissecting Physical and Biochemical Factors of Catalytic Effectiveness in Immobilized D-Amino Acid Oxidase by Real-Time Sensing of O2 Availability Inside Porous Carriers. *ChemCatChem* 6(4):981–986.

6 Appendix

6.1 Immobilization of $Z_{basic2\_}Lm$SPase

6.1.1 Stability of soluble $Z_{basic2\_}Lm$SPase at pH 7 and pH 8

The impact of the pH value present during immobilization on the stability of the enzymatic activity was assessed. Therefore a crude extract including soluble $Z_{basic2\_}Lm$SPase was diluted 1:500 in 50 mM KH_2PO_4 having a pH of 7.0 or 8.0, respectively, and incubated for up to 260 h at room temperature (22 °C). The courses of the volumetric activity in this period are shown in Figure 39.
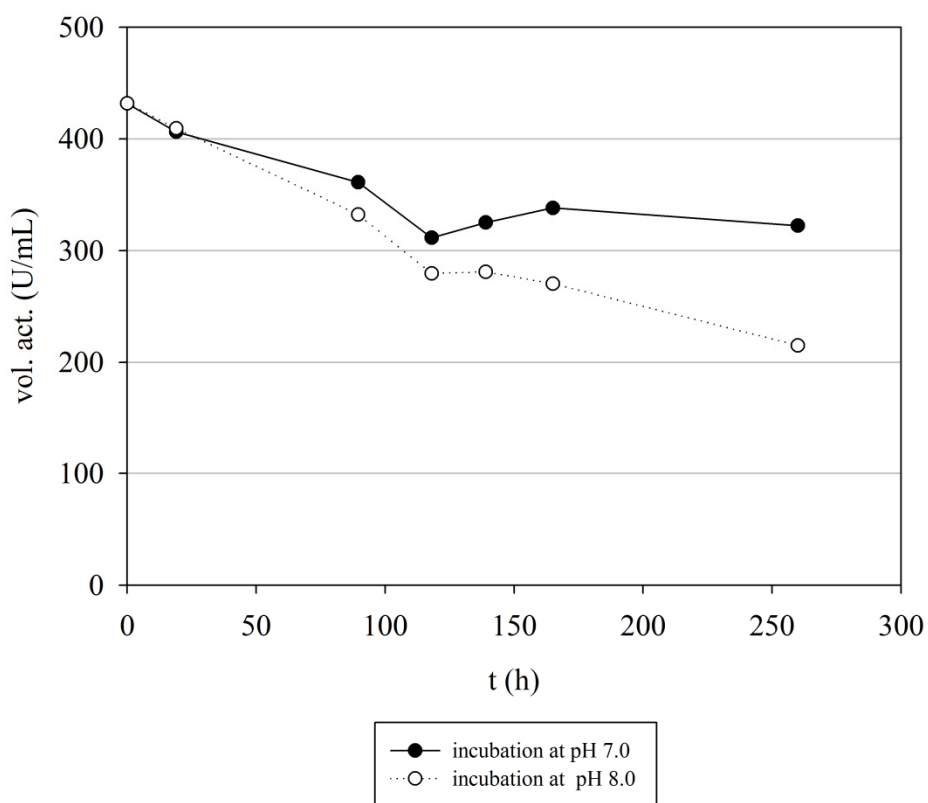
Figure 39: Volumetric activity of $Z_{basic2\_}Lm$SPase during incubation at different pH values

While being identical at the start of the experiment, activity was only slowly decreasing. However, after 260 h the activity was only 75% or 50% of its initial value after incubation at pH7.0 or pH8.0, respectively. It is therefore concluded that the activity is only insignificantly affected by the pH value present during the applied immobilization times.

6.1.2 Purification and concentration of Z_{basic2}_LmSPase

The crude extract deployed for purification had an initial volumetric activity of 406 U/mL and a protein content of 17.1 mg/mL. 3 mL of crude extract in a 1:10 dilution were added to 0.3034 g of the resin. Volumetric activities and protein contents were determined in the supernatant and the three washing steps after the incubation, as well as in the eluate after detaching the purified Z_{basic2}_LmSPase from the solid carrier. The eluted fraction was concentrated by reduction of the volume from 1000 µL to 240 µL, resulting in a solution with a volumetric activity of 149 U/mL (Table 13).

Table 13: Observed volumetric activities during purification of Z_{basic2}_LmSPase

fraction	volumetric activity (U/mL)
crude extract	32.90
supernatant	1.58
wash 1	0.34
wash 2	0.05
wash 3	0.00
eluate	30.35
concentrated enzyme	149.54

6.1.3 Particle size distribution in Z_{basic2}_LmSPase immobilization mixtures

For identifying a potential formation of aggregates in crude extracts prepared at different times of the experimental course – and therefore having different ages – immobilization mixtures were prepared and analyzed regarding their particle size count and distribution. On the date of the MFI measurement, the used crude extracts labeled SPase 2, SPase 3 and SPase 7 were 4 months, 3 weeks and 2 days old, respectively.

The counts classified for different particle sizes x are summarized in Table 14.

Table 14: Particle counts in different immobilization mixtures using crude extracts of different ages

x (µm)	concentration (particles/mL)		
	SPase 2	SPase 3	SPase 7
$2.00 \leq x < 5.00$	19540.70	8192.65	188817.60
$5.00 \leq x < 10.00$	1677.19	864.18	3559.06
$10.00 \leq x < 15.00$	488.94	267.21	636.76
$15.00 \leq x < 20.00$	250.16	119.39	261.53
$20.00 \leq x < 30.00$	267.21	90.97	261.53
$30.00 \leq x < 40.00$	79.60	62.54	17.06
$40.00 \leq x < 60.00$	11.37	5.69	22.74
$60.00 \leq x < 100.00$	0	0	0
$100.00 \leq x < 300.00$	5.69	0	0
total	22320.86	9602.63	193576.28

Total particle counts are strongly differing, but do not allow for a correlation with the age of the crude extract. The lowest number was identified in the mix containing the middle-aged crude extract SPase 3, while it was 2.3 times higher in the mix including the 4 months old SPase 2 extract. The highest value was observed in the mixture with the freshest extract SPase 7. While the differences in total particle count might be attributed to varying amounts of deployed crude extracts (for example the volume of SPase 2 added to the immobilization mix was in fact 2 times higher than that of SPase 3), the particle size distribution should offer more information on the characteristics of the mixtures (Figure 40).
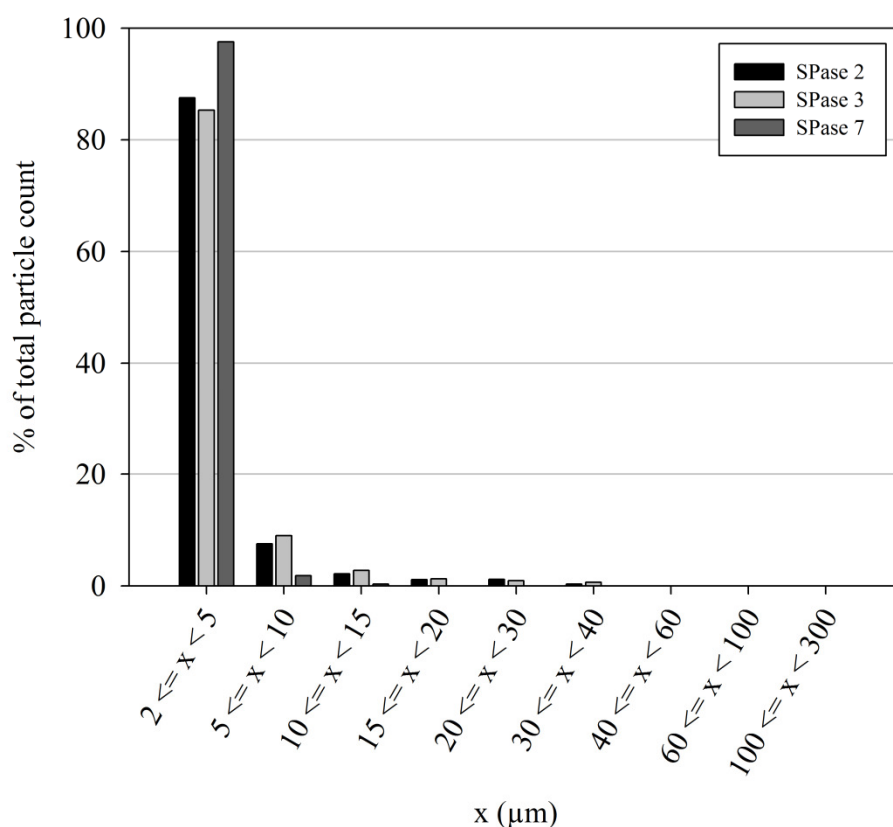
Figure 40: Particle size distribution in different immobilization mixtures using crude extracts of different ages

Ages of extracts: SPase 2: 4 months, SPase 3: 3 weeks, SPase 7: 2 days

In all samples, the by far highest number of particles was identified in the smallest detectable fraction between 2 and 5 µm. This implies that if the particles found in the strongest fraction are aggregates of proteins including Z_{basic2}_*Lm*SPase, most of them do not exceed a size of 5 µm. However, as the monomeric Z_{basic2}_*Lm*SPase has a maximum dimension of 40.5 nm (according to the data shown in 4.1.1), one aggregate might still comprise much more than 100 monomers. Independent from the total count, the size distributions are rather similar, although the smallest fraction is represented slightly stronger in the mix comprising the freshest extract, while exhibiting lower values for the higher particle sizes. Considering the size distribution does also not permit a connection with the respective ages.

It has to be noted that particles below 2 µm could not be identified with the available MFI instrument, while particles smaller than this size might still affect the immobilization process considering the small dimensions of Z_{basic2}_*Lm*SPase. However, employment of the MFI technology for further studies in this regard might benefit from including a comparative

"protein blank" in the measurements. An immediate suggestion is the preparation of a solution containing BSA in a protein concentration comparable to the crude extract.

6.1.4 Abbreviations

4-AAP	4-Aminoantipyrene
BSA	Bovine serum albumin
CLSM	Confocal laser scanning microscopy
dH$_2$O	Deionized water
DMA	N,N-Dimethylaniline
D-Met	D-Methionine
DNP	2,4-Dinitrophenylhydrazine
G1P	Glucose-1-phosphate
G6P	Glucose-6-phosphate
G6P-DH	Glucose-6-phosphate Dehydrogenase from *Leuconostoc mesenteroides*
GOX	Glucose oxidase
HCl	Hydrochloric acid
HRP	Horseradish peroxidase
IPTG	Isopropyl-β-D-thiogalactopyranoside
LB medium	Lysogeny broth medium
*Lm*SPase	Sucrose phosphorylase from *Leuconostoc mesenteroides*
MeOH	Methanol
MFI	Microflow Imaging
MOPS	3-morpholinopropane-1-sulfonic acid
NAD$^+$	Nicotinamide adenine dinucleotide, oxidized
NaOH	Sodium hydroxide
PGM	Phosphoglucomutase from rabbit muscle
SBM	Silica-binding module
SDS-PAGE	Sodium dodecyl sulfate polyacrylamid gel electrophoresis
SPTHS	3-(Trihydroxysilyl)-1-propanesulphonic acid
STY	Space-time yield
tot.act.	Total activity
TRIS	Tris(hydroxymethyl)aminomethane
*Tv*DAAO	D-amino acid oxidase from *Trigonopsis variabilis*
vol.act.	Volumetric activity